Title
Endothelial Mutagenesis Uncovers Key Regulatory Pathways that Maintain Vascular Homeostasis

Author
Ziyad, Safiyyah

Publication Date
2015

Peer reviewed|Thesis/dissertation

UNIVERSITY OF CALIFORNIA

Los Angeles

Endothelial Mutagenesis Uncovers Key Regulatory Pathways that Maintain Vascular Homeostasis

A dissertation submitted in partial satisfaction of the
requirements for the degree Doctor of Philosophy
in Molecular Cell and Developmental Biology

by

Safiyyah Ziyad

2015

ABSTRACT OF THE DISSERTATION

Endothelial Mutagenesis Uncovers Key Regulatory Pathways that Maintain Vascular Homeostasis

by

Safiyyah Ziyad
Doctor of Philosophy in Molecular, Cell and Developmental Biology
University of California, Los Angeles, 2015
Professor Luisa M. Iruela-Arispe, Chair

The purpose of the vascular system is to distribute oxygen rich blood to all organs and extremities, to mediate the transport of nutrients and waste, and to deliver immune cells to sites of infection. It is comprised of the heart and a complex, hierarchically branched network of blood vessels through which the blood is pumped. The principal cell type of the blood vessel is the endothelial cell (EC). They are a subclass of epithelial cells that line the blood vessels and like ceramic tiles, provide a flat-slippery surface for the blood to flow past. Healthy blood circulation is critical for organs to be well oxygenated with the transport of red blood cell and free of infection through the delivery of white blood cells.

Under normal physiological conditions, adult EC are quiescent and do not proliferate. However, in pathological conditions like wound healing and cancer, secreted growth factors and inflammatory cytokines induce endothelial cells to turn on an angiogenesis program. On the other hand, transformed ECs can be the primary cell type of pathology. One such endothelial cell pathology is vascular anomalies (VAs). The emergence of these lesions requires endothelial

cells to accumulate mutations causing them to form malformed vessels or solid tumors. It has been predicted that half of the mutations underlying vascular malformations are unknown, especially those that are non-hereditary and triggered by sporadic, somatic mutations. What is known has been determined through genetic linkage analysis of familial forms of the disease. Here we present the novel results of an *in vivo* forward genetic screen in murine endothelial cells that modeled vascular anomalies. The majority of the approximately 100 disrupted genes identified have not been previously associated with vascular anomalies. Furthermore, we validated a tumor suppressor (*Fndc3b*) and an oncogene (*Pdgfrb*) and demonstrated their causation in endothelial dysfunction. The major significant finding of this study is that endothelial cell homeostasis is heavily governed by regulation of the actin cytoskeleton, cytokine and growth factor signaling, and Hippo signaling pathways.

Also a result of the screen was the revelation that a pathological relationship exists between hemogenic endothelial cells and leukemia. Using the same forward genetic approach in a mouse model, we were able to induced mutagenesis at E9.5 in endothelial cells one day before they turned on their hemogenic program at E10.5. Not only were hematopoietic malignancies generated (both myeloid and lymphoid), but novel mutations associated with these cancers were identified. Here we also present data demonstrating the novel role of *Pi4ka* (identified in association with myeloid leukemia) in hematopoiesis. Together this work takes a look at the critical role of endothelial cells from three different perspectives (tumor angiogenesis, vascular anomalies, and hemogenic endothelial contribution to leukemia), highlighting their importance in physiology and pathology.

The dissertation of Safiyyah Ziyad is approved.

William Edward Lowry

Matteo Pellegrini

Aldons J. Lusis

Luisa M. Iruela-Arispe, Committee Chair

University of California, Los Angeles

2015

DEDICATION

This dissertation is dedicated to my mother and father who sacrificed and taught me that there is nothing that I cannot accomplish.

TABLE OF CONTENTS

LIST OF FIGURES

LIST OF TABLES

ACKNOWLEDGEMENTS

I would first like to thank Dr. M. Luisa Iruela-Arispe, my thesis advisor and mentor, for encouraging me to join her lab and for presenting me with this outstanding project. She has given me the chance to grow as a scientist, while being available for guidance when needed. Her positive outlook and confidence in my abilities is inspiring and has helped me along in tough times. She truly loves her job as a mentor and teacher and this quality greatly influences her passionate, yet cheerful approach to science.

I would also like to thank my doctoral committee members: Dr. William E. Lowry, Dr. Matteo Pellegrini and Dr. Aldons J. Lusis for their valuable guidance, support, and enthusiasm. I would like to thank Dr. Lowry for use of the CemaGenes expression dataset and advice on how to analyze it. I would also like to thank Dr. Pellegrini for putting me in contact with his Collaboratory fellow that has been very helpful in helping with data visualization.

I had great opportunities to form collaborations both at UCLA and at other institutions. In particular, I would like to thank Drs. Adam J. Dupuy and Jesse Riordan from the University of Iowas, who sent us the Sleeping Beauty Mice, performed the linker-mediated PCR, sequencing, and sent us the list of gCIS that were generated from the screen. Their excellent feedback and edits were invaluable to improving our manuscripts. I would also like to thank Drs. Jau-nian Chen and Ann Cavanaugh for allowing us to use their zebrafish facilities, train and help me to perform injections, and give insights and valuable feedback in zebrafish biology. Thanks also to Drs. Matthew Veldman, Jason Ear, and Ann Lindgren for their expertise in zebrafish hematopoiesis. I received valuable protocols, advice and reagents from Drs. Dan Cohn, Hanna Mikkola, Vincenzo Calvanese, Lydia Lee, and Diana Dou with regards to mouse hematopoiesis. I also want to give a big thank you to Drs. Michael Weinstein and Simon Mitchell for critical assistance in exome sequencing analysis and pathway visualization.

It has been a pleasure to be apart of the Arispe lab team and I would like to thank past and present members of the lab for their camaraderie, technical expertise, and advice during my career in the lab. Thanks to Michelle Steel, Ana Rivas, Georg Hilfenhaus, Anais Briot, Stephanie Lau, Liman Zhou, Lauren Goddard, Josephine Enciso, Austin McDonald, Onika Noel, Julia Mack, Taylor Lu, Kirsten Turlo, Huanhuan (Mahsa) He, Aaron Der, Carmen Warren, Courtney Domigan, Melanie Uebelhoer and my undergraduate students Kristine Huynh and Victoria Lee.

I also had the opportunity to work with several outstanding Core facilities on the UCLA campus. I would also like to thank Felicia Codrea and Jessica Scholes of the Broad Stem Cell Institute FACS Core for training and sorting appointments. I would also like to thank Dr. Xinmin Lee, Dr. Xiangming Ding, and members of the JCCC Clinical Microarray Core for exome sequencing expertise. I would like to thank the Zebrafish Core facility, the UCLA Vector Core, and a special thanks goes to members of the UCLA Translational Pathology Core Laboratory for thousands of specimen preparations and histology sections.

Research contained in this thesis was funded by the Eugene V. Cota-Robles Fellowship, the Cell and Molecular Biology Training Grant (Ruth L. Kirschtein National Service Award [DM007185]), the UNCF-Merck Graduate Dissertation Fellowship, and the UCLA Dissertation Year Fellowship.

Finally I would like to thank friends and family for their support and encouragement. They are always there when I need someone to talk to and remind me that with struggle there comes ease.

VITA

2005	Summer Research Grant Children's Hospital Oakland Research Institute Oakland, California
2006-2007	Biology Fellows Program Research Grant University of California Berkeley, California
2007	B.A., Molecular and Cell Biology University of California Berkeley, CA
2009-2011	Teaching Assistant Department of Molecular, Cell and Development Biology Department of Life Science University of California Los Angeles, California
2009	Isabel and Harvey Kibel Fellowship Award University of California, Los Angeles, California
2009-2013	Eugene V. Cota-Robles Fellowship Award University of California Los Angeles, California
2010-2013	Cell and Molecular Biology Training Grant Ruth L. Kirschtein National Service Award University of California Los Angeles, California
2014	Dissertation Year Fellowship University of California Los Angeles, California
2014	UNCF-MERK Graduate Research Fellowship
2015	Edward A. Bouchet Graduate Honor Society Member

PUBLICATIONS AND PRESENTATIONS

Ziyad S and Iruela-Arispe ML. 2011. Molecular Mechanisms of Tumor Angiogenesis. Genes & Cancer 2(12):1085-1096 [Cover Story]

Ziyad S, Goddard LM, Riordan JD, Brett BT, Scheetz TE, Dupuy AJ, and Iruela-Arispe ML. 2012. Endothelial Cell Restricted Sleeping Beauty Transposon Mutagenesis Yields Hemangiomas and Hematopoietic Malignancies. MBI Retreat October 2012, MCDB Retreat December 2012, Lake Arrowhead, CA

Ziyad S, Riordan JD, Dupuy AJ, Iruela-Arispe ML. 2012. Endothelial Cell Restricted Sleeping Beauty Transposon Mutagenesis Screen to Identify Causative Genes Underlying Vascular Tumors. North American Vascular Biology Organization- Genetics and Genomics of Vascular Disease Workshop, Asilomar Conference Grounds, Monterey, CA

Ziyad S, Riordan JD, Brett BT, Scheetz TE, Dupuy AJ, and Iruela-Arispe ML. 2013. Endothelial Cell Mutagenesis Identifies Genes Associated with Vascular Tumors. MCDB Retreat, Lake Arrowhead, CA

Warren CM, **Ziyad S**, Briot A, Der A, Iruela-Arispe ML. 2014. A Ligand-independent VEGFR2 Signaling Pathway Limits Angiogenic Responses in Diabetes. Science Signaling 7(307):ra1

Domigan CK, **Ziyad S**, Iruela-Arispe ML. 2014. Canonical and Noncanonical Vascular Endothelial Growth Factor Pathways: New Developments in Biology and Signal Transduction. Arteriosclerosis, Thrombosis, and Vascular Biology 35(1):30-9.

Ziyad S, Cavanaugh A, Riordan JD, Huynh K, Brett BT, Scheetz TE, Dupuy AJ, Chen Jau-Nian, Iruela-Arispe ML. August 2014. Endothelial Cell Mutagenesis During Development Yields Hematopoietic Abnormalities. International Society for Experimental Hematology, Montreal, Canada

Domigan CK, Warren CM, Antenesian V, Happel K, **Ziyad S**, Lee S, Krall A, Duan L, Torres-Collado AX, Castellani LW, Elashoff D, Christofk HR, Potente M, Iruela-Arispe LM. 2015. Autocrine VEGF Maintains Endothelial Survival Through Regulation of Energy Metabolism and Autophagy. Journal of Cell Science pii: jcs.163774

Ziyad S, Riordan J, Weinstein M, Mitchell S, Lee V, Huynh K, Brett BT, Sheetz TE, Bischoff J, Vikkula M, Gomes A, Dupuy AJ, Iruela-Arispe LM. May 2015 Endothelial Mutagenesis Yields Hematopoietic and Vascular Anomalies. Molecular, Cell and Developmental Biology Club, UCLA, Los Angeles, CA

Chapter 1:

Introduction- Disruptions of Endothelial Cell Homeostasis

Section 1.1. Endothelial Cell Homeostasis

Endothelial cells (ECs) are a specialized epithelial cell type that line blood and lymphatic vessels. Normally quiescent (0.1% doublings per day)[1], these cells line the vessels like ceramic tiles, providing a low friction conduit for blood to flow. ECs act to selectively allow the passage of small molecules and immune cells between the vessel lumen and surrounding organ structure by regulating the permeability of the single-layered sheet of tiled cells called the endothelium. Whether alone (capillaries) or surrounded by a layer of pericytes (veins and venules) or smooth muscle cells (artery and arteriole vessels and the aorta), they form the blood vessel unit. The vascular system is comprised of a highly ordered hierarchical system of branching vessels designed to effectively nourish the tissue through delivery of oxygen and metabolites and draining of toxic byproducts of normal organ function. Any perturbation of disruption of this critical system would ultimately lead to organ failure.

Endothelial cells are tightly anchored to the vessel wall via a layer of extracellular matrix (ECM), called the basement membrane (BM). The ECM is a network of intertwining fibrils of structural molecules like collagen, elastin, and fibronectin, but it also contains a rich electrostatically charged proteoglycan mileu than can hold onto growth factors and cytokines like a sponge. ECs use cell surface transmembrane molecules called integrins to hook onto the basement membrane and are stimulated for proliferation, migration, and survival by a combination of signals received though the integrins and growth factor and cytokine receptors [2]. It is believed that EC-EC contact, achieved through tight packing of the cells, inhibits growth *in vivo*, maintaining the inert monolayer of tiled cells [3]. Endothelial cell integrin, adhesion molecule, and cell surface receptor signaling is well understood in relation to endothelial cell function and will be summarized in Section 1.2 and in Chapter 2 in the context of tumor angiogenesis. However, imbalances in the known afore-mentioned regulators do not fully

explain the formation of a class of endothelial cell pathologies called vascular anomalies, which are the subject of this thesis.

Not only do ECs have to remain attached to the vessel wall under the shear and turbulent forces of blood flow, but they also have to maintain their shape, structure, and barrier function. The strength of the endothelial cells relies in its ability to flatten against the inside of the vessel and keep its shape despite pulsing fluid force from the blood. Endothelial cell resilience is maintained by an endoskeleton made of polymerized actin (actin cytoskeleton), tubulin (microtubule network), and vimentin (intermediate filaments). EC barrier function is regulated through the reorganization and contraction of the cytoskeletal component actin. Cell adhesion molecules at the surface are linked to the actin cytoskeleton through a protein complex comprised of catenins and p190RhoGAP. Disruption of EC-EC contacts are known to occur in response to inflammatory molecules and growth factors [4]. These permeability mediators initiate a signaling cascade that phosphorylates cell adhesion molecules like VE-Cadherin, which mark them for degradation via endocytosis. Without VE-Cadherin tethering beta-catenin to the surface, the latter can then translocate to the nucleus as a transcriptional regulator promoting endothelial cell proliferation. Endocytosis of VE-Cadherin results in vascular permeability. Resultant loss of p190RhoGAP at the cell surface releases inhibition of RhoA, which increases stress fiber formation, causing cells to contract away from each other. ECs that no longer have tight cell-cell growth exit the quiescent state and become activated to migrate and proliferate.

Section 1.2: Tumor Angiogenesis

Angiogenesis is the process by which new blood vessels bud, extend, and branch from existing blood vessels. After initial vasculogenesis (or de novo formation of the vascular plexus during development) it is key for normal development of embryos, growth of the organism and wound healing. However, the tumor organ can corrupt existing vasculature by secreting growth factors and cytokines to turn on an angiogenic program in the endothelial cells. Deregulation of VEGF/Neuropillin, Notch, Ang1/Tie2, Semaphorin, Ephrin/Eph axis, and Slt/Robo signaling can all lead to tumor angiogenesis . This is discussed in detail in Chapter 2.

Section 1.3: Vascular Anomalies

Vascular anomalies are a class of vascular diseases characterized by abnormal vessel morphogenesis (malformations) or endothelial cell overproliferation (tumors). Vascular malformation are further classified into slow flow and fast flow categories [5]. Slow flow malformations include lymphatic, capillary and venous malformations. Arterial and arteriovenous malformations and fistulas make up the fast flow malformations. On the other hand, vascular tumors are categorized into benign, malignant, and those of intermediate malignancy [6]. Angiosarcoma and epitheloid hemangioendothelioma are classified as malignant vascular tumors; hemangiomas (the most common tumor of infancy) and pyogenic granuloma are examples of benign vascular tumors; while Kaposiform hemangioendothelioma and Kaposi sarcoma are classified as vascular tumors of intermediate malignancy according to the most recent consensus of the International Society for the Study of Vascular Anomalies [7].

Decades of linkage analysis studies and deep sequencing, in more recent years, have been instrumental in finding vascular malformation causative mutations in families. The majority of phenotypes follow the Knudsonian two-hit hypothesis in which a predisposing inherited mutation requires a second somatic mutation for a lesion to occur [8]. Hereditary hemorrhagic telangiectasia (HHT), juvenile polyposis-HHT, and HHT-like are fast-flow inherited disorders shown to be caused by aberrant BMP/TGFbeta signaling. Loss of function (LOF) mutations have been found in *ENG* (HHT1), *ALK1* (HHT2), *SMAD4* (JP-HHT), and *BMP9* (HHT-like) [9-12]. Two more mapped loci have been associated with families, but the causative genes have yet to be identified [13,14]. HHT is one of the more rare forms of vascular malformation, occurring with a population frequency of about 0.01% to 0.02% [15].

The genetic basis of inherited forms of slow-flow malformations has also been studied. Capillary malformations are known to be caused by gain of function (GOF) mutations in *GNAQ* (a small G-protein coupled receptor) and LOF mutations in *RASA1* (p120RasGAP) [16-18].

Capillary malformations occur in about 0.3% to 0.5% of the population [19]. Cerebral cavernous malformations (CCM), slow-flow malformations of the brain, are known to be caused by mutations in *KRIT1* (CCM1) [20-23], *Malcavernin/OSM* (CCM2) [24,25], and PDCD10 (CCM3) [25-27]. Following the discovery of the genes, knockout animal models confirmed their causal role [28-32]. CCM1-3 proteins act in combination with each other or with other proteins and have multiple regulatory roles in the cell: cell-cell adhesion [33], cell-matrix interaction [34], DELTA-NOTCH signaling [32,35], RhoA activity and stress fiber formation [30,36,37], cell polarization [38,39], apoptosis [40], endothelial to mesenchymal transition [41], MAPK signaling [42-44], ROS signaling [45], and exocytosis. A lot of the CCM protein interactions have been discovered through structural studies [46]. There is a suspected fourth locus that has been mapped to a subset of patients, but the causative gene has yet to be isolated [47]. CCM is one of the more common types of vascular anomaly occurring in 0.4% to 0.5% of the population [48]. Venous malformations are known to be caused by endothelial mutations in the TIE2/TEK receptor tyrosine kinase and those mutations have been shown to decrease endothelial PDGF-BB production (via Akt dependent inhibition of Foxo1) required to maintain smooth muscle cell support of vessel integrity [49-51]. The first mutations were identified in familial forms of the disease, but subsequent mutations have been identified using next-generation sequencing. Venous malformations occur in abut 0.01% of the population [52]. Much work has also focused on lymphatic anomalies including lymphatic malformation and lymphedema and it has been shown that the majority of the mutation surround VEGFR3 signaling axis [53].

Studies have also focused on understanding the etiology of vascular tumors, particularly Infantile Hemangioma (IH), which is the most common tumor of infancy [54]. IH follows a predicatable life cycle of proliferation of endothelial cells forming luminated vessels, followed by replacement of endothelial lesions with fibro-fatty tissue [55]. Investigation into the underlying genetic cause of this pathology has pointed to VEGFR controlling endothelial cell proliferation [56],

Tie2 disrupting endothelial cell homeostasis [57,58], and Notch signaling in HemSC (hemangioma stem cell) to pericyle/smooth muscle cell differentiation [58,59]. Less is known about the malignant vascular tumors, but there is recent interest in the field beyond immunohistochemical characterization [60,61]. Whole genome sequencing was performed on angiosarcoma specimens, which revealed recurrent mutation in PTPRB (a VEGFR phosphotase) and PLCgamma (known to function downstream of VEGFR) [62]. Informed by hemangioendothelioma and angiosarcoma response to beta-blockers, studies have focused on dissecting pathways downstream of beta-adrenergic receptor [63,64]. It is known that Kaposi sarcoma is caused by the Kaposi sarcoma virus, and it has been reveals that it is the vGPCR present in the viral genome that triggers lesion formation via the PI3K/Akt/mTOR pathway [65-67].

While great strides have been made in understanding the genetic mechanism of inherited vascular malformations, the majority of malformations are the result of somatic mutations [8]. It is predicted that over half of the mutations, when considering all malformation together, are yet to be identified. Next-generation sequencing is one approach to determine mutations in sporadic vascular anomalies. However in this venture, distinguishing driver, passenger, and benign mutations becomes the challenge. To surmount this challenge, we have generated a list of mutated genes found in association with our mouse model of vascular anomalies and used that list to narrow down likely drivers mutations found in human next-generation sequencing samples. This work is summarized in Chapter 3.

Section 1.4: Hematopoietic Stem Cell Birth from Endothelium

A normal disruption of the endothelial cell program occurs at midgestation and resuls in the emergence of hematopoietic cells from the endothelium. During this narrow time window (mouse embryonic days 9.5-13.5), hematopoietic stem and progenitor cells (HSPC) round up and bud off from endothelial cells with hemogenic capacity. This requires the budding cells to lose their ability to attach to both the basement membrane and other EC and be released into the circulation, where they will travel to the fetal liver for expansion, and later home to the bone marrow. Nearly ten years ago, a series of papers were published establishing the endothelial origin of the HSC[68-76]. The ECs with hemogenic capacity are derived from the lateral plate mesoderm [77] and are always arterial in nature as opposed to venous or lymphatic [78]. COUPTFII (a marker of arteries) knockout mice convert "veins" to arteries (as evidenced by staining for arterial markers) and HSC budding can be seen from venous channels expressing arterial markers [79] and Notch1 (another marker of arterial identify) knockout mice lack hematopoietic budding from endothelium [80]. Notch signaling is not only important for hemogenic EC arterial identity, but is also required for turning on the HSC program. [81] VEGF secreted from the sclerotome activates VEGFR2 pathway in endothelial progenitor cells. These cells express Notch as a result. Activated Notch NICD acts as a transcription factor to turn on not only EphrinB2 (arterial marker), but also Gata2 which goes onto cause Runx1 expression. Runx1 knockout endothelial cells do not produce hematopoietic stem cell progeny. The budding HSC quickly lose endothelial markers like claudin-5 and express HSC markers like CD41, followed by the pan leukocyte marker CD45 [68].

Given this physiological link between the hemogenic endothelium (HE), we sought to investigate a pathological role between mutagenesis initiated in the HE and the development of leukemia. The findings are detailed in Chapter 4.

Section 1.5: Sleeping Beauty Transposon Mutagenesis

One approach to uncovering genes and pathways critical to normal cell function is to perform a forward genetic screen to identify genes that when mutated lead to pathology. Genetic screens have been key to discovering important signaling pathways in Drosophila[82], yeast [83], zebrafish [84], and even mice [85]. Forward genetic screening in mice was greatly improved with introduction of engineered transposon tools, particularly the Sleeping Beauty (SB) transposon system [86-89]. Further strides were gained when somatic transposition was able to create cancer and linker mediated PCR was used to identify disprupted genes [88,90,91]. The system has been further refined to model tissue specific cancers through the use of Cre-loxP technology [92-95].

The SB system is comprised of transposable genetic elements (transposons) and the transposase enzyme, which cuts and pastes the transposon randomly into TA dinucleotides distributed throughout the genome [96]. The transposon gets spliced into the mRNA of disrupted genes through splice acceptor and donor sites that are apart of its sequence. The transposon sequence contains a viral promoter/enhancer that can drive overexpression of gene and polyA sequences in both directions that can truncate the disrupted gene. In this way, gain and loss of function phenotypes can be captured. Global mutagenesis (activity in every cell) can be induced when the transposase is controlled by a ubiquitously expressed promoter like Rosa26 [90]. This type of mutagenesis produced mainly blood cancers. Targeted or tissue-restricted mutagenesis can be tailored by placing the transpose downstream of a tissue specific promoter and/or inducible promoter [92,97]. The viral promoter/enhancer can influence tumor type: MSCV promoter is strong in the hematopoietic compartment whereas the CAG promoter is not [98]. Finally, the number of transposons in the starting concatemer (or home site of insertion) also influences mutagenesis [90,91]. Mouse models with a higher starting number or tranpsosons have more opportunities for mutagenesis.

Coupled with linker-mediated PCR, the SB system is able to identify the associated mutations [88,99]. The transposon genome junctions can be sequenced and mapped back to the reference genome. In this way, the exact site of insertion can be determined. Multiple insertions within a gene more often that would be expected by random chance suggest a role for that gene in the pathogenesis of the lesion. Transposon orientation and distribution into a locus has been shown to be a predictor of the resulting phenotype [100]. Gain-of-function is predicted by transposon insertions clustered and all in the direction of transcription of the gene. Loss of function is predicted by distribution of the transposon throughout the gene, with the transposon oriented in either direction. Confirmation of these hypotheses needs to be confirmed with functional studies in which gene of interest is overexpressed or knocked down.

The SB mutagenesis platform is an especially powerful tool for understanding the mechanism of diseases with understudied etiology [95]. This tool has been central to the present study, which is aimed to dissect the genetic mutations and pathways that drive vascular anomaly formation.

Section 1.6: Central Hypothesis and Specific Aims of the Dissertation

Our governing hypothesis was that endothelial cell targeted mutagenesis would yield vascular anomaly formation and would allow for the identification of novel causative genes and regulatory pathways of endothelial cell homeostasis. The specific aims were four: (1) Use endothelial-cell-restricted mutagenesis to generate vascular anomalies. (2) Identify mutated genes using linker-mediated PCR and next-generation sequencing. (3) Validate the causative role of specific genes using *in vitro* and *in vivo* studies (4) Interrogate the human anomaly samples for the presence of variants that could be causative mutations by direct comparison with the SB-transposon screen.

References

1. Cines, D. B. *et al.* Endothelial cells in physiology and in the pathophysiology of vascular disorders. *Blood* **91,** 3527–3561 (1998).

2. Chen, T. T. *et al.* Anchorage of VEGF to the extracellular matrix conveys differential signaling responses to endothelial cells. *J Cell Biol* **188,** 595–609 (2010).

3. Giannotta, M., Trani, M. & Dejana, E. VE-Cadherin and Endothelial Adherens Junctions: Active Guardians of Vascular Integrity. *Dev Cell* **26,** 441–454 (2013).

4. Goddard, L. M. & Iruela-Arispe, M. L. Cellular and molecular regulation of vascular permeability. *Thromb. Haemost.* **109,** 407–415 (2013).

5. Greene, A. K. Current Concepts of Vascular Anomalies. *Journal of Craniofacial Surgery* **23,** 220–224 (2012).

6. Weiss, S. W., Goldblum, J. R. & Folpe, A. L. Enzinger and Weiss's Soft Tissue Tumors. (2013).

7. Wassef, M. *et al.* Vascular Anomalies Classification: Recommendations From the International Society for the Study of Vascular Anomalies. *PEDIATRICS* **136,** e203–e214 (2015).

8. Nguyen, H.-L., Boon, L. M. & Vikkula, M. Genetics of vascular malformations. *Seminars in Pediatric Surgery* **23,** 221–226 (2014).

9. McAllister, K. A. *et al.* Endoglin, a TGF-beta binding protein of endothelial cells, is the gene for hereditary haemorrhagic telangiectasia type 1. *Nat Genet* **8,** 345–351 (1994).

10. Johnson, D. W. *et al.* Mutations in the activin receptor-like kinase 1 gene in hereditary haemorrhagic telangiectasia type 2. *Nat Genet* **13,** 189–195 (1996).

11. Gallione, C. *et al.* Overlapping spectra of SMAD4 mutations in juvenile polyposis (JP) and JP-HHT syndrome. *Am J Med Genet A* **152A,** 333–339 (2010).

12. Wooderchak-Donahue, W. L. *et al.* BMP9 mutations cause a vascular-anomaly syndrome with phenotypic overlap with hereditary hemorrhagic telangiectasia. *Am J Hum Genet* **93,** 530–537 (2013).

13. Cole, S. G., Begbie, M. E., Wallace, G. M. F. & Shovlin, C. L. A new locus for hereditary haemorrhagic telangiectasia (HHT3) maps to chromosome 5. *Journal of medical genetics* **42,** 577–582 (2005).

14. Bayrak-Toydemir, P. *et al.* A fourth locus for hereditary hemorrhagic telangiectasia maps to chromosome 7. *Am J Med Genet A* **140,** 2155–2162 (2006).

15. Albiñana, V., Sanz-Rodríguez, F., Recio-Poveda, L., Bernabeu, C. & Botella, L. M. Immunosuppressor FK506 increases endoglin and activin receptor-like kinase 1 expression and modulates transforming growth factor-β1 signaling in endothelial cells. *Mol Pharmacol* **79,** 833–843 (2011).

16. Shirley, M. D. *et al.* Sturge-Weber syndrome and port-wine stains caused by somatic

mutation in GNAQ. *N Engl J Med* **368,** 1971–1979 (2013).

17. Eerola, I. *et al.* Locus for susceptibility for familial capillary malformation ('port-wine stain') maps to 5q. *Eur J Hum Genet* **10,** 375–380 (2002).

18. Eerola, I. *et al.* Capillary malformation-arteriovenous malformation, a new clinical and genetic disorder caused by RASA1 mutations. *Am J Hum Genet* **73,** 1240–1249 (2003).

19. Orme, C. M., Boyden, L. M., Choate, K. A., Antaya, R. J. & King, B. A. Capillary malformation--arteriovenous malformation syndrome: review of the literature, proposed diagnostic criteria, and recommendations for management. *Pediatr Dermatol* **30,** 409–415 (2013).

20. Sahoo, T. *et al.* Mutations in the gene encoding KRIT1, a Krev-1/rap1a binding protein, cause cerebral cavernous malformations (CCM1). *Hum Mol Genet* **8,** 2325–2333 (1999).

21. Laberge-le Couteulx, S. *et al.* Truncating mutations in CCM1, encoding KRIT1, cause hereditary cavernous angiomas. *Nat Genet* **23,** 189–193 (1999).

22. Günel, M., Awad, I. A., Anson, J. & Lifton, R. P. Mapping a gene causing cerebral cavernous malformation to 7q11.2-q21. *Proc Natl Acad Sci USA* **92,** 6620–6624 (1995).

23. Dubovsky, J. *et al.* A gene responsible for cavernous malformations of the brain maps to chromosome 7q. *Hum Mol Genet* **4,** 453–458 (1995).

24. Liquori, C. L. *et al.* Mutations in a gene encoding a novel protein containing a phosphotyrosine-binding domain cause type 2 cerebral cavernous malformations. *Am J Hum Genet* **73,** 1459–1464 (2003).

25. Craig, H. D. *et al.* Multilocus linkage identifies two new loci for a mendelian form of stroke, cerebral cavernous malformation, at 7p15-13 and 3q25.2-27. *Hum Mol Genet* **7,** 1851–1858 (1998).

26. Guclu, B. *et al.* Mutations in apoptosis-related gene, PDCD10, cause cerebral cavernous malformation 3. *Neurosurgery* **57,** 1008–1013 (2005).

27. Bergametti, F. *et al.* Mutations within the programmed cell death 10 gene cause cerebral cavernous malformations. *Am J Hum Genet* **76,** 42–51 (2005).

28. Boulday, G. *et al.* Tissue-specific conditional CCM2 knockout mice establish the essential role of endothelial CCM2 in angiogenesis: implications for human cerebral cavernous malformations. *Disease Models & Mechanisms* **2,** 168–177 (2009).

29. Cunningham, K. *et al.* Conditional deletion of Ccm2 causes hemorrhage in the adult brain: a mouse model of human cerebral cavernous malformations. *Hum Mol Genet* **20,** ddr225–3206 (2011).

30. Whitehead, K. J. *et al.* The cerebral cavernous malformation signaling pathway promotes vascular integrity via Rho GTPases. *Nat Med* **15,** 177–184 (2009).

31. He, Y. *et al.* Stabilization of VEGFR2 signaling by cerebral cavernous malformation 3 is critical for vascular development. *Science Signaling* **3,** ra26–ra26 (2010).

32. Mcdonald, D. A. *et al.* A novel mouse model of cerebral cavernous malformations based on the two-hit mutation hypothesis recapitulates the human disease. *Hum Mol Genet* **20,** 211–222 (2011).

33. Glading, A., Han, J., Stockton, R. A. & Ginsberg, M. H. KRIT-1/CCM1 is a Rap1 effector that regulates endothelial cell cell junctions. *J Cell Biol* **179,** 247–254 (2007).

34. Faurobert, E. *et al.* CCM1-ICAP-1 complex controls β1 integrin-dependent endothelial contractility and fibronectin remodeling. *J Cell Biol* **202,** 545–561 (2013).

35. Wüstehube, J. *et al.* Cerebral cavernous malformation protein CCM1 inhibits sprouting angiogenesis by activating DELTA-NOTCH signaling. *Proceedings of the National Academy of Sciences* **107,** 12640–12645 (2010).

36. Richardson, B. T., Dibble, C. F., Borikova, A. L. & Johnson, G. L. Cerebral cavernous malformation is a vascular disease associated with activated RhoA signaling. *Biological Chemistry* **394,** 35–42 (2013).

37. Stockton, R. A., Shenkar, R., Awad, I. A. & Ginsberg, M. H. Cerebral cavernous malformations proteins inhibit Rho kinase to stabilize vascular integrity. *Journal of Experimental Medicine* **207,** 881–896 (2010).

38. Goudreault, M. *et al.* A PP2A phosphatase high density interaction network identifies a novel striatin-interacting phosphatase and kinase complex linked to the cerebral cavernous malformation 3 (CCM3) protein. *Mol Cell Proteomics* **8,** 157–171 (2009).

39. Fidalgo, M. *et al.* CCM3/PDCD10 stabilizes GCKIII proteins to promote Golgi assembly and cell orientation. *J Cell Sci* **123,** 1274–1284 (2010).

40. Chen, L. *et al.* Apoptotic functions of PDCD10/CCM3, the gene mutated in cerebral cavernous malformation 3. *Stroke* **40,** 1474–1481 (2009).

41. Maddaluno, L. *et al.* EndMT contributes to the onset and progression of cerebral cavernous malformations. *Nature* **498,** 492–496 (2013).

42. Uhlik, M. T. *et al.* Rac–MEKK3–MKK3 scaffolding for p38 MAPK activation during hyperosmotic shock. *Nature* **5,** 1104–1110 (2003).

43. Zhou, X., Izumi, Y., Burg, M. B. & Ferraris, J. D. Rac1/osmosensing scaffold for MEKK3 contributes via phospholipase C-gamma1 to activation of the osmoprotective transcription factor NFAT5. *Proceedings of the National Academy of Sciences* **108,** 12155–12160 (2011).

44. Zhou, Z. *et al.* The cerebral cavernous malformation pathway controls cardiac development via regulation of endocardial MEKK3 signaling and KLF expression. *Dev Cell* **32,** 168–180 (2015).

45. Goitre, L. *et al.* KRIT1 Regulates the Homeostasis of Intracellular Reactive Oxygen Species. *PLoS ONE* **5,** e11786 (2010).

46. Fisher, O. S. & Boggon, T. J. Signaling pathways and the cerebral cavernous malformations proteins: lessons from structural biology. *Cell. Mol. Life Sci.* **71,** 1881–1892 (2014).

47. Liquori, C. L. *et al.* Low frequency of PDCD10 mutations in a panel of CCM3 probands: potential for a fourth CCM locus. *Hum Mutat* **27,** 118–118 (2006).

48. Fischer, A., Zalvide, J., Faurobert, E., Albiges-Rizo, C. & Tournier-Lasserve, E. Cerebral cavernous malformations: from CCM genes to endothelial cell homeostasis. *Trends Mol Med* **19,** 302–308 (2013).

49. Limaye, N. *et al.* Somatic mutations in angiopoietin receptor gene TEK cause solitary and multiple sporadic venous malformations. *Nat Genet* **41,** 118–124 (2009).

50. Uebelhoer, M. *et al.* Venous malformation-causative TIE2 mutations mediate an AKT-dependent decrease in PDGFB. *Hum Mol Genet* **22,** 3438–3448 (2013).

51. Limaye, N. & Boon, L. From germline towards somatic mutations in the pathophysiology of vascular anomalies. *Hum Mol Genet* (2009).

52. Brouillard, P. & Vikkula, M. Genetic causes of vascular malformations. *Hum Mol Genet* **16 Spec No. 2,** R140–9 (2007).

53. Brouillard, P., Boon, L. & Vikkula, M. Genetics of lymphatic anomalies. *J Clin Invest* **124,** 898–904 (2014).

54. Greenberger, S. & Bischoff, J. Infantile Hemangioma—Mechanism (s) of Drug Action on a Vascular Tumor. *Cold Spring Harb Perspect Med* (2011).

55. Greenberger, S. & Bischoff, J. Pathogenesis of infantile haemangioma. *Br J Dermatol* **169,** 12–19 (2013).

56. Jinnin, M. *et al.* Suppressed NFAT-dependent VEGFR1 expression and constitutive VEGFR2 signaling in infantile hemangioma. *Nat Med* **14,** 1236–1246 (2008).

57. Perry, B. N. *et al.* Pharmacologic Blockade of Angiopoietin-2 Is Efficacious against Model Hemangiomas in Mice. *J Investig Dermatol* **126,** 2316–2322 (2006).

58. Calicchio, M. L., Collins, T. & Kozakewich, H. P. Identification of signaling systems in proliferating and involuting phase infantile hemangiomas by genome-wide transcriptional profiling. *Am J Pathol* **174,** 1638–1649 (2009).

59. Boscolo, E., Stewart, C. & Greenberger, S. JAGGED1 Signaling Regulates Hemangioma Stem Cell–to–Pericyte/Vascular Smooth Muscle Cell Differentiation. *… and Vascular Biology* (2011).

60. Lahat, G. *et al.* Angiosarcoma. *Annals of Surgery* **251,** 1098–1106 (2010).

61. Rao, P. *et al.* Angiosarcoma: A Tissue Microarray Study With Diagnostic Implications. *Am J Dermatopathol* **35,** 432–437 (2013).

62. Behjati, S. *et al.* Recurrent PTPRB and PLCG1 mutations in angiosarcoma. *Nat Genet* **46,** 376–379 (2014).

63. Stiles, J. M. *et al.* Targeting of Beta Adrenergic Receptors Results in Therapeutic Efficacy against Models of Hemangioendothelioma and Angiosarcoma. *PLoS ONE* **8,** e60021 (2013).

64. Stiles, J. *et al.* Propranolol treatment of infantile hemangioma endothelial cells: A molecular analysis. *Exp Ther Med* **4,** 594–604 (2012).

65. Martin, D. *et al.* PI3Kγ mediates kaposi's sarcoma-associated herpesvirus vGPCR-induced sarcomagenesis. *Cancer Cell* **19,** 805–813 (2011).

66. Sodhi, A. *et al.* The TSC2/mTOR pathway drives endothelial cell transformation induced by the Kaposi's sarcoma-associated herpesvirus G protein-coupled receptor. *Cancer Cell* **10,** 133–143 (2006).

67. Montaner, S. *et al.* Endothelial infection with KSHV genes in vivo reveals that vGPCR initiates Kaposi's sarcomagenesis and can promote the tumorigenic potential of viral latent genes. *Cancer Cell* **3,** 23–36 (2003).

68. Eilken, H. M., Nishikawa, S.-I. & Schroeder, T. Continuous single-cell imaging of blood generation from haemogenic endothelium. *Nature* **457,** 896–900 (2009).

69. Boisset, J.-C. *et al.* In vivo imaging of haematopoietic cells emerging from the mouse aortic endothelium. *Nature* **464,** 116–120 (2010).

70. Kissa, K. & Herbomel, P. Blood stem cells emerge from aortic endothelium by a novel type of cell transition. *Nature* **464,** 112–115 (2010).

71. Lancrin, C. *et al.* The haemangioblast generates haematopoietic cells through a haemogenic endothelium stage. *Nature* **457,** 892–895 (2009).

72. Zovein, A. C. *et al.* Vascular remodeling of the vitelline artery initiates extravascular emergence of hematopoietic clusters. *Blood* **116,** 3435–3444 (2010).

73. Chen, M. J., Yokomizo, T., Zeigler, B. M., Dzierzak, E. & Speck, N. A. Runx1 is required for the endothelial to haematopoietic cell transition but not thereafter. *Nature* **457,** 887–891 (2009).

74. Bertrand, J. Y. *et al.* Haematopoietic stem cells derive directly from aortic endothelium during development. *Nature* **464,** 108–111 (2010).

75. Rhodes, K. E. *et al.* The Emergence of Hematopoietic Stem Cells Is Initiated in the Placental Vasculature in the Absence of Circulation. *Cell Stem Cell* **2,** 252–263 (2008).

76. Zovein, A. C. *et al.* Fate tracing reveals the endothelial origin of hematopoietic stem cells. *Cell Stem Cell* **3,** 625–636 (2008).

77. Zovein, A. C. *et al.* Vascular remodeling of the vitelline artery initiates extravascular emergence of hematopoietic clusters. *Blood* **116,** 3435–3444 (2010).

78. Zape, J. P. & Zovein, A. C. Hemogenic endothelium: Origins, regulation, and implications for vascular biology. *Seminars in Cell and Developmental Biology* 1–12 (2011). doi:10.1016/j.semcdb.2011.10.003

79. Kroymann, J. & Mitchell-Olds, T. Epistasis and balanced polymorphism influencing complex trait variation. *Nature* **435,** 95–98 (2005).

80. Kumano, K. *et al.* Notch1 but not Notch2 is essential for generating hematopoietic stem cells from endothelial cells. *Immunity* **18,** 699–711 (2003).

81. Clements, W. K. & Traver, D. Signalling pathways that control vertebrate haematopoietic stem cell specification. *Nat Rev Immunol* **13,** 336–348 (2013).

82. St Johnston, D. The art and design of genetic screens: Drosophila melanogaster. *Nat. Rev. Genet.* **3,** 176–188 (2002).

83. Forsburg, S. L. The art and design of genetic screens: yeast. *Nat. Rev. Genet.* **2,** 659–668 (2001).

84. Patton, E. E. & Zon, L. I. The art and design of genetic screens: zebrafish. *Nat. Rev. Genet.* **2,** 956–966 (2001).

85. Kile, B. T. & Hilton, D. J. The art and design of genetic screens: mouse. *Nat. Rev. Genet.* **6,** 557–567 (2005).

86. Ivics, Z., Hackett, P. B., Plasterk, R. H. & Izsvák, Z. Molecular reconstruction of Sleeping Beauty, a Tc1-like transposon from fish, and its transposition in human cells. *Cell* **91,** 501–510 (1997).

87. Luo, G., Ivics, Z., Izsvák, Z. & Bradley, A. Chromosomal transposition of a Tc1/mariner-like element in mouse embryonic stem cells. *Proc Natl Acad Sci USA* **95,** 10769–10773 (1998).

88. Carlson, C. M. *et al.* Transposon mutagenesis of the mouse germline. *Genetics* **165,** 243–256 (2003).

89. Dupuy, A. J. *et al.* Mammalian germ-line transgenesis by transposition. *Proc Natl Acad Sci USA* **99,** 4495–4499 (2002).

90. Dupuy, A. J., Akagi, K., Largaespada, D. A., Copeland, N. G. & Jenkins, N. A. Mammalian mutagenesis using a highly mobile somatic Sleeping Beauty transposon system. *Nature* **436,** 221–226 (2005).

91. Collier, L. S., Carlson, C. M., Ravimohan, S., Dupuy, A. J. & Largaespada, D. A. Cancer gene discovery in solid tumours using transposon-based somatic mutagenesis in the mouse. *Nature* **436,** 272–276 (2005).

92. Keng, V. W. *et al.* A conditional transposon-based insertional mutagenesis screen for genes associated with mouse hepatocellular carcinoma. *Nat Biotechnol* **27,** 264–274 (2009).

93. Starr, T. K. *et al.* A transposon-based genetic screen in mice identifies genes altered in colorectal cancer. *Science* **323,** 1747–1750 (2009).

94. Dupuy, A. J. *et al.* A modified sleeping beauty transposon system that can be used to model a wide variety of human cancers in mice. *Cancer Res* **69,** 8150–8156 (2009).

95. Moriarity, B. S. *et al.* A Sleeping Beauty forward genetic screen identifies new genes and pathways driving osteosarcoma development and metastasis. *Nat Genet* **47,** 615–624 (2015).

96. Copeland, N. G. & Jenkins, N. A. Harnessing transposons for cancer gene discovery. *Nat Rev Cancer* **10,** 696–706 (2010).

97. Starr, T. K. *et al.* A transposon-based genetic screen in mice identifies genes altered in colorectal cancer. *Science* **323,** 1747–1750 (2009).

98. Rad, R. *et al.* PiggyBac Transposon Mutagenesis: A Tool for Cancer Gene Discovery in Mice. *Science* 1–5 (2010). doi:10.1126/science.1193004

99. Brett, B. T. *et al.* Novel Molecular and Computational Methods Improve the Accuracy of Insertion Site Analysis in Sleeping Beauty-Induced Tumors. *PLoS ONE* **6,** 1–11 (2011).

100. Been, R. A. *et al.* Genetic Signature of Histiocytic Sarcoma Revealed by a Sleeping Beauty Transposon Genetic Screen in Mice. *PLoS ONE* **9,** e97280 (2014).

Chapter 2:

Molecular Mechanisms of Tumor Angiogenesis

Abstract

Tumors have been recently recognized as aberrant organs composed of a complex mixture of highly interactive cells that in addition to the cancer cell include stroma (fibroblasts, adipocytes, and myofibroblasts), inflammatory (innate and adaptive immune cells), and vascular cells (endothelial and mural cells). While initially cancer cells co-opt tissue-resident vessels, the tumor eventually recruits its own vascular supply. The process of tumor neovascularization proceeds through the combined output of inductive signals from the entire cellular constituency of the tumor. During the last two decades, the identification and mechanistic outcome of signaling pathways that mediate tumor angiogenesis have been elucidated. Interestingly, many of the genes and signaling pathways activated in tumor angiogenesis are identical to those operational during developmental vascular growth, but they lack feedback regulatory control and are highly affected by inflammatory cells and hypoxia. Consequently, tumor vessels are abnormal, fragile, and hyperpermeable. The lack of hierarchy and inconsistent investment of mural cells dampen the ability of the vessels to effectively perfuse the tumor, and the resulting hypoxia installs a vicious cycle that continuously perpetuates a state of vascular inefficiency. Pharmacological targeting of blood vessels, mainly through the VEGF signaling pathway, has proven effective in normalizing tumor vessels. This normalization improves perfusion and distribution of chemotherapeutic drugs with resulting tumor suppression and moderate increase in overall survival. However, resistance to antiangiogenic therapy occurs frequently and constitutes a critical barrier in the inhibition of tumor growth. A concrete understanding of the chief signaling pathways that stimulate vascular growth in tumors and their cross-talk will continue to be essential to further refine and effectively abort the angiogenic response in cancer.

Introduction: Tumors Are Organs

The transformation of normal cells into a neoplasm and subsequently into a malignant tumor is a stepwise process through which the tumor acquires what Hanahan and Weinberg named the "hallmarks of cancer".[1] In order for tumors to succeed in situ, they have to develop ways to sustain proliferative signaling, evade antiproliferative safeguards, resist apoptotic programming, achieve replicative immortality, and summon new vasculature to import nutrients and export waste. If a tumor is able to gain the necessary mutations to migrate and survive in new niches, it can then take advantage of available vascular networks and travel to colonize new frontiers (Fig. 1). In fact, death from cancer is due less to the primary tumor outcompeting surrounding tissue and more due to cachexia, immune suppression, and thromboembolisms.[2,3]

As interdisciplinary information reached cancer biology, the field has moved away from the concept of cancer as an isolated self-sufficient ball of aberrant cells. Currently, tumors are viewed as "organs" composed of multiple and highly interactive cell types.[3-6] Thus, the tumor is made up of the primary cancer cells and of a court of stromal cells that actively contribute to its maintenance. The tumor stroma includes mesenchymal derived cells (like fibroblasts, adipocytes, and smooth muscle cells), inflammatory cells (innate and adaptive immune cells), and vascular cells (endothelial cells and pericytes). Each of these cell types can be found in normal stroma; but in a tumorigenic setting, the cancer has appropriated, modified, and corrupted these cells to do its bidding.

The cancer cell element of the tumor organ, through growth factor paracrine signaling, stimulates the differentiation of fibroblasts from a tumor-suppressing cell to a tumor-supporting cell. These cancer/ tumor-associated fibroblasts (CAFs or TAFs) are characterized by smooth muscle α actin, fibroblast activation protein, and Thy-1 expression.[7,8] The acquisition of these features is gradual and, at some point, irreversible. First, upon a breach in tissue integrity,

tissue-resident fibroblasts become myofibroblasts due to the upregulation of smooth muscle α actin. Myofibroblasts are normally involved in wound healing and display an increased capacity for secreting extracellular matrix (ECM) proteins and cytokines, such as IL-6 and RANTES, which relay distress calls to the immune system. If healing is resolved, myofibroblasts revert back to tissue- resident fibroblasts.[7,8] However, continued pressure from tumor cells can impose additional changes on myofibroblasts that now evolve into CAFs. These can no longer revert into tissue fibroblasts and, in addition, gain resistance to apoptosis.[8] The ECM secreted by CAFs can hoard and store cytokines and growth factors produced by the tumor and the assortment of stromal cells in the microenvironment. CAFs also secrete matrix metalloproteinases (MMPs) that further enable tumor invasion.[9] Degradation of the ECM also makes stored growth factors and cytokines biologically available to spark proliferation and migration via the activation of signal transduction cas- cades.[9] The presence of CAFs, along with the influx of inflammatory cells to the tumor site, inspired the concept of the tumor as “a wound that never heals”.[10]

In addition to the cancer cells and fibroblast components, the tumor organ has a substantial inflammatory cell constituency. The notion that immune cells aid in cancer growth is counterintuitive if we think of the immune system as a mechanism to fight against foreign and abnormal insults. In fact, customarily, immune cells do identify and eliminate abnormally growing cells.[6] A tumor only develops once the cancer cells have evolved to bypass immune recognition and have co-opted inflammatory cells to their own advantage.[3] The inflammatory cells seen in the tumor microenvironment include tumor-associated macrophages (TAMs), mast cells, eosinophils, neutrophils, and dendritic cells.[3,11] TAMs most closely resemble the M2 branch.[3] They secrete cytokines and growth factors that induce tumor growth, invasion, metasta- sis, and angiogenesis. They also have been shown to suppress cytotoxic T-cell activity.[3,11] In addition to TAMs, N2 lineage neutrophils and mast cells release ECM-degrading enzymes and angiogenesis-stimulating factors.[3,11] As a consequence, the recruitment of

immune cells to the tumor amplifies an already upregulated network of growth factor cross-talk that promotes tumor growth.

Tumor-associated vascular beds provide the tumor with nutrients and oxygen and with a mode of waste removal. If a tumor develops in a well-vascularized region, the co-option of pre-existing vessels might be employed. Otherwise, angiogenesis, or the branching of new blood vessels from established vascular networks, is a necessity for tumor expansion beyond 400 μm.[12] The induction of vascular growth is only possible by building a proangiogenic environment through the collective effort of tumor cells, CAFs, and resident inflammatory cells.[7] Growth factors secreted by the tumor create a chemotactive gradient to recruit endothelial cells and pericytes away from their existent vascular beds. In addition, MMPs generate a large variety of matrix protein fragments that facilitate migration and vascular morphogenesis.[3,7] Once a vascular network is established, it can further support the tumor by shuttling in nutrients and oxygen and exporting away waste products. With the aid of the cooperative tumor microenvironment, the cancer continues to have the opportunity to accumulate mutations and metastasize. The fact that angiogenesis is required for tumors to achieve two of the “hallmarks of cancer” highlights its importance in cancer progression. Understanding the tumor as an organ requires an understanding of angiogenesis. This review will summarize the current knowledge on the molecular mechanisms that underlie this process.

The Tumor Vasculature

Within a tumor, immune, stromal and cancer cells, immune and stromal cells engage in altruism, the goal of which is to nurture cancer cell growth and facilitate expansion of the tumor to alternative niches.[1] Blood vessels are an essential component of this goal, as they provide metabolic means and routes for meta- static expansion. Nonetheless, how frequent is “true” angiogenesis (growth of new blood vessels) in tumors? Is the formation of new blood vessels necessary for tumor growth? Or are local tissue- resident vessels sufficient to feed tumor cells?

While the notion that angiogenesis is triggered as soon as the tumor reaches 0.4 mm is conceptually appealing, it is unclear how frequent new blood vessels versus existent blood vessel utilization occurs in tumors (Figure 2). New vascular invasion is essential for tumors originating from avascular tissues such as the epidermis. Yet, even in this environ- ment, once tumor cells disrupt the basement membrane and invade the underlying dermis, a wealth of dermal resident vessels is available to the incipient tumor cells. Vascular co-option is prominent in carcinomas originating from single epithelia (e.g., many types of breast cancer) as well as in any tumor of mesenchymal origin (sarcomas). Thus, as tumor cells expand, they pro- gressively take over the local vasculature through co-option of vessels[13] (Figure 2). However, it should be stressed that these co-opted vessels are no longer normal. The association of tumor cells with resident vessels alters their morphology, physiology, and responses to therapy.[14,15] It is critical to acknowledge that we do not know how much co-option versus tumor-initiated vascular growth occurs in any given tumor. It is experimentally difficult to distinguish between the 2 processes. However, a future clear delineation between co-option and new vascular sprouting might be particularly important for better selection of therapeutic intervention.

Whether co-opted or the result of legitimate angiogenesis, tumor-associated vessels differ from normal vessels morphologically and functionally. Normal vessels are hierarchic,

evenly distributed, and because of their effective coating of smooth muscle cells/pericytes, are able to efficiently deliver nutrients to the tissue they serve. In contrast, tumor vasculature tends to be inefficient because of structural transformations induced by paracrine signaling and tumor-endothelium cell contact. Tumor vessels tend to be unevenly distributed and form chaotic, tortuous networks with irregular branching patterns.[16] Tumor vessels exhibit bidirectional blood flow and are not constantly perfused.17 Using artificial methods like tumor cell injection or adenoviral delivery of VEGF into mice, investigators have been able to generate surrogate vessels to understand the pathology of blood vessels in crisis. Whereas adenovirally delivered VEGF (adeno-VEGF) mimics an acute spike of VEGF (the most prominent angiogenic growth factor), as seen in wound healing, injection of tumor cells is meant to model the chronic, sustained exposure of vessels to VEGF. Adeno-VEGF injection creates a fast and amplified production of VEGF that tapers off to normal levels after about a month.[16] These studies have shown "tumor" blood vessels to be larger than normal vessels, with an altered surface area to volume ratio that results in poor nutrient delivery and waste removal.[16] Efforts have been made to categorize and follow the evolution of these surrogate vessels as a method of understanding the vessels commonly found in tumors.

Using morphological and physiological criteria, investigators have identified 6 distinct types of tumor vessels[16,18]: 1) Mother vessels (MVs) are the first type of vessels to form after exposure to high levels of VEGF and/or after injection of tumor cells. These vessels have been also seen in healing wounds and human tumors. They are maintained as long as high concentrations of VEGF164 are present. MVs originate from pre- existing capillaries and venules and form in a 3-step process. After injection, there is an initial peak in cell proliferation after about 3 to 5 days. To accommodate a 3- to 5-fold increase in vessel diameter, the MV must shed the associated pericytes and degrade the vessel basement membrane (VBM). Cathepsin cystein proeases, secreted by pericytes, are responsible for this degradation of the

VBM. Normally, cystein protease inhibitors (CPIs) would prevent VBM degradation, but they are found at low levels at the injection site. The individual endothelial cells lining the vessel wall have to stretch and flatten. To accommodate the increase in endothelial cell surface area, vesiculo-vacuolar organelles fuse with plasma membrane. MVs are transitional vessels that evolved into 1 of 3 types of daughter vessels. 2) After VEGF levels start to fall, capillaries are formed in a process called luminal bridging: when MV endothelial cells extend processes across the lumen. The blood flow gets divided into the capillaries, which can sustain in the presence of low VEGF levels. 3) Alternatively, in the presence of high levels of VEGF, MVs can evolve into glomeruloid microvascular proliferations. These vessels are formed when an overproliferation of CD31-VEGFR2+ endothelial cells bridge the lumen of MVs. These smaller vessels acquire pericytes and an excess of abnormal VBM. When VEGF levels fall, these vessels regress into capillaries. 4) Vascular malformations, the last type of daughter vessel, form when MVs obtain a thin asymmetrical coat of smooth muscle cells that might supply the endothelial cells with VEGF. Vascular Malformations (VMs) main- tain the large diameter of MVs and can survive independent of an exoge- nous source of VEGF. 5) and 6) Feeder arteries and draining veins are vessels directly upstream and downstream from the tumor. They are large, tortuous vessels that are not a product of angiogenesis.

Functionally, tumor vessels are inappropriately permeable to large macro- molecules and are inefficient at oxygenating the tumor and clearing waste. Tumor-associated vessels leak not just water but “exudate” a fluid close to the composition of whole plasma.[19] This is in contrast to normal vessels that are able to filter large macromolecules and prevent them from passing into the tissue. In the tumor microenvironment, plasma proteins like fibrinogen leak into the stroma and encounter tissue factor, which polymerizes fibrinogen into fibrin gel clots, which aids in tumor expansion in a number of ways[19]: a) The fibrin gel absorbs water and prevents the clearance of fluid, causing edema and a pressure gradient that favors diffusion from the

interstitial space into the vessel lumen. This is in direct contrast to the function of a normal blood vessel, which should deliver nutrients to the tissue. b) Fragment E, cleaved from fibrin by MMPs, is directly angiogenic. c) Growth factors can become trapped in the gel, protecting them from degradation and making them available to transform stromal cells. So, not only are tumor vessels unable to perform their normal functions, but they also actively contribute to the formation of the tumor-promoting microenvironment. Tumor vessels are unable to effectively oxygenate tumor tissues and are also inefficient at removing waste metabolites because of the aforementioned structural abnormalities.[20] Some areas of the tumor are chronically hypoxic and acidic because they are hypovascular, and other regions are acutely hypoxic and acidic due to intermittent blood flow.[20] One can imagine how this hostile microenvironment could select only for the most aggressive tumors that are able to switch to signaling pathways that allow adaptation. In addition, both hypoxia and acidosis induce the expression of growth factors like VEGF, Ang2, PDGF, PlGF, TGFα, IL8, and HGF in vitro.[21] These growth factors can induce both cancer cell and stromal cell proliferation. In mice, it has been shown that low pH controls VEGF promoter activity by way of the Ras-ERK1/2-AP1 pathway, while hypoxia induces VEGF promoter activity via the HIF1α route.[22] So, as the tumor shapes the microenvironment to promote abnormal blood vessels, the deviant vasculature in turn promotes a microenvironment that selects for and nurtures a more aggressive cancer phenotype.

The abnormal tumor vasculature is a formidable barrier to chemotherapeutic agents administered to fight the tumor. Hypoxia itself can cause resistance to radiation and other therapies.[23] Certain DNA-hydrolyzing chemotherapeutic agents can only work in the presence of oxygen, and the highly acidic microen- vironment can attract weakly basic drugs, preventing access to the cancer cell targets.[20] The chaotic structure of the vasculature, poor smooth muscle cell/pericyte coverage, and the dysfunc- tional ability of the endothelium to transport fluid create a high intratumoral pressure that perpetuates difficulties in perfusion of the growing

tumor.[23-25] Due to the hyperpermeability of tumor ves- sels and the focal leaks often seen in tumor vessels, blood flow rates are reduced as measured by red blood cell velocity.[20,26] Studies have shown that tumors often have increased interstitial pressure[23] and that they can affect the interstitial pressure of surrounding nor- mal tissue.[25] Hydraulic conductivity studies using intratumoral injection of Evans blue dye into tumor centers have shown that tumors vary in their resistance to fluid flow.[24] This resistance could be relieved using hyaluronase to hydrolyze the ECM, demonstrating that tumoral ECM composition and density influence interstitial pressure. Interestingly, the injected dye did not reabsorb into blood vessels as expected perhaps due to the lack of blood flow observed around the area of injection.[24] In sum, the corrupted tumor-associated vasculature can protect the cancer from antitumor chemotherapeutic agents.

With our new understanding of the tumor as a complex organ, the current focus is on targeting the supportive tumor stroma. Based on observations that abnormal tumor vessels present difficulties in drug delivery to the tumor, efforts have been made to “normalize” tumor blood vessels in order to make for a more efficient delivery of antitumor drugs. By using neutralizing antibodies against VEGFR-2, hyperpermeable vessels can be “normalized”, and drug access to cancer cells can be improved.[23] Studies in mice have shown that VEGFR2-neutralizing antibodies are able to correct leaking vessels, restore a more normal VBM, decrease tumor interstitial pressure, and increase tumor oxygenation.[27,28] Similar effects are seen in human tumors after treatment with bevacizumab (also known as Avastin [Genentech Inc., South San Francisco, CA], an antibody against VEGF) in coordination with chemotherapy and radiation.[29] Since VEGF-targeted therapies have been shown to have limited efficacy, the concept of targeting stromal cells in general has been brought to the forefront.[30] Guidance molecules including semaphorins, ephrins, netrins, and slit, well known to influence neuronal guidance, also have a role in vascular remodeling.[31] More specifically, semaphorins interact with Neuropilin-1 (NRP1) receptors to inhibit migration of endothelial and tumor cells alike. It was

recently demonstrated that targeted and systemic delivery of Sema3A in a mouse tumor model abrogates tumor cell migration and metastasis as well as tumor angiogenesis.[32] By targeting the endothelium, the Sema3A starves the tumor for oxygen and nutrients and concomitantly prevents the tumor cells from migrating to seek out a new source of sustenance. The dual effect of this therapy has great potential. Moreover, understanding the various signaling molecules can provide further opportunities to effectively suppress the multiple survival pathways exploited by tumors.

Operational Signaling Pathways in Tumor Angiogenesis

In the last two decades, much has been learned about the tumor vasculature. As the tumor expands, growth factors secreted by tumor cells mediate the induction of angiogenesis and control the inflammatory infiltrate. Multiple ligand-receptor complexes have been associated with tumor angiogenesis. The network of growth factors and receptors during tumor growth is indeed similar to the one operative in developmental angiogenesis and during angiogenesis- driven inflammation[33,34] (Figure 3). Nonetheless, the lack of cross-regulatory control with the host tissue and the misregulation of downstream signals result in an aberrant vascular supply, one that is frequently inefficient with irregular flow patterns and abnormal delivery of oxygen and nutrients.[16,17]

To date, the following ligand-receptor signaling networks have been identified ascontributorstotumorangiogenesis:1) VEGF ligand with receptors VEGFR-1, VEGFR-2, and NRP1; 2) angiopoietin ligandswiththeTiereceptors; 3)Delta- like and Jagged ligands with Notch recep- tors; 4) Ephrin ligands with the Eph receptors; and 5) Slit ligand with the Robo receptors. Combined, the circuitry of growth factors and the respective receptors mediates the proliferation and migration of endothelial cells and the organization of vascular networks that feed the tumor and provide avenues for metastatic spread.[35] Stimulation of the endothelium by growth factors is critical to attain two of the hallmarks of cancer: angiogenesis and metastasis.[1] Thus, much effort has been placed in the suppression of tumor angiogenesis via targeting specific growth factors and receptors.[36,37]

Differential Effects of Soluble Versus ECM-Bound VEGF-A on Endothelial Cells

As a tumor outgrows the oxygen diffusion gradient, it either co-opts existing vasculature or induces angiogenesis. Prolyl hydroxylases (PHDs) allow cells (tumor and stromal) to sense the oxygen levels in the environment.[38] Specifically, under normoxic conditions, PHDs use the

abundance of oxygen molecules to hydroxylate HIF transcription factors. Hydroxylated HIF associates with VHL (von Hippel-Lindau) and becomes targeted for degradation by the proteasome. Conversely, under hypoxic conditions, the HIF2α transcription factor in endothelial cells is able to induce the expression of target genes like VEGF-A (henceforth, referred to as VEGF).

VEGF is secreted in multiple iso- forms, as a result of alternative splicing of a single gene, with VEGF164 being the most common.[39] Every isoform retains the receptor-binding domain encoded by exons 2 to 5 but differ in their carboxy-terminal end (encoded by exons 6a, 6b, 7, and 8). These differences alter their respective abilities to bind to the ECM and to the nonenzymatic single-pass transmembrane proteins Neuropilin-1 and -2 (NRP1 and 2). In addition to splicing events, these changes can be imposed by posttranslational proteolytic cleavage of the matrix binding VEGF C-terminus, creating soluble forms. MMP and plasmin processing of VEGF generates 113 and 110 amino acid receptor–binding products, respectively.[40,41] VEGF matrix associations increase the stability of the VEGF molecules in vitro.[42] More importantly, association of VEGF with NRP1 and the ECM confers different VEGFR2- mediated downstream signaling compared to soluble VEGF.[42,43]

Endothelial cells respond to the VEGF ligand through 2 receptor tyrosine kinases: VEGFR-1 and VEGR-2 (VEGF receptor-1 and -2, respectively). Most of the proangiogenic responses are conveyed by VEGFR-2, while VEGFR-1 is thought to act as a decoy modulator. Upon VEGF dimer-ligand binding, VEGFR-2 homodimerizes and induces cross-phosphorylation. Active VEGFR-2 sparks downstream signaling that can induce endothelial cell proliferation, migration, and vascular permeability. Soluble VEGF signals differently than matrix-bound VEGF. Mice expressing only the soluble VEGF isoform 120 have less vascular branching during embryo- genesis, and more than half succumb to death as neonates.[44] Similarly, blood vessels induced by recombinant VEGF113 (made to mimic MMP-cleaved VEGF) had dramatically less branching than those induced by VEGF164. In contrast, VEGF that cannot be

released from the matrix (VEGF Δ108-118) resulted in highly branched vasculature with a high density of thin vessels.[41] Similar findings were obtained using tumor cells that overexpressed VEGF113, 164, or Δ108-118.[41] These data demonstrate that soluble VEGF appears to be responsible for increasing the girth of vessels, while bound VEGF signaling influences vessel branching.

Recently, we have shown that the difference in human umbilical vein endothelial cell response to bound versus soluble VEGF can be explained by divergent downstream signaling pathways.[42] Both soluble and collagen matrix–bound VEGF can bind VEGFR-2 through the amino acids encoded by VEGF exons 2 to 5 and activate the receptor as measured by tyrosine 1175 phosphorylation. However, several differences exist in the nature of the signal and downstream activation. In particular, prolonged phosphorylation of VEGFR-2 at tyrosine 1214 is specifically found when VEGF is bound to matrix. Both soluble and collagen-bound VEGF can lead to phosphorylation of the secondary messengers p38MAPK and Akt; but collagen matrix–bound VEGF leads to prolonged p38MAPK activation, while soluble VEGF causes prolonged Akt activation. Interestingly, matrix-bound VEGF stimulates VEGFR-2 clustering and association with β1-integrin at focal adhesions. Inhibition of β1-integrin dampens the prolonged phosphorylation at VEGFR-2 Y1214, p28MAPK phosphorylation, and the levels of internalization of VEGFR-2. This implies that collagen-bound VEGF bridges the β1-integrin association with VEGFR-2 and that this interaction is responsible for the divergent signaling pathways. Thus, association of VEGF with the ECM brings VEGFR-2 in proximity to β1-integrin, which recruits an additional set of secondary messengers to be activated. These data suggest a mechanism for the differential cellular response to soluble versus bound VEGF. Alterna- tive to or in addition to this pathway is the signaling pathway downstream of the VEGF coreceptor Neuropilin-1, which also binds to this C-terminal domain of VEGF.

VEGF/Neuropilin Signaling

The C-terminal domain of VEGF, encoded by exons 7 and 8, mediates binding to the nonreceptor tyrosine kinase Neuropilin-1 (NRP1).[45-47] The role of NRP in vascular development is underscored by the observation that NRP1 null mice die of cardiovascular and neuronal defects between E12 and E13.5.[48] Neuropilin-1 and -2 are trans- membrane glycoproteins expressed in multiple cell types including neurons, cancer cells, smooth muscle cells, and endothelial cells.[49] NRPs are capable of binding at least 2 different ligands: the semaphorins, which inhibit cell migra- tion, and the growth factors like VEGF, PDGF, and HGF that promote cell migration.[50] Because NRP1 and 2 are expressed on both tumor and endothelial cells, it has been demonstrated that Sema3A can be used to target cancer with a dual approach.[30]

The interacting region of NRP with VEGF is distinct from that of semaphorins, and it is mediated via its b1b2 extra- cellular domains.[51,52] NRP1 has a short cytoplasmic tail with a single PDZ- binding domain, but it contains no inherent enzymatic activity, and its ability to signal on its own is not clear at this point.[49] For this reason, NRPs have been considered as co-receptors for VEGF rather than independent receptors. Indeed, NRPs have been shown to enhance VEGF interaction with VEGFR-2.[53] Despite this long-held assumption, the NRP1 cytoplasmic domain is capable of initiating endothelial cell migration.[54] Intracellularly, Synectin/GIPC1/NIP binds to the NRP1 PDZ motif using yeast 2-hybrid studies, and it is necessary for NRP1-mediated endothelial cell migration.[55,56] Further downstream, P130Cas phosphorylation mediates VEGF-induced NRP1-dependent migration of endothe- lial cells.[57] A recent study pinpointed functional relevance to amino acids Y297 and D320 in NRP1. These residues, located in the b1b2 domain, are critical for VEGF binding to NRP1 and neces- sary for VEGF stimulation of endothelial cell migration.[58] In contrast, inhibition of VEGF binding to NRP1 had no effect on VEGFR-2–mediatedendothelialcellpro- liferation and permeability. The emerging theme is that NRPs are relevant to the migratory function initiated downstream of VEGF signaling.

Small molecule inhibitors against NRP1, as well as NRP1-targeting anti- bodies, have shown potential in cancer therapy. In particular, the small molecule EG00229, a VEGF exon 7 and 8 mimetic, is able to compete for VEGF binding to NRP1 and inhibit VEGF- induced endothelial cell migration.[57,59] Coupled with targeted delivery, this molecule holds clinical promise. Along the same lines, an antibody aimed at disrupting the interaction between NRP1 and VEGF yields reduction in pericyte coverage of tumor vessels.[60] Further- more, simultaneous anti-NRP1 and anti- VEGF antibody treatment of tumor xenograft models resulted in inhibition of tumor volume and prolonged survival compared to either agent alone. The authors argue that the removal of pericytes by targeting NRP1 makes the vessels more vulnerable to anti-VEGF treatment.

Notch Signaling Determines Tip Versus Stalk Cell Fate in the Vascular Sprout

Notch signaling regulates the initial pro- cess of vascular sprouting by establish- ing critical differences between leading (tip) and following (stalk) cells. The Notch pathway has been well estab- lished as a regulator of cell fate and homeostasis in multiple settings includ- ing branching morphogenesis in tracheal sprouting and neuronal cell fate.[61,62] Interestingly, sprouting angiogenesis has commonalities with both tracheal sprouting and neuronal development, including sensing and responding to environmental chemotactic and inhibi- tory guidance cues.[63,64]

Notch receptors and ligands are cell- surface single-pass transmembrane pro- teins that can engage in juxtacrine or autocrine signaling.[65] In mammals, there are 4 Notch receptors (Notch 1-4) and 5 ligands (Delta-like 1, 3, and 4 and Jagged 1 and 2). Within the secretory path- way, Notch receptors are cleaved by furin-like convertases into 2 fragments that later associate into a heterodimeric form. Thus, the mature cell surface receptor includes a membrane- spanning domain that is connected to an extracellular domain through noncovalent inter-

actions. Upon ligand binding, the Notch receptor changes conformation of the juxtamembrane region, exposing a pro- tease-sensitive domain to ADAM 10/17 that cleaves the extracellular portion of the receptor. The cleaved Notch extra- cellular domain–ligand complex is endocytosed by the ligand-expressing cell. The Notch intracellular membrane– tethered receptor is further cleaved by γ-secretase, a process that releases the Notch intracellular domain (NICD) from the cell membrane and enables its translocation into the nucleus. There, the NICD acts as a transcription factor, reg- ulating the expression of various target genes like VEGFR-1, 2, and 3 in endo- thelial cells.[66]

Notch activation by Dll4 (Delta-like 4) results in the formation of an angiogenic sprout with 2 distinct types of endothelial cells: tip and stalk cells. The tip cells lack Notch signaling and are responsible for sensing environmental cues through filopodia armed with VEGFR-2.[67] Upon VEGF binding to VEGFR-2, Dll-4 is upregulated via the PI3K/Akt pathway in arterial endothelial cells in vitro.[68] VEGF treatment increases Dll4 in mouse retinas ex vivo.[69] Tip cells and stalk cells closest to migrating front of the mouse retina express more Dll4 than do stalk cells, which express more Notch receptors than do the tip cells.[70] The tip endothelial cells at the leading edge of the vascular plexus receive the most exposure to VEGF and express the most Dll4, which in turn signal to the following endothelial cells to become stalk cells. Because Dll4 haploinsufficiency and pharmacological blockade of Notch signaling (by DAPT treatment) lead to more branching morphogenesis in the developing retina, the default phenotype would appear to be that of a tip cell.[70] Confocal imaging of developing mouse retinas shows that while tip cells are responsible for branching morphogenesis, the stalk cells form the blood-perfused tubes.[67] To accomplish this task, stalk cells must rapidly proliferate to fill in the plexus behind leading tip cells. In fact, the developing mouse retina shows a lack of proliferation in tip cells, in contrast to profuse proliferation by the stalk cells.[67]

The Dll4-Notch cascade also regulates tip/stalk cell specification in tumor angiogenesis. Interestingly, several groups have shown that inhibiting Dll4 signaling paradoxically results in smaller tumors. Injection of Dll4 inhibitory antibodies into several xenograft mouse models yields smaller tumors than control-treated animals.[71] The mechanism by which tumor size was reduced lies in the observation that while there appeared to be more endothelial cells present in the tumor, they were unproductive and unable to form perfused vessels. Furthermore, while the vasculature of tumors overexpressing Dll4 had increased vessel density, they exhibited increased hypoxia due to insufficient vascular perfusion.[72] Given that information, the possibility of targeting Dll4 as a modality of cancer therapy has been explored in preclinical models.[73] However, because Notch signaling is involved in many cellular processes, concerns related to side effects are high. Furthermore, the concept of increasing the number of endothelial cells (tip cells) within a tumor is worrisome. While the presence of the Dll4 antibody would block their intrinsic ability to organize patent vascular tubes, it is likely that a short suppression of therapy might enable the formation of a vascular network, which would no longer be suppressed by antibodies. Additional experiments that explore the consequences of interruption of treatment are warranted.

Angiopoietin/Tie2 Signaling Maintains Vascular Quiescence

VEGF/VEGFR-2 stimulates angiogenesis, and the Dll4/Notch signaling axis controls endothelial tip/stalk cell fate promoting angiogenic growth. Nonetheless, functional vessels require the establish- ment of a quiescent phenotype to stabilize the new vascular network. Active cell signaling is needed to squelch further branching morphogenesis and to maintain homeostatic vessel integrity. Thus, after the establishment of a vascular plexus, a maturation process follows and it includes enhancement of tight junctions, secretion of a basement membrane, and recruitment of perivascular cells. For arteries and veins, this means recruitment of smooth muscle cells; for capillaries and small venules, it represents recruitment of pericytes.[74]

Perivascular (mural) cells join the outer vessel wall through the stimulatory action of PDGFB/PDGFβ, HB-EGF/EGFR/ HER2, HGF/c-Met, seratonin, sphingosine-1 phosphate, and TGF-β signaling.[74-78] The recruitment of mural cells has been studied during development, but it is also relevant to tumor angiogenesis.[79,80] In tumor vessels, the relative density and degree of adhesion of pericytes have been associated with alterations in response to therapy. The greater the number of pericytes and their degree of attachment to the endothelium, the more difficult it is to induce vascular regression. Furthermore, perivascular cells signal to the endothelium to maintain vessel quiescence and regulate permeability. Both perivascular paracrine and endothelial autocrine Tie/angiopoietin (Ang) signaling have been shown to influence quiescence and homeostasis of the vascular plexus.

The Tie/Ang signaling system comprises 2 Ang glycoprotein ligands (Ang-1 and -2) and 2 Tie tyrosine kinase receptors (Tie1 and 2). Tie1 and 2 are mainly, but not exclusively, expressed by endothelial and hematopoietic cells.[81-83] Perivascular cells are the main producers of Ang-1, which once secreted is incorporated into the ECM.[74] Ang-2 is found mainly in endothelial cells, where it is stored intracellularly in Weibel- Palade bodies.[84] Perivascular Ang-1 has been shown to maintain quiescence by promoting endothelial cell survival, inhibition of vascular permeability, inhibition of proinflammatory signaling, and promotion of vascular maturation.[85]

While Ang-1 signaling through Tie2 is thought to have an agonistic effect, the signaling outcome depends on how the ligand is presented to the receptor. Ang-1/Tie2 binding induces distinct signaling complexes when presented in cell-cell versus cell-matrix contexts.[86,87] Endothelial cells engaged in cell-cell contacts show Tie2/Ang-1 in trans-homotypic complexes. In contrast, endothelial cells that are not confluent or forming cell-cell connections showed Tie2 in association with the ECM. These distinct contextual localizations of Tie2 beget strikingly different signaling cascades. While cell-matrix Ang-1/Tie2 interac- tions lead to Erk/MAPK

pathway stimulation, the cell-cell homotypic Ang-2/ Tie2 complexes stimulate PI3K/Akt signaling. Further work demonstrated that Ang-2/Tie2 complex signaling leads to Dll4 expression via AKT-dependent activation of β-catenin and subsequent vessel maturation via basement membrane deposition.[78] Dll4 signaling via Notch induces the tip cell phenotype. Also con- textual, the outcome of Ang-2 signaling through Tie2 is framed by the activation state of the endothelium. For example, Ang-2 activity destabilizes quiescent vasculature by competing with Ang-1 for Tie2 binding.[88] It has also been shown to destabilize the endothelium through an intracrine feedback loop.[89] Conversely, Ang-2 stimulation leads to the phosphorylation and activation of Tie2 and the inhibition of vessel leakage.[90] Less is knownabouttheTie1receptor, but studies have shown that it can be cleaved to generate a soluble form91 and that it can interact with and modulate the signaling ofTie2.[92]

The Ang-2/Tie2 downstream signaling cascade has a role in cancer progression through activation of the endothelium. Interestingly, Tie2 is also expressed in multiple tumor cell types including Kaposi sarcoma, cutaneous angiosarcoma, melanoma, breast cancer, non–small cell lung cancer, hepatocellular carcinoma, prostate cancer, hemangioma, and astrocytoma.[93] Tumor-secreted Ang-2 can destabilize the endothelium and promote more branching morphogenesis. A special class of TAMs, named Tie2-expressing macrophages (TEMs), are able to home to tumors due to the local upregulation of Ang-2. These TEMs nurture tumor angiogenesis[94] and pro- mote endothelial cell survival.[95] Accordingly, efforts are being made to target the Ang-2/Tie2 axis to suppress tumor angio- genesis by targeting these cells and the endothelium as well.[30] In particular, anti–Ang-2 monoclonal antibodies and the pharmacokinetically improved peptide-antibody conjugate called CovX-Bodies have been successful in preclinical trials.[96,97] Furthermore, one such antibody, AMG386, has shown promise in ovarian cancer during phase II clinical trials.[98]

Ephrin/Eph Axis in Arterial/Venous Patterning and Angiogenesis

Ephrin ligands and their Eph receptors generally provide repulsive signals for neurons.[99] They are divided into 2 classes, A and B, based on similarities in structure and binding affinities.[100] For example, class A Eph receptors typically bind all class A ephrin ligands and the same for class B receptors and ligands. However, there are some exceptions: EphA4 binds both class A and class B ephrins, while ephrinA4 binds both class A and class B receptors.[100] The Eph receptors are tyrosine kinases that are activated upon ephrin ligand binding.[101] The ephrin ligands are either GPI anchored (class A) or transmembrane (class B) cell-surface proteins. The Eph/ ephrin receptor is unique, as it can initiate both forward and reverse signaling and, like Notch signaling, results in ligand/receptor endocytosis. Upon receptor/ligand binding, the ligand is cleaved from the cell surface. When the Eph receptors are endocytosed, the ligand goes along for the ride.[102]

The contribution of Eph/ephrin signaling to vascular morphogenesis varies depending on the stage of vascular development, receptor class, and cancer type. Evaluation of reporter-transgenic mice showed EphB4 expression in veins and ephrinB2 in arteries.[103,104] Homologous inactivation studies have shown that both EphB4 and ephrinB2 are critical for vascular development, as ablation of either gene causes embryonic lethality before E11.5.105-107 EphrinB2 expression is controlled by microenvironmental cues like VEGF exposure, smooth muscle cell association, and arterial flow stress.[108,109] Given this and the fact that ephrinB2 and EphB4 tend to result in repulsion, it has been suggested that they define the vascular border. In addition, endothelial studies under culture conditions have revealed that activation of ephrinB2 by EphB4-Fc prevents migration and cell adhesions.[110] Additionally, ephrinB2/ EphB4 appears to regulate the size of arteries and veins.[111] Furthermore, studies have demonstrated that ephrinB2 reverse signaling has a role in vessel maturation by influencing perivascular associations with the endothelium.[112,113] Less is understood about the class A EphA2/

ephrinA1receptorligandpairindevelop- mental angiogenesis. However, ephrinA1 is expressed at sites of developmental angiogenesis, and soluble EphA2-Fc has been shown to inhibit endothelial cell migration, sprouting, survival, and corneal angiogenesis induced by VEGF.[114,115]

Disregulation of the ephrin/Eph molecules is observed in a wide variety of cancers.[116] Furthermore, both the class A ephrinA1 and EphA2 receptors are expressed by the endothelium and by tumor cells.[117,118] Interestingly, hypoxia (a common feature of cancer) induces increased mRNA and protein levels of EphB4, ephrinB2, EphA2, and ephrinA1 in mouse skin.[119] Evidence that the ephrinA1/EphA2 axis plays a role in tumor angiogenesis lies in studies that show that tumors from EphA2 null mice are smaller and less vascularized.[120,121] In addition, injection of soluble EphA2 and EphA3-Fc chimeras into tumor-bearing mice was able to inhibit tumor growth and angiogenesis.[122-124]

Two recent studies revealed a role for ephrinB2 in VEGFR-2 and VEGFR-3 endocytosis with consequences to developmental and tumor angiogenesis.[125,126] Because VEGFR endocytosis is crucial for signaling, loss of ephrinB2 results in less VEGF receptor endocytosis, lower downstream signaling, and decreased tip cell filopodial extension. The net result is lower sprouting in the retina and a decrease in vessels permeating tumors in ephrin-deficient mice. Furthermore, injection of soluble EphA4 extracellular domains into mouse xenograft models of cancer results in reduced tumor size and tumor angiogenesis.[127-129] In addition to their role in tumor angiogenesis, the majority of the studies have focused on the conflicting roles of Eph/ephrin in various types of tumor cells, in some instances promoting and in other times inhibiting tumor cell survival and metastasis.[116] In sum, further work should be done to tease out the nuances of Eph/ ephrin signaling in cancer before using it as a target for cancer therapy.

Slit/Roundabout in Blood Vessel Guidance

Another group of neuronal signaling molecules recently found to modulate developmental and tumor angiogenesis is the Slit ligand/Roundabout (Robo) receptor duo. Mammals express 3 Slit ligands (Slit-1, -2, and -3) and 4 Robo receptors (Robo 1-4), which contribute to the morphogenesis and physiology of a wide variety of tissue types in addition to neurons.[130] Robo1 and Robo4 are the main Robo receptors in angiogenesis. Because our understanding of Robo/Slit signaling in angiogenesis is recent and limited, there exists some controversy surrounding the subject. However, it is clear that as in neuronal development, the Slit/Robo system participates in blood vessel guidance. In addition to its effects in developmental angiogenesis, Robo1 was shown to have a role in tumor neovascularization.[131] In a tumor context, Slit-2 is expressed by tumor cells, while the ligand, Robo1, is present in the endothelium. Slit-2 was shown to induce endothelial cell migration and tube formation in a PI3K-dependent manner.

Discovered within the last decade, Robo4, also known as magic Round- about, is the only Robo receptor exclusively found in the endothelium.[132] Efforts made to further understand the role of Robo4 in blood vessel homeostasis have yielded conflicting results: some studies conclude that Robo4 activation inhibits endothelial cell migration, while others claim that it actually has promigratory effects. Evidence for Robo4 acting to induce endothelial cell migration lies in the findings that soluble Robo4-Fc inhibits both in vitro and in vivo angiogenesis by competing with the ligand for endogenous Robo4.[133] Interestingly, this group also argues that Slit-1 to -3 do not bind the Robo4 receptor, given measurements of weak interactions between purified forms of the two using the BiaCore system (Amersham Biosciences, Pittsburgh, PA). This finding is possibly due to the use of purified recombinant protein interactions in the absence of heparin, which is known to aid in the interaction between Robo and Slit.[134,135] Another investigation into the promigratory role of Robo4 in endothelial cells demonstrates that Slit-2 binds to a Robo1/Robo4 heterodimer, which recruits WASP, leading to Robo4-depen-

dent filopodia formation.[136] Alternatively, there are also data demonstrating that Robo4 inhibits angiogenesis and stabilizes the vasculature.[137] First, the authors showed that Robo4 is expressed predominantly in stalk cells of developing retinas. Next, they used Robo4 knockout mice to show that Robo4 inhibits VEGF-induced migration, tube formation, and permeability. Finally, they show that Slit-2 prevents Robo- mediated oxygen-induced retinopathy. The same group went on to illustrate that Slit/Robo signaling inhibits Arf6, an effector molecule downstream of VEGFR-2, which controls VEGF- induced endothelial cell migration, angiogenesis, and vascular permeability.[138] Interestingly, inactivation of Robo4 in endothelial cells produces more VEGF, has higher levels of activated VEGFR-2, and has increased angiogenic capacity in a mammary fat pad transplant assay.[139] This study also identified smooth muscle cells as the source of Slit-2 and Slit-3 in the developing mammary fat pad, underscoring the relevance of the microenvironment in angiogenesis. Seeking to reconcile the different effects that Slit-2 has on Robo signaling, one group has presented evidence that suggests that ephrinA1 inhibits the normally proangiogenic effects of Slit-2–induced mTORC2-Akt-Rac signaling pathway by inhibiting Akt and Rac.[140] Unfortunately, this article does not address specific Robo receptors. In addition, recent data demonstrate that Robo4 binds and activates Unc5b, inhibits Src signaling downstream of VEGF, and prevents VEGF-induced hyperpermeability and angiogenesis.[141]

Conclusions

The last 20 years of research in vascular signaling have revealed a significant degree of complexity and cross-talk between signaling systems. Not surprisingly, all of the essential players noted to be active in tumor angiogenesis are reiterations of those operational during developmental angiogenesis. Major strides in the last 3 years have been made in clarifying the contribution of “context” in endothelial signaling. Thus, soluble versus matrix-bound VEGF or cell-cell versus cell-matrix activation of Tie2 both result in distinct downstream activation pathways and offer altered cellular responses. In addition, the contribution of inflammatory cells, particularly with respect to the production of matrix metalloproteases and their ability to modify the stroma, cytokines, and responding receptors has also gained visibility. While not currently being considered in the clinic, combination therapies that target tumor macrophages with antiangiogenic therapy might offer significant benefits. Increased knowledge on the contributions of Notch signaling and its ligands has propelled the generation of antibodies for pharmacological blockade of this pathway in cancer. These, now in clinical trials, will offer complementation to the current anti-VEGF therapy and clarify one of the current questions in the field, namely whether inhibition of multiple signaling arms would be more effective than single therapies.

The quest to gain additional depth in the mechanisms that regulate vascular growth in tumors will continue to expand and deliver new ideas for therapeutic exploration. However, a more effective follow-up on how therapy alters tumor vasculature is needed to effectively translate these therapies when resistance to the therapy surfaces in the clinic, as it has with Avastin. Future experiments and more integrated efforts on the evaluation of the therapy at the molecular level will further aid to refine targeted treatments in tumor biology.

Figure 2.1: Tumor Angiogenesis in the Lung

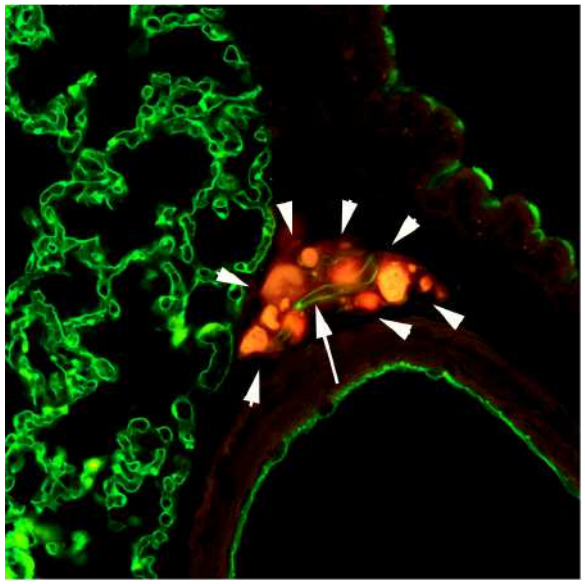

Figure 2.2: Co-option of normal vasculature by tumor cells

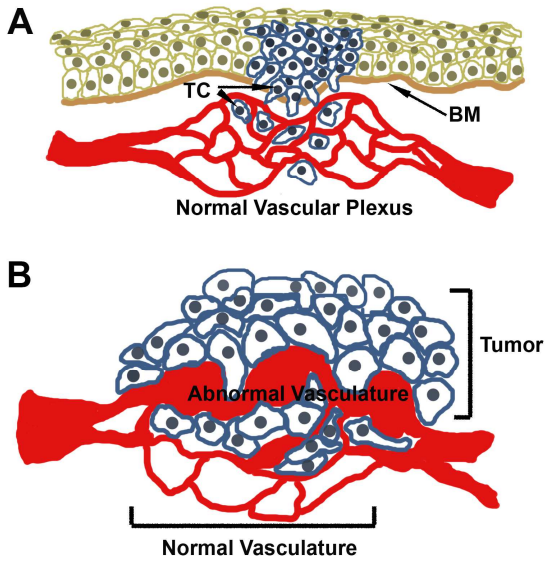

Figure 2.3: Signaling pathways in angiogenesis

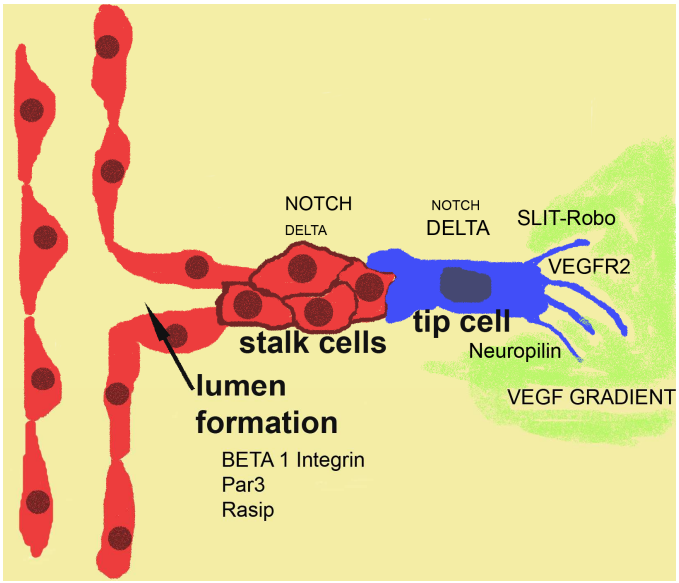

Figure Legends

Figure 2.1: Tumor Angiogenesis in the Lung

Prostate epithelial cells are labeled in red, and vasculature is labeled with anti-PECAM antibody in green. Note the way a very small cluster of tumor cells (white arrowheads) has recruited a single vessel (arrow).

Figure 2.2: Co-option of normal vasculature by tumor cells

(A) Skin carcinoma cells (tumor cells [TC]) are shown migrating across the basement membrane (BM) and associating with the normal vasculature in the dermis in a process known as co-option. **(B)** Over time, co-opted vessels are highly modified by the tumor cells. These tumor vessels exhibit alterations in lumen size, increased permeability, and dysfunctional association with pericytes/smooth muscle cells.

Figure 2.3: Signaling pathways in angiogenesis

The key cellular events associated with tumor angiogenesis are very similar to those described in developmental angiogenesis. A vascular sprout is composed of stalk and tip cells. The distinction between stalk and tip is conveyed by Notch signaling, which is higher in the stalk than in the tip cell. Tip cells received signals from a gradient of VEGF and from the Slit-Robo pathway.

References

1. Hanahan D, Weinberg RA. Hallmarks of cancer: the next generation. Cell. 2011;144:646-74.

2. Chaffer CL, Weinberg RA. A perspective on cancer cell metastasis. Science. 2011;331:1559-64.

3. Egeblad M, Nakasone ES, Werb Z. Tumors as organs: complex tissues that interface with the entire organism. Dev Cell. 2010;18:884-901.

4. Bissell MJ, Hines WC. Why don't we get more cancer? A proposed role of the microenvironment in restraining cancer progression. Nat Med. 2011;17:320-9.

5. Chouaib S, Kieda C, Benlalam H, Noman MZ, Mami-Chouaib F, Ruegg C. Endothelial cells as key determinants of the tumor microenvironment: interaction with tumor cells, extracellular matrix and immune killer cells. Crit Rev Immunol. 2010;30:529-45.

6. Schreiber RD, Old LJ, Smyth MJ. Cancer immunoediting: integrating immunity's roles in cancer suppression and promotion. Science. 2011;331:1565-70.

7. Baglole CJ, Ray DM, Bernstein SH, *et al*. More than structural cells, fibroblasts create and orchestrate the tumor microenvironment. Immunol Invest. 2006;35:297-325.

8. Xing F, Saidou J, Watabe K. Cancer associated fibroblasts (CAFs) in tumor microenvironment. Front Biosci. 2010;15:166-79.

9. Kessenbrock K, Plaks V, Werb Z. Matrix metalloproteinases: regulators of the tumor microenvironment. Cell. 2010;141:52-67.

10. Dvorak HF. Tumors: wounds that do not heal. Similarities between tumor stroma generation and wound healing. N Engl J Med. 1986;315:1650-9.

11. Demaria S, Pikarsky E, Karin M, *et al*. Cancer and inflammation: promise for biologic therapy. J Immunother. 2010;33:335-51.

12. Hanahan D, Folkman J. Patterns and emerging mechanisms of the angiogenic switch during tumorigenesis. Cell. 1996;86:353-64.

13. Leenders WP, Kusters B, de Waal RM. Vessel co-option: how tumors obtain blood supply in the absence of sprouting angiogenesis. Endothelium. 2002;9:83-7.

14. Hillen F, Griffioen A. Tumour vascularization: sprouting angiogenesis and beyond. Cancer Metastasis Rev. 2007;26:489-502.

15. Zhao C, Yang H, Shi H, *et al*. Distinct contributions of angiogenesis and vascular co-option during the initiation of primary microtumors and micrometastases. Carcinogenesis. 2011;32:1143-50.

16. Nagy JA, Chang S-H, Shih S-C, Dvorak AM, Dvorak HF. Heterogeneity of the tumor vasculature. Semin Thromb Hemost. 2010;36:321-31.

17. Chaplin DJ, Olive PL, Durand RE. Intermittent blood flow in a murine tumor: radiobiological effects. Cancer Res. 1987;47:597-601.

18. Nagy JA, Chang SH, Dvorak AM, Dvorak HF. Why are tumour blood vessels abnormal and why is it important to know? Br J Cancer. 2009;100:865-9.

19. Nagy J, Benjamin L, Zeng H, Dvorak A, Dvorak H. Vascular permeability, vascular hyperpermeability and angiogenesis. Angiogenesis. 2008; 11:109-19.

20. Fukumura DAI, Duda DG, Munn LL, Jain RK. Tumor microvasculature and microenvironment: novel insights through intravital imaging in pre- clinical models. Microcirculation. 2010;17:206-25.

21. Harris AL. Hypoxia: a key regulatory factor in tumour growth. Nat Rev Cancer. 2002;2:38-47.

22. Xu L, Fukumura D, Jain RK. Acidic extracellular pH induces vascular endothelial growth factor (VEGF) in human glioblastoma cells via ERK1/2 MAPK signaling pathway: mechanism of low pH-induced VEGF. J Biol Chem. 2002;277:11368-74.

23. Fukumura D, Jain RK. Tumor microenvironment abnormalities: causes, consequences, and strate- gies to normalize. J Cell Biochem. 2007;101: 937-49.

24. Boucher Y, Brekken C, Netti PA, Baxter LT, Jain RK. Intratumoral infusion of fluid: estimation of hydraulic conductivity and implications for the delivery of therapeutic agents. Br J Cancer. 1998;78:1442-8.

25. Boucher Y, Salehi H, Witwer B, Harsh GRt, Jain RK. Interstitial fluid pressure in intracranial tumours in patients and in rodents. Br J Cancer. 1997;75:829-36.

26. Yuan F, Salehi HA, Boucher Y, Vasthare US, Tuma RF, Jain RK. Vascular permeability and microcirculation of gliomas and mammary carcinomas transplanted in rat and mouse cranial windows. Cancer Res. 1994;54:4564-8.

27. Tong RT, Boucher Y, Kozin SV, Winkler F, Hicklin DJ, Jain RK. Vascular normalization by vascular endothelial growth factor receptor 2 blockade induces a pressure gradient across the vasculature and improves drug penetration in tumors. Cancer Res. 2004;64:3731-6.

28. Winkler F, Kozin SV, Tong RT, *et al*. Kinetics of vascular normalization by VEGFR2 blockade governs brain tumor response to radiation: role of oxygenation, angiopoietin-1, and matrix metalloproteinases. Cancer Cell. 2004;6: 553-63.

29. Willett CG, Boucher Y, di Tomaso E, *et al*. Direct evidence that the VEGF-specific antibody bevacizumab has anti-vascular effects in human rectal cancer. Nat Med. 2004;10:145-7.

30. Weick A, Augustin HG. Double attack on tumors by targeting with guidance molecules. Arterioscler Thromb Vasc Biol. 2011;31:721-2.

31. Adams RH, Eichmann A. Axon guidance molecules in vascular patterning. Cold Spring Harb Perspect Biol. 2010;2:a001875.

32. Casazza A, Fu X, Johansson I, *et al*. Systemic and targeted delivery of semaphorin 3A inhibits tumor angiogenesis and progression in mouse tumor models. Arterioscler Thromb Vasc Biol. 2011;31:741-9.

33. Warren CM, Iruela-Arispe ML. Signaling circuitry in vascular morphogenesis. Curr Opin Hematol. 2010;17:213-8.

34. Arroyo AG, Iruela-Arispe ML. Extracellular matrix, inflammation, and the angiogenic response. Cardiovasc Res. 2010;86:226-35.

35. Carmeliet P, Jain RK. Angiogenesis in cancer and other diseases. Nature. 2000;407:249-57.

36. Carmeliet P, Jain RK. Molecular mechanisms and clinical applications of angiogenesis. Nature. 2011;473:298-307.

37. Ferrara N, Mass RD, Campa C, Kim R. Targeting VEGF-A to treat cancer and age-related macular degeneration. Annu Rev Med. 2007;58:491-504.

38. Germain S, Monnot C, Muller L, Eichmann A. Hypoxia-driven angiogenesis: role of tip cells and extracellular matrix scaffolding. Curr Opin Hematol. 2010;17:245-51.

39. Grunewald FS, Prota AE, Giese A, Ballmer- Hofer K. Structure-function analysis of VEGF receptor activation and the role of coreceptors in angiogenic signaling. Biochim Biophys Acta. 2010;1804:567-80.

40. Ferrara N. Binding to the extracellular matrix and proteolytic processing: two key mechanisms regulating vascular endothelial growth factor action. Mol Biol Cell. 2010;21:687-90.

41. Lee S, Jilani SM, Nikolova GV, Carpizo D, Iruela-Arispe ML. Processing of VEGF-A by matrix metalloproteinases regulates bioavailability and vascular patterning in tumors. J Cell Biol. 2005;169:681-91.

42. Chen TT, Luque A, Lee S, Anderson SM, Segura T, Iruela-Arispe ML. Anchorage of VEGF to the extracellular matrix conveys differential signaling responses to endothelial cells. J Cell Biol. 2010; 188:595-609.

43. Evans IM, Yamaji M, Britton G, *et al*. Neuropilin-1 signaling through p130Cas tyrosine phosphorylation is essential for growth factor- dependent migration of glioma and endothelial cells. Mol Cell Biol. 2011;31:1174-85.

44. Ruhrberg C, Gerhardt H, Golding M, *et al*. Spatially restricted patterning cues provided by heparin-binding VEGF-A control blood vessel branching morphogenesis. Genes Dev. 2002;16:2684-98.

45. Soker S, Fidder H, Neufeld G, Klagsbrun M. Characterization of novel vascular endothelial growth factor (VEGF) receptors on tumor cells that bind VEGF165 via its exon 7-encoded domain. J Biol Chem. 1996;271:5761-7.

46. Soker S, Takashima S, Miao HQ, Neufeld G, Klagsbrun M. Neuropilin-1 is expressed by endothelial and tumor cells as an isoform-specific receptor for vascular endothelial growth factor. Cell. 1998;92:735-45.

47. Pan Q, Chathery Y, Wu Y, *et al*. Neuropilin-1 binds to VEGF121 and regulates endothelial cell migration and sprouting. J Biol Chem. 2007;282:24049-56.

48. Kitsukawa T, Shimizu M, Sanbo M, *et al*. Neuropilin-semaphorin III/D-mediated chemorepulsive signals play a crucial role in peripheral nerve projection in mice. Neuron. 1997;19:995-1005.

49. Zachary IC, Frankel P, Evans IM, Pellet-Many C. The role of neuropilins in cell signalling. Biochem Soc Trans. 2009;37:1171-8.

50. Pellet-Many C, Frankel P, Jia H, Zachary I. Neuropilins: structure, function and role in disease. Biochem J. 2008;411:211-26.

51. Mamluk R, Gechtman Z, Kutcher ME, Gasiunas N, Gallagher J, Klagsbrun M. Neuropilin-1 binds vascular endothelial growth factor 165, placenta growth factor-2, and heparin via its b1b2 domain. J Biol Chem. 2002;277:24818-25.

52. Gu C, Limberg BJ, Whitaker GB, *et al*. Charac- terization of neuropilin-1 structural features that confer binding to semaphorin 3A and vascular endothelial growth factor 165. J Biol Chem. 2002;277:18069-76.

53. Soker S, Miao HQ, Nomi M, Takashima S, Klagsbrun M. VEGF165 mediates formation of complexes containing VEGFR-2 and neuropi- lin-1 that enhance VEGF165-receptor binding. J Cell Biochem. 2002;85:357-68.

54. Wang L, Zeng H, Wang P, Soker S, Mukhopadhyay D. Neuropilin-1-mediated vascular permeability factor/vascular endothelial growth factor-dependent endothelial cell migration. J Biol Chem. 2003;278:48848-60.

55. Cai H, Reed RR. Cloning and characterization of neuropilin-1-interacting protein: a PSD-95/Dlg/ ZO-1 domain-containing protein that interacts with the cytoplasmic domain of neuropilin-1. J Neurosci. 1999;19:6519-27.

56. Wang L, Mukhopadhyay D, Xu X. C terminus of RGS-GAIP-interacting protein conveys neuro- pilin-1-mediated signaling during angiogenesis. FASEB J. 2006;20:1513-5.

57. Evans IM, Yamaji M, Britton G, *et al*. Neu- ropilin-1 signaling through p130Cas tyrosine phosphorylation is essential for growth factor- dependent migration of glioma and endothelial cells. Mol Cell Biol. 2011;31:1174-85.

58. Herzog B, Pellet-Many C, Britton G, Hartzoulakis B, Zachary IC. VEGF binding to neuropilin-1 (NRP1) is essential for VEGF stimulation of endothelial cell migration, complex formation between NRP1 and VEGFR2 and signalling via FAK Tyr407 phosphorylation. Mol Biol Cell. 2011;22:2766-76.

59. Jarvis A, Allerston CK, Jia H, *et al*. Small mole- cule inhibitors of the neuropilin-1 vascular endo- thelial growth factor A (VEGF-A) interaction. J Med Chem. 2010;53:2215-26.

60. Pan Q, Chanthery Y, Liang WC, *et al*. Blocking neuropilin-1 function has an additive effect with anti-VEGF to inhibit tumor growth. Cancer Cell. 2007;11:53-67.

61. Ghabrial AS, Krasnow MA. Social interactions among epithelial cells during tracheal branching morphogenesis. Nature. 2006;441:746-9.

62. Louvi A, Artavanis-Tsakonas S. Notch signalling in vertebrate neural development. Nat Rev Neurosci. 2006;7:93-102.

63. Carmeliet P, Tessier-Lavigne M. Common mechanisms of nerve and blood vessel wiring. Nature. 2005;436:193-200.

64. Uv A, Cantera R, Samakovlis C. Drosophila tracheal morphogenesis: intricate cellular solutions to basic plumbing problems. Trends Cell Biol. 2003;13:301-9.

65. Kopan R, Ilagan MXG. The canonical Notch signaling pathway: unfolding the activation mechanism. Cell. 2009;137:216-33.

66. Jakobsson L, Bentley K, Gerhardt H. VEGFRs and Notch: a dynamic collaboration in vascular patterning. Biochem Soc Trans. 2009;37:1233-6.

67. Gerhardt H, Golding M, Fruttiger M, *et al*. VEGF guides angiogenic sprouting utilizing endothelial tip cell filopodia. J Cell Biol. 2003;161:1163-77.

68. Liu Z-J, Shirakawa T, Li Y, *et al*. Regulation of Notch1 and Dll4 by vascular endothelial growth factor in arterial endothelial cells: implications for modulating arteriogenesis and angiogenesis. Mol Cell Biol. 2003;23:14-25.

69. Lobov IB, Renard RA, Papadopoulos N, *et al*. Delta-like ligand 4 (Dll4) is induced by VEGF as a negative regulator of angiogenic sprouting. Proc Natl Acad Sci U S A. 2007;104:3219-24.

70. Hellstrom M, Phng L-K, Hofmann JJ, *et al*. Dll4 signalling through Notch1 regulates for- mation of tip cells during angiogenesis. Nature. 2007;445:776-80.

71. Ridgway J, Zhang G, Wu Y, *et al*. Inhibition of Dll4 signalling inhibits tumour growth by deregulating angiogenesis. Nature. 2006;444:1083-7.

72. Noguera-Troise I, Daly C, Papadopoulos NJ, *et al*. Blockade of Dll4 inhibits tumour growth by promoting non-productive angiogenesis. Nature. 2006;444:1032-7.

73. Thurston G, Noguera-Troise I, Yancopoulos GD. The Delta paradox: DLL4 blockade leads to more tumour vessels but less tumour growth. Nat Rev Cancer. 2007;7:327-31.

74. Gaengel K, Genove G, Armulik A, Betsholtz C. Endothelial-mural cell signaling in vascular development and angiogenesis. Arterioscler Thromb Vasc Biol. 2009;29:630-8.

75. Iivanainen E, Nelimarkka L, Elenius V, *et al*. Angiopoietin-regulated recruitment of vascular smooth muscle cells by endothelial-derived heparin binding EGF-like growth factor. FASEB J. 2003;17:1609-21.

76. Kobayashi H, DeBusk LM, Babichev YO, Dumont DJ, Lin PC. Hepatocyte growth factor mediates angiopoietin-induced smooth muscle cell recruitment. Blood. 2006;108:1260-6.

77. Lindahl P, Johansson BR, Leveen P, Betsholtz C. Pericyte loss and microaneurysm formation in PDGF-B-deficient mice. Science. 1997;277:242-5.

78. Zhang J, Fukuhara S, Sako K, *et al*. Angiopoietin-1/Tie2 signal augments basal Notch signal controlling vascular quiescence by inducing delta-like 4 expression through AKT-mediated activation of beta-catenin. J Biol Chem. 2011; 286:8055-66.

79. Abramsson A, Lindblom P, Betsholtz C. Endothelial and nonendothelial sources of PDGF-B regulate pericyte recruitment and influence vas- cular pattern formation in tumors. J Clin Invest. 2003;112:1142-51.

80. Hellstrom M, Kalen M, Lindahl P, Abramsson A, Betsholtz C. Role of PDGF-B and PDGFR-beta in recruitment of vascular smooth muscle cells and pericytes during embryonic blood vessel formation in the mouse. Development. 1999;126:3047-55.

81. Korhonen J, Polvi A, Partanen J, Alitalo K. The mouse tie receptor tyrosine kinase gene: expres- sion during embryonic angiogenesis. Oncogene. 1994;9:395-403.

82. De Palma M, Venneri MA, Galli R, *et al*. Tie2 identifies a hematopoietic lineage of proangiogenic monocytes required for tumor vessel formation and a mesenchymal population of pericyte progenitors. Cancer Cell. 2005;8:211-26.

83. Dumont DJ, Yamaguchi TP, Conlon RA, Rossant J, Breitman ML. tek, a novel tyrosine kinase gene located on mouse chromosome 4, is expressed in endothelial cells and their presumptive precursors. Oncogene. 1992;7:1471-80.

84. Fiedler U, Scharpfenecker M, Koidl S, *et al*. The Tie-2 ligand angiopoietin-2 is stored in and rapidly released upon stimulation from endothelial cell Weibel-Palade bodies. Blood. 2004;103:4150-6.

85. Augustin HG, Young Koh G, Thurston G, Ali- talo K. Control of vascular morphogenesis and homeostasis through the angiopoietin-Tie sys- tem. Nat Rev Mol Cell Biol. 2009;10:165-77.

86. Fukuhara S, Sako K, Minami T, *et al*. Differential function of Tie2 at cell-cell contacts and cell-sub- stratum contacts regulated by angiopoietin-1. Nat Cell Biol. 2008;10:513-26.

87. Saharinen P, Eklund L, Miettinen J, *et al*. Angio- poietins assemble distinct Tie2 signalling com- plexes in endothelial cell-cell and cell-matrix contacts. Nat Cell Biol. 2008;10:527-37.

88. Maisonpierre PC, Suri C, Jones PF, *et al*. Angiopoietin-2, a natural antagonist for Tie2 that disrupts in vivo angiogenesis. Science. 1997;277:55-60.

89. Scharpfenecker M, Fiedler U, Reiss Y, Augustin HG. The Tie-2 ligand angiopoietin-2 destabilizes quiescent endothelium through an internal autocrine loop mechanism. J Cell Sci. 2005;118: 771-80.

90. Daly C, Pasnikowski E, Burova E, *et al*. Angio- poietin-2 functions as an autocrine protective fac- tor in stressed endothelial cells. Proc Natl Acad Sci U S A. 2006;103:15491-6.

91. Marron MB, Singh H, Tahir TA, *et al*. Regulated proteolytic processing of Tie1 modulates ligand responsiveness of the receptor-tyrosine kinase Tie2. J Biol Chem. 2007;282:30509-17.

92. Yuan HT, Venkatesha S, Chan B, *et al*. Activation of the orphan endothelial receptor Tie1 modifies Tie2-mediated intracellular signaling and cell survival. FASEB J. 2007;21:3171-83.

93. Martin V, Liu D, Fueyo J, Gomez-Manzano C. Tie2: a journey from normal angiogenesis to cancer and beyond. Histol Histopathol. 2008;23:773-80.

94. Lewis CE, Ferrara N. Multiple effects of angiopoietin-2 blockade on tumors. Cancer Cell. 2011;19:431-3.

95. Schubert SY, Benarroch A, Monter-Solans J, Edelman ER. Primary monocytes regulate endo- thelial cell survival through secretion of angio- poietin-1 and activation of endothelial Tie2. Arterioscler Thromb Vasc Biol. 2011;31:870-5.

96. Huang H, Lai J-Y, Do J, *et al*. Specifically targeting angiopoietin-2 inhibits angiogen- esis, Tie2-expressing monocyte infiltration, and tumor growth. Clin Cancer Res. 2011;17: 1001-11.

97. Mazzieri R, Pucci F, Moi D, *et al*. Targeting the ANG2/TIE2 axis inhibits tumor growth and metastasis by impairing angiogenesis and disabling rebounds of proangiogenic myeloid cells. Cancer Cell. 2011;19:512-26.

98. Huang H, Bhat A, Woodnutt G, Lappe R. Tar- geting the ANGPT-TIE2 pathway in malig-nancy. Nat Rev Cancer. 2010;10:575-85.

99. Bashaw GJ, Klein R. Signaling from axon guid- ance receptors. Cold Spring Harb Perspect Biol. 2010;2:a001941.

100. Mosch B, Reissenweber B, Neuber C, Pietzsch J. Eph receptors and ephrin ligands: important players in angiogenesis and tumor angiogenesis. J Oncol. 2010;2010:135285.

101. Heroult M, Schaffner F, Augustin HG. Eph receptor and ephrin ligand-mediated interactions during angiogenesis and tumor progression. Exp Cell Res. 2006;312:642-50.

102. Kuijper S, Turner CJ, Adams RH. Regulation of angiogenesis by Eph-ephrin interactions. Trends Cardiovasc Med. 2007;17:145-51.

103. Gale NW, Baluk P, Pan L, *et al*. Ephrin-B2 selectively marks arterial vessels and neovascularization sites in the adult, with expression in both endothelial and smooth-muscle cells. Dev Biol. 2001;230:151-60.

104. Shin D, Garcia-Cardena G, Hayashi S-I, *et al*. Expression of EphrinB2 identifies a stable genetic difference between arterial and venous vascular smooth muscle as well as endothelial cells, and marks subsets of microvessels at sites of adult neovascularization. Dev Biol. 2001;230:139-50.

105. Adams RH, Wilkinson GA, Weiss C, *et al*. Roles of ephrinB ligands and EphB receptors in cardiovascular development: demarcation of arterial/venous domains, vascular morphogenesis, and sprouting angiogenesis. Genes Dev. 1999;13:295-306.

106. Gerety SS, Wang HU, Chen ZF, Anderson DJ. Symmetrical mutant phenotypes of the receptor EphB4 and its specific transmembrane ligand ephrin-B2 in cardiovascular development. Mol Cell. 1999;4:403-14.

107. Wang HU, Chen ZF, Anderson DJ. Molecular distinction and angiogenic interaction between embryonic arteries and veins revealed by ephrin-B2 and its receptor Eph-B4. Cell. 1998;93:741-53.

108. Korff T, Dandekar G, Pfaff D, *et al*. Endothelial ephrinB2 is controlled by microenvironmental determinants and associates context-dependently with CD31. Arterioscler Thromb Vasc Biol. 2006;26:468-74.

109. le Noble F, Moyon D, Pardanaud L, *et al*. Flow regulates arterial-venous differentiation in the chick embryo yolk sac. Development. 2004;131:361-75.

110. Fuller T, Korff T, Kilian A, Dandekar G, Augus- tin HG. Forward EphB4 signaling in endothelial cells controls cellular repulsion and segregation from ephrinB2 positive cells. J Cell Sci. 2003;116:2461-70.

111. Kim YH, Hu H, Guevara-Gallardo S, Lam MT, Fong SY, Wang RA. Artery and vein size is balanced by Notch and ephrin B2/EphB4 during angiogenesis. Development. 2008;135:3755-64.

112. Foo SS, Turner CJ, Adams S, *et al*. Ephrin-B2 controls cell motility and adhesion during blood- vessel-wall assembly. Cell. 2006;124:161-73.

113. Salvucci O, Maric D, Economopoulou M, *et al*. EphrinB reverse signaling contributes to endo- thelial and mural cell assembly into vascular structures. Blood. 2009;114:1707-16.

114. Cheng N, Brantley DM, Liu H, *et al*. Blockade of EphA receptor tyrosine kinase activation inhibits vascular endothelial cell growth factor-induced angiogenesis. Mol Cancer Res. 2002;1:2-11.

115. McBride JL, Ruiz JC. Ephrin-A1 is expressed at sites of vascular development in the mouse. Mech Dev. 1998;77:201-4.

116. Pasquale EB. Eph receptors and ephrins in cancer: bidirectional signalling and beyond. Nat Rev Cancer. 2010;10:165-80.

117. Ogawa K, Pasqualini R, Lindberg RA, Kain R, Freeman AL, Pasquale EB. The ephrin-A1 ligand and its receptor, EphA2, are expressed during tumor neovascularization. Oncogene. 2000;19:6043-52.

118. Walker-Daniels J, Hess AR, Hendrix MJ, Kinch MS. Differential regulation of EphA2 in normal and malignant cells. Am J Pathol. 2003;162:1037-42.

119. Vihanto MM, Plock J, Erni D, Frey BM, Frey FJ, Huynh-Do U. Hypoxia up-regulates expression of Eph receptors and ephrins in mouse skin. FASEB J. 2005;19:1689-91.

120. Fang WB, Brantley-Sieders DM, Parker MA, Reith AD, Chen J. A kinase-dependent role for EphA2 receptor in promoting tumor growth and metastasis. Oncogene. 2005;24:7859-68.

121. Brantley-Sieders DM, Fang WB, Hicks DJ, Zhuang G, Shyr Y, Chen J. Impaired tumor microenvironment in EphA2-deficient mice inhibits tumor angiogenesis and metastatic progression. FASEB J. 2005;19:1884-6.

122. Brantley DM, Cheng N, Thompson EJ, *et al*. Soluble Eph A receptors inhibit tumor angiogenesis and progression in vivo. Oncogene. 2002;21:7011-26.

123. Dobrzanski P, Hunter K, Jones-Bolin S, *et al*. Antiangiogenic and antitumor efficacy of EphA2 receptor antagonist. Cancer Res. 2004;64:910-9.

124. Cheng N, Brantley D, Fang WB, *et al*. Inhibition of VEGF-dependent multistage carcinogenesis by soluble EphA receptors. Neoplasia. 2003;5:445-56.

125. Sawamiphak S, Seidel S, Essmann CL, *et al*. Ephrin-B2 regulates VEGFR2 function in developmental and tumour angiogenesis. Nature. 2010;465:487-91.

126. Wang Y, Nakayama M, Pitulescu ME, *et al*. Ephrin-B2 controls VEGF-induced angiogenesis and lymphangiogenesis. Nature. 2010; 465:483-6.

127. Kertesz N, Krasnoperov V, Reddy R, *et al*. The soluble extracellular domain of EphB4 (sEphB4) antagonizes EphB4-EphrinB2 inter- action, modulates angiogenesis, and inhibits tumor growth. Blood. 2006;107:2330-8.

128. Martiny-Baron G, Korff T, Schaffner F, *et al*. Inhibition of tumor growth and angiogenesis by soluble EphB4. Neoplasia. 2004;6:248-57.

129. Djokovic D, Trindade A, Gigante J, *et al*. Combination of Dll4/Notch and Ephrin-B2/ EphB4 targeted therapy is highly effective in disrupting tumor angiogenesis. BMC Cancer. 2010;10:641.

130. Liao WX, Wing DA, Geng JG, Chen DB. Perspectives of SLIT/ROBO signaling in placental angiogenesis. Histol Histopathol. 2010;25:1181-90.

131. Wang B, Xiao Y, Ding B-B, *et al*. Induction of tumor angiogenesis by Slit-Robo signaling and inhibition of cancer growth by blocking Robo activity. Cancer Cell. 2003;4:19-29.

132. Huminiecki L, Gorn M, Suchting S, Poulsom R, Bicknell R. Magic roundabout is a new member of the roundabout receptor family that is endothelial specific and expressed at sites of active angiogenesis. Genomics. 2002;79:547-52.

133. Suchting S, Heal P, Tahtis K, Stewart LM, Bicknell R. Soluble Robo4 receptor inhibits in vivo angiogenesis and endothelial cell migration. FASEB J. 2005;19:121-3.

134. Fukuhara N, Howitt JA, Hussain SA, Hohenester E. Structural and functional analysis of slit and heparin binding to immunoglobulin-like domains 1 and 2 of Drosophila Robo. J Biol Chem. 2008;283:16226-34.

135. Legg JA, Herbert JM, Clissold P, Bicknell R. Slits and Roundabouts in cancer, tumour angiogenesis and endothelial cell migration. Angiogenesis. 2008;11:13-21.

136. Sheldon H, Andre M, Legg JA, *et al*. Active involvement of Robo1 and Robo4 in filopodia formation and endothelial cell motility mediated via WASP and other actin nucleation-promoting factors. FASEB J. 2009;23:513-22.

137. Jones CA, London NR, Chen H, *et al*. Robo4 stabilizes the vascular network by inhibiting pathologic angiogenesis and endothelial hyper- permeability. Nat Med. 2008;14:448-53.

138. Jones CA, Nishiya N, London NR, *et al*. Slit2- Robo4 signalling promotes vascular stability by blocking Arf6 activity. Nat Cell Biol. 2009;11:1325-31.

139. Marlow R, Binnewies M, Sorensen LK, *et al*. Vascular Robo4 restricts proangiogenic VEGF signaling in breast. Proc Natl Acad Sci U S A. 2010;107:10520-5.

140. Dunaway CM, Hwang Y, Lindsley CW, *et al*. Cooperative signaling between Slit2 and Ephrin-A1 regulates a balance between angiogenesis and angiostasis. Mol Cell Biol. 2011;31:404-16.

141. Koch AW, Mathivet T, Larrivee B, *et al*. Robo4 maintains vessel integrity and inhibits angiogenesis by interacting with UNC5B. Dev Cell. 2011;20:33-46.

Chapter 3:

Endothelial Cell Homeostasis is Disrupted by Mutations in Signaling Pathways Controlling the Cytoskeleton and Cell Surface Receptors

Abstract

After development has been completed, endothelial cells, which line the blood and lymphatic vessels, are normally quiescent. Their main functions are to regulate the exchange of oxygen, metabolites, and trafficking of cells between the circulating blood and the underlying tissue, processes critical to the physiology of the organism. However, there are instances when endothelial cells break their dormancy and become proliferative, migratory, and/or lose their barrier function. Vascular anomalies are a class of pathology in which endothelial disruption leads to vascular malformations and endothelial cell tumors. While linkage analysis has been critical to identify the etiology of heritable vascular anomalies, the mechanisms that trigger the onset of the vast majority of anomalies, remains elusive, particularly when the mutations are somatic in nature. Here we present a mouse model for the identification of mutations contributing to the pathogenesis of spontaneous vascular anomalies. We performed a transposon mediated forward genetic screen to induce vascular anomalies followed by the identification of genetic insertions associated with those lesions. In doing so we were able to identify approximately 100 genes associated with vascular anomalies in mice, discover novel regulatory pathways in endothelial cell homeostasis, confirm causation of a subset of those genes, find mutations in those genes in human vascular anomaly samples, and ultimately gain a more discerning understanding of the mechanisms of endothelial cell physiology.

Introduction

The endothelial cell is a specialized type of epithelial cell that lines the blood and lymphatic vessel walls to provide a normally quiescent and stable barrier that tightly regulates the passage of small molecules between the blood and tissue parenchyma. The term "vascular anomaly" describes a set of pathologies that are characterized by abnormal vascular morphology or endothelial cell proliferation. They manifest as malignant tumors, fragile brain blood vessels that are prone to hemorrhage, facial and limb disfigurations, and skin discolorations. Familial linkage analysis has been crucial in demonstrating the genetic basis of a subset of vascular anomalies that are inherited. Known genetic mutations include those in *TIE2/TEK* and *Glomulin* (venous anomalies); *RASA1, KRIT1/CCM1, Malcavernin/CCM2,* and *PDCD10/CCM3* (capillary anomalies); *ENG, ALK1,* and *SMAD4* (arterial/combined anomalies); and *VEGFR3/FLT4, FOXC2,* and *SOX18* (lymphatic anomalies)[1].

Unfortunately, the majority of vascular anomalies form spontaneously and little information has been obtained to uncover the genetic mutations that cause these non-inherited lesions. One method to identify the genetic causation underlying spontaneous vascular anomalies is to perform exome sequencing on human vascular anomaly tissue. This approach is limited by factors such as sample availability and non-endothelial variant mutations and is overwhelmed by the shear number of genetic variants that may or may not be causative.

To overcome these challenges, we have chosen to model vascular anomalies in mice using an endothelial specific forward genetic screen. Sleeping Beauty transposon mutagenesis has previously been used to model blood and solid cancers and has aided in the identification of novel causative genes in leukemia (*Csf2*), colorectal cancer (miR-181a-2, 181b-2), hepatocellular carcinoma (miR-370), skin squamous cell carcinoma (*Zmiz1*, *Ppp1r3c*), and glioma (*Csf1*) (Howell 2012). By using VE-Cadherin driven Cre-recombinase, we restricted the transposase enzyme activity specifically to endothelial cells and performed two separate screens (VEC-Cre;T2/Onc2 and VEC-Cre;T2/Onc3). The transposons contain a viral

promoter/enhancer (T2/onc2: MSCV and T2/onc3: CMV) and truncation sequences that, when spliced into the mRNA of a gene, can cause overexpression or premature truncation of causative proteins. In this way, both gain- and loss-of-function mutations can be associated with specific lesions.

In this study, we showed the range of vascular anomaly phenotypes created from our endothelial specific *in vivo* forward genetic screen. Overall we have identified the genetic mutations associated with these lesions and through this process highlighted the cellular pathways that maintain endothelial cell homeostasis. Importantly, we investigated overlaps between the genetic mutations found in the mouse and in the exome sequencing data from human vascular anomaly samples. Finally, we performed independent validation studies using endothelial genetic overexpression and knockdown assays that show causation of *PDGFRB* and *FNDC3B* in endothelial cell dysfunction. In this way, we have identified previously unknown genetic mutations in endothelial cells that cause vascular anomalies.

Results

In vivo endothelial cell mutagenesis induces vascular anomalies in adult mice.

The advantages of using an endothelial specific forward genetic screen to identify mutations that cause vascular anomalies were several: to spontaneously model a broad range vascular anomalies, to maximize the total number of samples analyzed, to focus specifically on mutations in the endothelium, and distinguish potential driver over passenger mutations. To execute this screen, we first bred VE-Cadherin-Cre; Rosa26-LacZ mice to either Sleeping Beauty transposase mice containing either the T2/onc2 or T2/onc3 transposable element (Figure 3. 1A). Inclusion of the T2/onc2 (MSCV) transposon yielded a cohort of animals in which 22.4% (n=17) developed vascular anomalies, while the cohort with the T2/onc3 (CMV) transposon induced 58.9% (n= 53) of the animals to develop vascular anomalies (Figure 3. 1B). T2/onc2 animals with vascular tumors had a mean survival of 262 days, while T2/onc3 animals had a slightly longer mean survival of 362 days (Figure 3. 1C). The T2/onc2 transposon cause vascular anomalies most often in muscle and subcutaneous fat (Figure 3. 1D, G (second row), H). While the T2/onc3 animals also often developed vascular anomalies in subcutaneous fat, the most common site of lesion development was the uterus of female mice (Fig 1E, G (first row), H). The T2/onc3 cohort had a greater variety of organ beds affected and more lesions present per animal (Figure 3. 1D-F). All lesions were vascular in nature.

Spontaneously generated vascular anomalies included tumors and malformations.

To better characterize the type of vascular anomalies created in the two screens, we assessed tissue morphology and performed histological analysis to characterize the cellular basis of the lesions. Upon microscopic analysis, it became clear that the vascular anomalies modeled by the T2/onc2 and T2/onc3 screens mirrored the tissue morphology of human vascular tumors and vascular malformations, respectively. T2/onc2 lesions more often contained large solid masses of endothelial cells, while T2/onc3 lesions were more

characterized by enlarged vascular cavernous spaces surrounded by varying layers of endothelial cells (Figure 3. 2A-C). VE-Cadherin-Cre/LacZ lineage tracing of the vascular anomalies from both cohorts demonstrate that lesions were endothelial in origin (Figure 3. 2A). CD31 staining was used to further confirm the endothelial character of the lesions and Ki67 staining showed that the endothelial cells comprising the tumors were actively proliferating (Figure 3. 2B-C).

gCIS analysis identified novel genes associated with vascular anomalies

Because the promoter of the T2/onc2 and T2/onc3 mice differed, we were curious to know if this had an influence on the average number of gCIS per lesion and the predicted type of mutations generated. The T2/onc2 and T2/onc3 cohorts also differed in the number of transposable DNA elements. The T2/onc2 contained 200 transposons on chromosome 4, while the T2/onc3 cohort contained 11 transposons on chromosome 9. This is reflected in differences in number of total tranposon hits per chromosome per cohort (Figure 3. 3G), the number of insertions per lesion per chromosome (Figure 3. 3H-I), and the total number of insertions per lesions when comparing the two cohorts (there were 3.6x as many in onc2) (Figure 3. 3A). Interestingly, despite these differences in genetic background and transposable element mutagenic capacity, the average number of significant gene centric insertions (gCIS) was about 4.5 in both cohorts of lesions (Figure 3. 3B). Transposon orientation and distribution throughout a specific gene could predict whether gain- or loss-of-function mutations were being created. Given this, it is also interesting to note that the majority of mutations were loss-of-function in both cohorts (Figure 3. 3C,D inset). The onc2 screen showed 57% LOF and 36% GOF predicted gCIS with only 7% undetermined. Onc3 showed 78% LOF and 33% GOF predicted gCIS. Of the 28 onc2 gCIS, the predicted gain-of-function mutations in the *Pdgfrb* gene were most commonly associated with vascular anomalies (Figure 3. 3C). Other top gCIS from the

T2/onc2 cohort included *Erg*, *Zfp521,* and *Arid2* (Figure 3. 3E). For the onc3 screen, loss-of-function mutations in the *Rasa1* gene were most commonly associated with vascular anomalies out of the 80 gCIS identified (Figure 3. 3D). The next most common onc3 genes were *Skint5*, *Lrch1*, *Nf1*, and *HRas* (Figure 3. 3F).

Endothelial cell homeostasis is disrupted by mutations in signaling pathways controlling the cytoskeleton and cell surface receptor signaling

In order to better understand the normal cellular signaling pathways governing endothelial cell homeostasis, we asked which cellular pathways were disrupted in association with vascular anomalies. To do this we assessed which pathways were enriched by the gCIS found in the vascular anomalies generated from our screen. Two common themes could be drawn from the affected pathways and these included cytoskeleton and receptor signaling cascades (Figure 3. 4A). The affected pathways related to the cytoskeleton included focal adhesions, axon guidance, regulation of actin cytoskeleton, gap junctions, and endocytosis. The other common theme among the affected pathways was cell signaling: chemokine signaling, VEGF signaling, and ErbbB signaling. In addition, the gCIS populated pathways previously recognized to be involved with other cancers: glioma, melanoma, prostate cancer, endometrial cancer, and renal cell carcinoma. Pathway visualization shows how the gCIS from both onc2 and onc3 screens populate the cytoskeletal regulatory (Figure 3. 4B) and cancer regulatory pathways (Figure 3. 4C).

To assess how the gCIS from our screen might be interacting to create vascular anomalies from the perspective of the whole lesion, we visually represented the co-occurrence of having two genes in the same lesion. For the onc2 screen we can see that there are strong co-occurrences between *Pdgfrb and Arid2, App and Arid2, 2610307P16Rik and Pdgfrb,*

2610307P16Rik and Arid2, as well as between Zfp521 and Zfp608 (Figure 3. 4D). For the onc3 screen we can see strong co-occurrences between *Rasa1* and *Kdr*, *Rasa1* and *Nf1*, *Rasa1* and *Skint5*, *Rasa1* and *Flt1*, *Rasa1* and *Met*, and *Rasa1* and *Nfib*. This was not suprising as *Rasa1* was the most frequently mutated gene (Figure 3. 4E). There were also some notable onc3 gCIS co-occurrences between *Ptprm* and *Wnk1*, *Nf1* and *Foxj3*, *Nfib* and *Fli1*, *Nf1* and *Hras1*, and *Nf1* and *Elmo1* (Figure 3. 4E).

Some endothelial beds are more frequently affected by specific genetic mutations

The three most common sites for occurrence of vascular tumor formation were muscle (T2/onc2), subcutaneous fat (T2/onc2 and onc3), and uterus (T2/onc3). Since it is known that different vascular beds differ functionally and morphologically, we wondered if the mutational signature of the vascular anomalies differed in these distinct vascular beds. Indeed certain mutations occurred proportionally more often in vascular anomalies derived from specific endothelial beds (Figure 3. 5). From the onc2 screen, the gCIS occurring most often in association with muscle lesions (>60%) were *Pdgfrb, Arid2, Rarg, App, Eras, Rasa1, Rictor, Sh3pxd2a*, and *Slk* (Figure 3. 5A). Also from the onc2 screen, the gCIS occurring most often in association with adipose-based-lesions (perigonadal, visceral, subcutaneous, and brown) included: *4931406P16Rik, Ctif, Kalrn, Kmt2c, Pcsk6, Phlpp1, Ppp6r3, Tbl1x*, and *Tcf4* (Figure 3. 5A). From the onc3 screen, the gCIS occurring most often in association with uterus were: *Rasa1, Nfib, Flt1, Ppp6r3, Elmo1, Wac, Pten, Hdac4, Smek1, 2010111I01Rik, Ift140, Birc6, Top1*, and *Foxj3* (Figure 3. 5B). gCIS from the onc3 screen occurring most often with fat were: *Egr2, Meox2, Magi1, Pdgfrb, Ttc28, Taok1, Rnf144a, Nedd9, Stk3, Hnrnpm, Sos1, 9430020K01Rik, Ubr3, Pdgfra, Ankrd11, Hook3, Stox2*, and *Tmem164* (Figure 3. 5B).

***In vitro* validation demonstrates the role of Fnd3cb and Pdgfrb in endothelial dysfunction**

Predicted LOF mutations in *Fndc3b* were found in association with some of the more aggressive vascular anomaly lesions from the onc3 screen (Figure 3. 6A, left). Complementary histology shows that the lesion is comprised of large cavernous spaces (Figure 3. 6A, right). Distribution of transposons in either orientation through the gene (4 insertions found in 4 different lesions) was indicative of a LOF function phenotype (Figure 3. 6B). Previous reports suggest that increased Fndc3b decreased prostate cancer cell migration and repression of Fndc3b increased hepatocellular carcinoma migration and melanoma cell migration [2-4], so we decided to test if knocking down Fndc3b in endothelial cells (HUVECs) increased migration. Knockdown efficiency is quantified by mRNA expression (Figure 3. 6C) and protein Western blot (Figure 3. 6D). Knockdown of Fndc3b lead to a more elongated cell morphology (Figure 3. 6E). As hypothesized, siFndc3b treated HUVECs migrate faster than siScrmb control cells in a wound migration assay (Figure 3. 6F).

Predicted GOF mutations in Pdgfrb were associated with highly aggressive and solid (in contrast to cavernous) endothelial tumors frequently found in skeletal muscle. Figure 3. 6G (left) shows the rear leg muscle of an animal to be completely overtaken by the vascular tumor. Histological analysis shows invasion of endothelial cells into to the muscle fibers (Figure 3. 6G, right). Figure 3. 6H shows that transposons were clustered near the beginning of the gene, all in the direction of gene transcription (suggesting GOF phenotype). Several reports in the literature show associations between Pdgfrb expression and canine angiosarcoma [5-7], while treatments with Imatinib and Dasatinib (which target Pdgfrb) slowed angiosarcoma growth [8]. Furthermore, there is evidence of PDGFRB and its ligands in cerebral arteriovenous and cavernous malformations [9]. Reports show that PDGFRB is important for lymphatic endothelial cell migration in a tumor lymphangiogenesis model as reduced expression resulted in less migration toward PDGF-BB [10]. Thus we predicted that *Pdgfrb* overexpression in HUVECS would result in more migration. In support of our hypothesis, HUVECS expressing *Pdgfrb*

migrate faster when cultured in media containing PDGF-BB in a wound-healing assay (Figure 3. 6J). Biochemical analysis confirms that *Pdgfrb* overexpression results in phosphorylation in response to PDGF-BB, and downstream activation of Akt and Erk (Figure 3. 6I).

Viewing exome sequencing data through the lens of mouse gCIS identified novel candidate driver mutations in human vascular anomalies

In order to assess the genetic mutations underlying human vascular anomalies, we selected 15 human samples. These specimens were aimed at surveying a variety of vascular anomaly subtypes and included angiosarcoma, hemangioma, lymphangioma, venous malformations, ateriovenous malformations, hemangioendothelioma, and kaposiform hemagioendothelioma. Mutations in gCIS genes were filtered to only consider those that occurred in the ExAC database at a frequency of less than 1%. Since vascular anomalies are rare in the population, we highlighted mutations that were less that 0.1% in light blue and those that occurred 0% in the ExAC database in red. Those occurring between 0.1% and 1% are in dark blue. Protein damage predictions were made using CADD C and Polyphen scores. Those with CADD C scores above 15 and Polyphen scores close to 1 are italicized. The majority of these mutations were likely somatic, as reads percentages were around 50%. Of the known mutated genes associated with human vascular anomalies, only mutations in *CCM2, FLT4, and TEK* were seen in these samples (Figure 3. 7A and B). Translation start-site mutation was found in *CCM2*, a protein kinase domain mutation was seen in *FLT4*, while a mutation in the FN repeats domain was seen in *TEK*.

In validation of our screen, mutations were found in 25 of the gCIS genes in the human samples. Missense and stop-gained mutations in *KMT2C (Lysine-specific methyl transferase 2C)* were found more preferentially in vascular malformations (AVM, VM, Lymphangioma, H w/ AVM) as compared to the vascular tumors (Figure 3. 7C). Other genes preferentially mutated in

association with vascular malformations included *NEDD9, ROCK1, KALRN, CDK13, WNK1, RSF1, PDGFR1, MAPKAP1, PTPRM, MLLT10, PDGFRB, MAGI1, SOS1,* and *ZMIZ1*. Genes found to be mutated preferentially in tumors (A, HE, and KHE) were *EPC2, KDR, ANKRD11, MAP3K3, BURC6, IFT140, SEMA6A, MACF1, SH3PXD2A, AND WWC2*. Damaging mutations were seen in a subset of genes in Figure 3. 7D: mutations near regulatory serine residues in *MAP3K3;* in zinc finger binding domain of *KMT2C,* including a stop-gain mutation; in the transmembrane and cytoplasmic domains of *KDR*; in the protein kinase domain of *PDGFRB*, in the phosphatase domain of *PTPRM*, in the proline rich domain of *ZMIZ1*, in the protein kinase domain of *CDK13*, and in the Src family substrate domain of *NEDD9*. In some cases, acquired mutations were detected in *KALRN* and *KMT2C* in AVM tissue versus blood from one patient (Figure 3. 7E). Also, an acquired mutation in *IFT140* was detected in one tumor compared to another from a patient with multifocal hemangioendothelioma (Figure 3. 7F). Interestingly, we detected a *PDGFRB* missense mutation in a human lymphangioma sample (Figure 3. 6C-D).

Discussion

Endothelial cells, which line the blood and lymphatic vessels are quiescent under normal physiological conditions. However, in instances of wound healing and in the context of tumor biology, endothelial cells can be induced to undergo a proliferative and migratory phenotype that can result in angiogenesis [11,12]. Vascular anomalies are a rare class of diseases, which include vessel malformations or tumors that are comprised of endothelial cells [13,14]. We performed this study with the goal of not only expanding our understanding regarding the underlying cause of somatically-derived vascular anomalies, but we also hoped to learn what keeps the endothelial cells highly resistant to transformation. It is often helpful to understand the normal function of a cell by investigating the mechanism of the pathological state.

Genetic screens have been used in the past to dissect critical cellular processes in Drosophila, yeast, zebrafish, and mouse [15-18]. Here we proposed to understand the pathways critical to endothelial homeostasis by performing a forward genetic screen in endothelial cells *in vivo*. We utilized the Sleeping Beauty transposon platform, which has been very successful at identifying novel genes in association with various solid cancers and leukemia [19-22]. More specifically, we used VEC-Cre to release mutagenesis specifically in endothelial cells to model vascular anomalies in a murine system. The DNA from these endothelial-based lesions were then sequenced and the exact location of the transposon was detected. In this way, we were able to discover approximately 100 genes in association with 110 vascular anomaly samples.

We then went further to validate the ability of the predicted GOF and LOF mutations in association with the vascular anomalies. The screen was self-validating in that we were able to identify insertions in *Rasa1* (p120RasGap), *Nf1, HRas1, Pcdc10* (CCM3) which have been previously known to be associated with or causative of vascular anomalies (Table 3.1). *RASA1* is well documented to be associated with human CM-AVM (capillary malformation-arteriovenous malformation) through linkage analysis studies [23,24], mouse models demonstrate its role in developmental angiogenesis and blood and lymphatic EC homeostasis [25-27], and *in vitro* fibroblast studies point to the role of Rasa1 in cytoskeletal regulation and motility [28-32]. Although most commonly known as one of the causative genes in neurofibromatosis, *NF1* has also been previously implicated in endothelial cell dysfunction through knockout mouse and zebrafish studies [25,33-35] and *in vitro* studies in endothelial cell proliferation [36]. Mutations have been found in angiosarcoma samples [37] and vascular anomalies and vasculopathy are found in patients with neurofibramatosis caused by NF1 mutations [38-43]. *HRas1* has been associated with the benign vascular tumor pyogenic granuloma [44]. Vascular anomalies are also found in patients with various syndromes caused by mutations in the gCIS we have identified: Proteus-like syndrome, Cowden syndrome, and Bannayan-Riley-Ruvalcaba syndrome (*PTEN*) with AVM [45-47] , Costello Syndrome (*HRAS1*)[48], and Noonan syndrome (*SOS1*) with pulmonary

arteriovenous fistulas and lymphatic abnormalities [49,50]. *PCDC10* (CCM3) is one of three currently known genes that when mutated cause cerebral cavernous malformations [51,52]. CCM3 binds to in complex with CCM1 and CCM2 to adhesion molecules to regulate cell-cell contacts and also sits in the STIPAK comlex with Stk24 and Mst4 to regulate endothelial cell migration [53].

Importantly, the value of this study was that we were able to also identify new genes associated with the emergence of vascular anomalies and endothelial cell dysfunction. The vast majority of the gCIS from our screen are to date unlinked with vascular anomalies. Here, we chose to validate two of those genes in isolation: Fndc3b and Pdgfrb. These choices were based on the severity of the lesions with which it was associated and previous findings in the literature that hint towards their role in vascular anomalies. LOF of Fndc3b was the first thing we tested in an in vitro migration assay. In accordance with our hypothesis, knockdown of Fndc3b in endothelial cells increased migration in a wound healing away. Interestingly, studies looking for a fourth CCM (cerebral cavernous malformation) locus identified a region in human chromosome 3q26.3–27.2 in which it is predicted to be found [54]. We discovered the predicted LOF gene *Fndc3b* to be located in this region and decided to tests its effects on endothelial function. Pdgfrb protein expression by immunohistochemistry had been detected in angiosarcoma samples from canine and human [5,6]. RNA analysis of human cerebral arteriovenous malformations demonstrate increased expression of Pdgfrb [55]. Interestingly, Pdgfrb falls in the 5q31.3-32 region predicted to contain the currently unidentified HHT3 gene [56]. A predicted LOF gCIS from our screen that falls in this region is Nr3c1, which codes for the glucocorticoid receptor. In our screen, predicted GOF mutations in Pdgfrb was heavily associated with solid endothelial tumors. We therefore tested the migration in response to PDGF-BB of endothelial cells overexpressing *Pdgfrb* and found indeed that those cells expressing the receptor had a migratory phenotype. This was found to coincide with increased p-Akt and p-Erk signaling, which are known to mediate survival and proliferation in endothelial cells.

One major finding is that endothelial cells from certain vascular beds are more likely to be transformed and they are preferentially transformed by a distinct set of genes. Uterine, adipose and muscle endothelial beds were most affected. We hypothesize that this is due to the dynamic nature of these tissues in the adult. The uterus is constantly being overturned and revascularization is required during the estrus cycle of the mouse. Adipose tissue is subjected to frequent metabolic alterations and changes in size, particularly expansion upon aging. Skeletal muscle is constantly undergoing damage and rebuilding through normal usage and, therefore, new vasculature would be required to support these processes. Angiogenesis is required in these tissues and this imposes proliferative needs on endothelial cells that then enter the cell cycle, a time when they become most susceptible to mutagenesis. Therefore it is understandable that these tissues were the most affected by vascular anomaly burden. Furthermore, when we used a cutoff of a gene occurring preferentially in a specific vascular bed of 60%, we saw that certain gCIS occurred preferentially with vascular anomalies originating in specific vascular beds. For example, *Rasa1* was heavily prevalent in vascular anomalies from the uterus, while *Pdgfrb* was prevalent in those from adipose and muscle.

Of special significance was the major finding that regulation of the actin cytoskeleton is central to endothelial cell homeostasis because mutations in genes regulating this pathway are associated with endothelial cell dysfunction. gCIS from our screen most enriched Kegg pathways related to the actin cytoskeleton: focal adhesion, axon guidance, regulation of the actin cytoskeleton, and gap junction pathways. This is significant since one would expect deregulation of the angiogenesis signaling (growth factor a cytokine) pathways to be the primary regulators of endothelial cell homeostasis since they are well known to regulate proliferation and migration. Interestingly, known causative genes in vascular like the CCM1-3 proteins are known to regulate the connection between the actin cytoskeleton and cell surface adhesion molecules in association with endothelial malignancy. Here we expand the breadth of cytoskeletal regulators that when disrupted caused vascular anomalies. Our data highlighted that Rho and

Rac GTPase regulation is critical to endothelial cell homeostasis as is regulation of actin polymerization. Interestingly, the genes we identified also point to a common connection between regulation of the actin cytoskeleton and regulation of cell growth through the Hippo pathway.

In conclusion, this work heavily impacts our understanding of endothelial cell homeostasis. It opens up new fields of study with the discovery of important genetic interactions. More importantly, it points towards previously unknown targets for vascular anomaly treatment.

Methods

Mouse Models

For the mutagenesis screen, quadruple transgenic mice were bred to include the following transgenes: VE-Cadherin-Cre, Rosa26-LacZ, Sleeping Beauty Transposase, and either the T2/onc2 or T2/onc3 transposon. Studies were conducted in accordance with UCLA Department of Laboratory Animal Medicine's Animal Research Committee guidelines.

Sequencing of transposon insertion sites

Genomic DNA was isolated from vascular lesions and fragmented. Transposon-genome junction fragments were amplified by ligation-mediated PCR (LM-PCR) and sequenced using the Illumina HiSeq machine [57,58].

Identification of common insertion sites (CISs)

Gene-centric CIS (gCIS) analyses were used to identify candidate genes implicated in vascular anomaly lesion formation as previously described (Brett et al., 2011).

Immunohistochemistry and X-gal staining

Mouse and human tissue were isolated from vascular anomalies and fixed with 2% paraformaldehyde for immunohistochemistry. Mouse tissue was fixed with 0.2% glutaraldehyde for X-gal reactions. Mouse primary antibodies: CD31 (Dianova Clone:SZ31, 1:20), Ki67 (Cell Signaling Clone: D3H10, 1:400). Human primary antibodies: CD31 (Dako Clone: JC70A, 1:40), smooth muscle alpha-actin (Millipore Clone:EPR5368, 1:400). Secondary antibodies used at 1:1000: anti-rabbit Dylight 594 (Pierce), anti-mouse Dylight 488 (Pierce), anti-rabbit biotin

(Vector Labs), anti-rat biotin (Vector Labs). A Zeiss LSM710 confocal microscope (Carl Zeiss Microscopy, Thornwood, NY) was used to image and Zen software was used for acquisition. Olympus DP73 camera and cellSens software was used to capture light microscope images.

Exome Sequencing Analysis

Genomic DNA was isolated from human vascular anomaly samples using Wizard SV genomic DNA Kit (Promega). Sequencing data was aligned to the GRCH37 human reference genome using BWA v0.7.7-r411. PCR duplicates were marked using MarkDuplicates program in Picard-tools-.1.115 tool set. GATK v3.2-2 was used for INDEL realignment and base quality recalibration. Exome coverage was calculated using bedtools. Samtools was used to call the SNVs and small INDELs. All variants were annotated using the Annovar program. Variant call files were further annotated using SeattleSeq[59] and ExAC Database (Exome Aggregation Consortium (ExAC), Cambridge, MA). Data was transferred to an SQL database, where data was sorted for rare (< 1% in ExAC) and potentially damaging variants (functionGVS not equal to intron, synonymous, 5-prime-UTR', '3-prime-UTR, non-coding-exon, upstream-gene, downstream-gene, intergenic). Lists were further sorted for known vascular anomaly genes[1] or those identified in the present study.

Cell Culture

HUVECs (Lonza) were cultured in MCDB-131 (VEC technologies) supplemented with 10% FBS. In certain conditions, media was supplemented with 100ng/ml PDGF-BB (Peprotech).

Lenti-viral transduction

HUVECs were transduced with lenti-virus expressing the CMV-Pdgfrb construct. The cds of Pdgfrb was purchased from Origene and cloned into the pRRL-X-IRES-GFP vector (UCLA Vector Core).

siRNA Transfection

siPORT AMINE reagent was used to transfect HUVECs with siRNA targeting Fndc3b. siFndc3b Silencer Select was purchased from Ambion (ID:s1500).

Western Blotting

HUVECs were serum starved for 5 hours, treated with 200uM sodium orthovanadate to inhibit phosphatases for 5 minutes, and were then treated with 100ng/ml PDGF-BB (Peprotech) for 10 minutes. Protein was collected in RIPA buffer (Warren et al., 2013).

Figure 3.1: Transposon mutagenesis in endothelial cells yield vascular anomalies

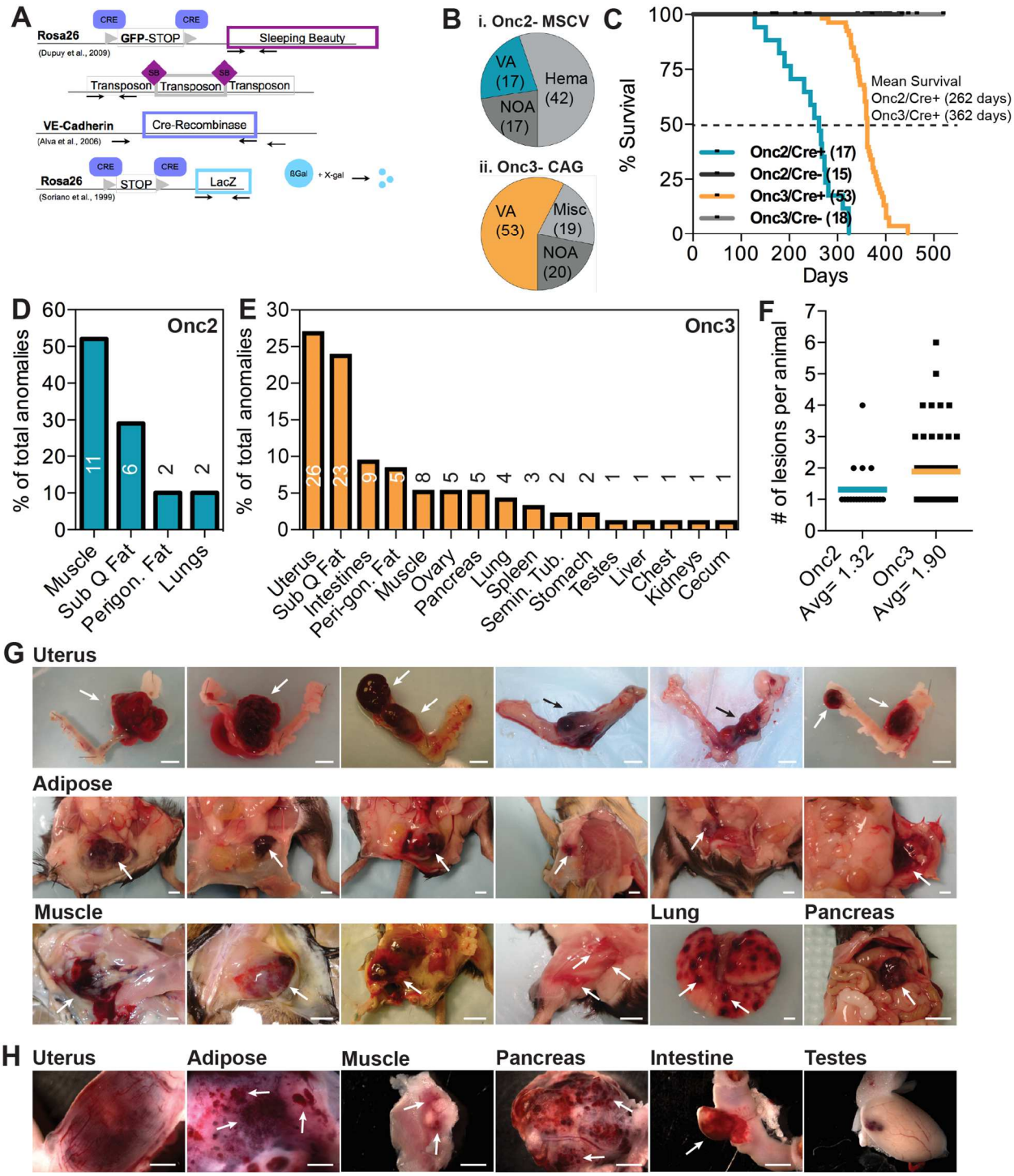

Figure 3.2: Vascular anomalies of endothelial origin were comprised of solid and cavernous lesions

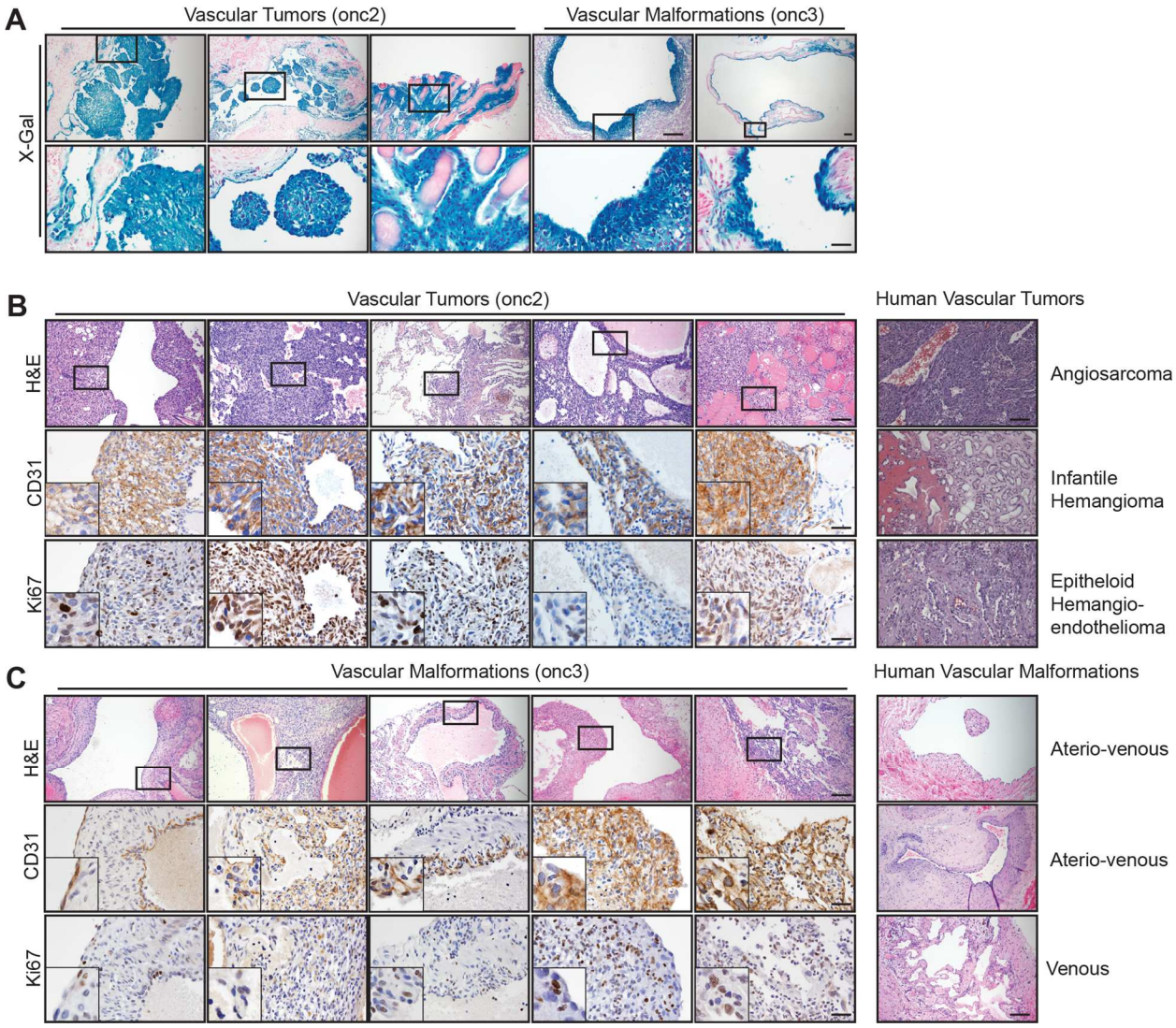

Figure 3.3: Endothelial mutagenesis identified known and novel mutations association with vascular anomalies

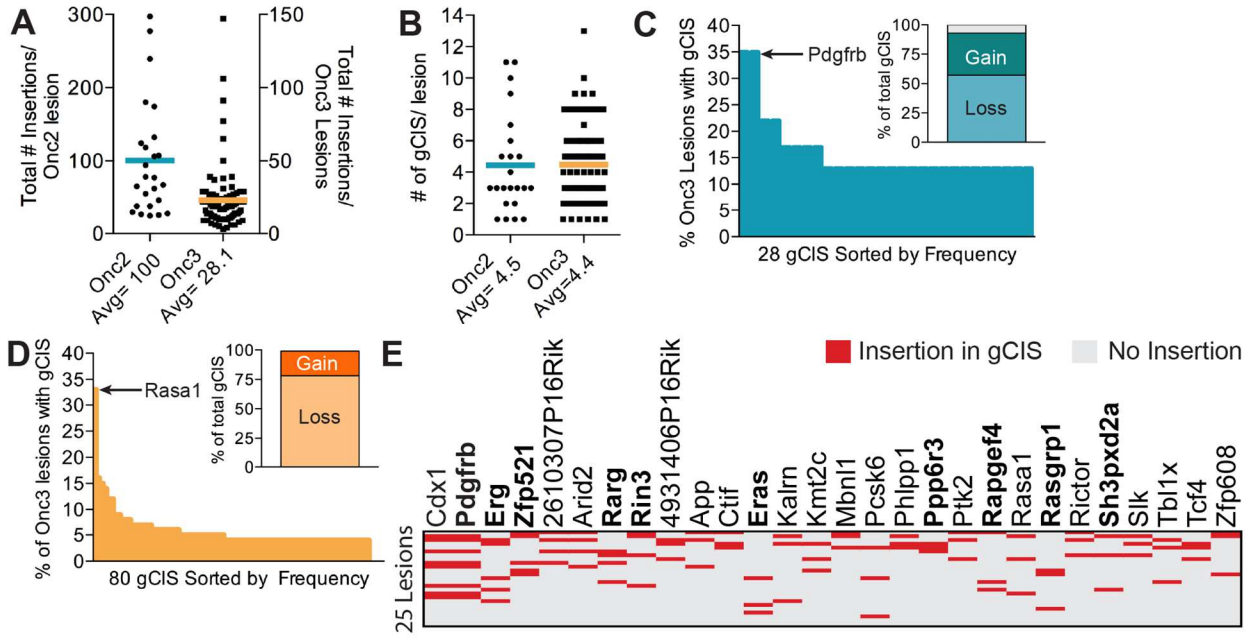

Figure 3.3: Endothelial mutagenesis identified known and novel mutations association with vascular anomalies

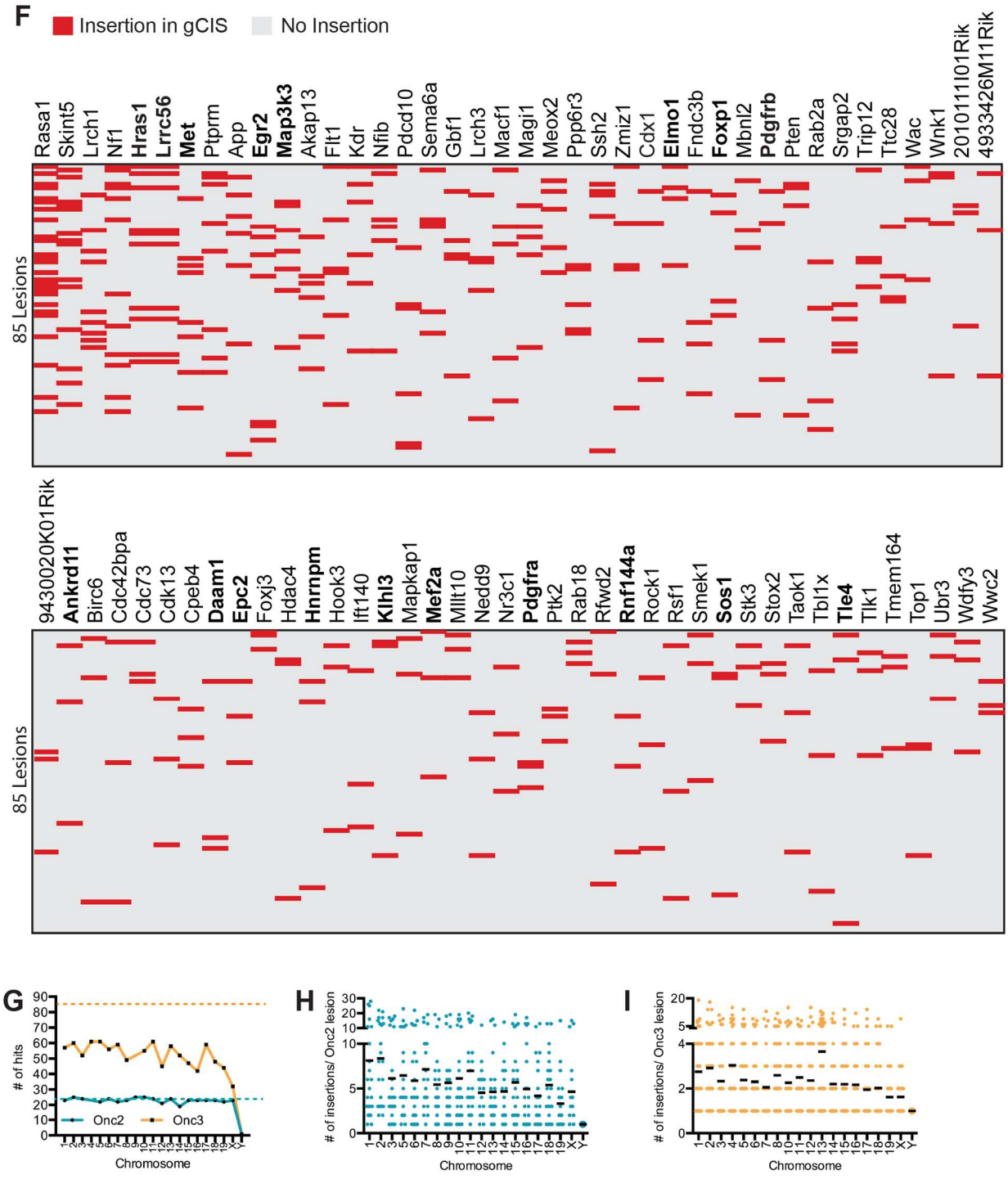

Figure 3.4: Regulation of the actin cytoskeleton is critical to maintain endothelial cell homeostasis

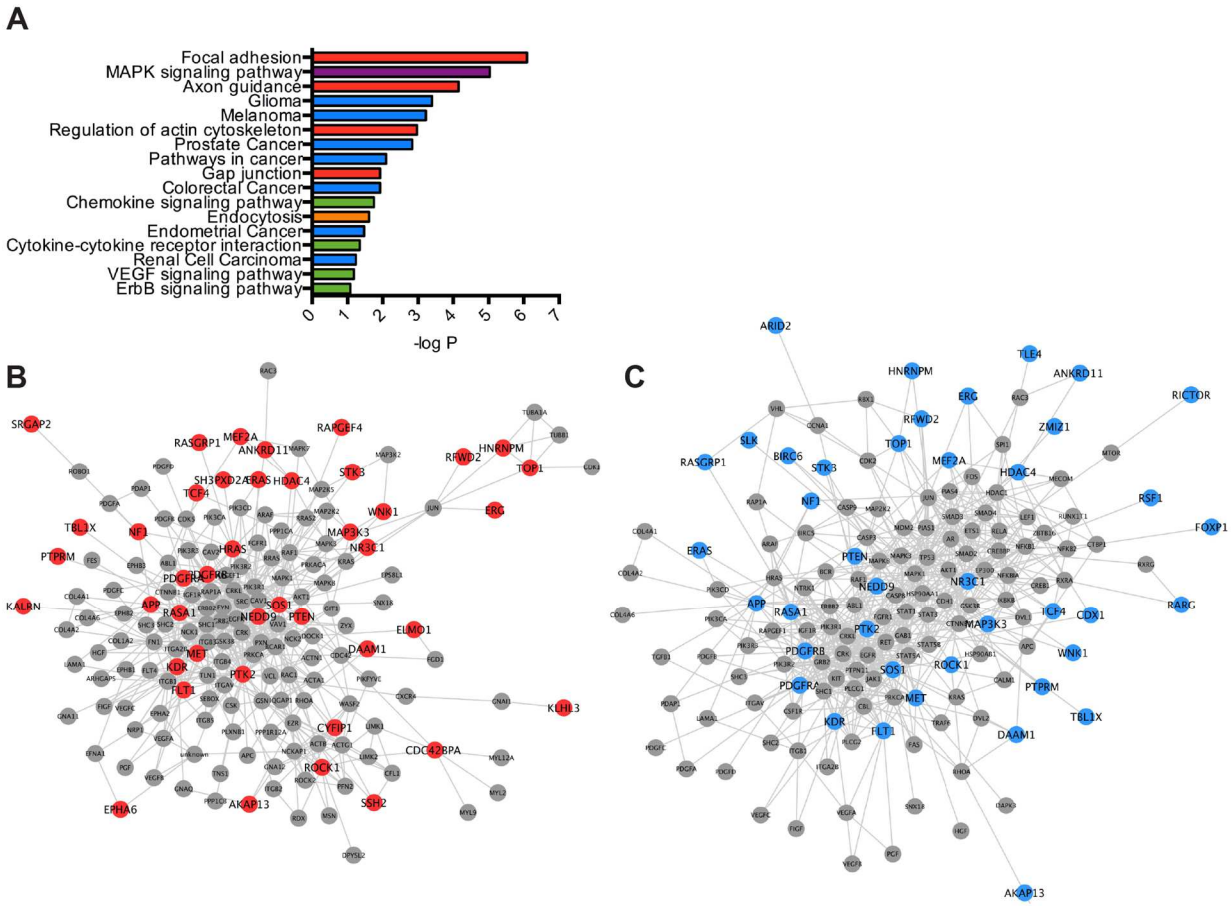

Figure 3.4: Regulation of the actin cytoskeleton is critical to maintain endothelial cell homeostasis

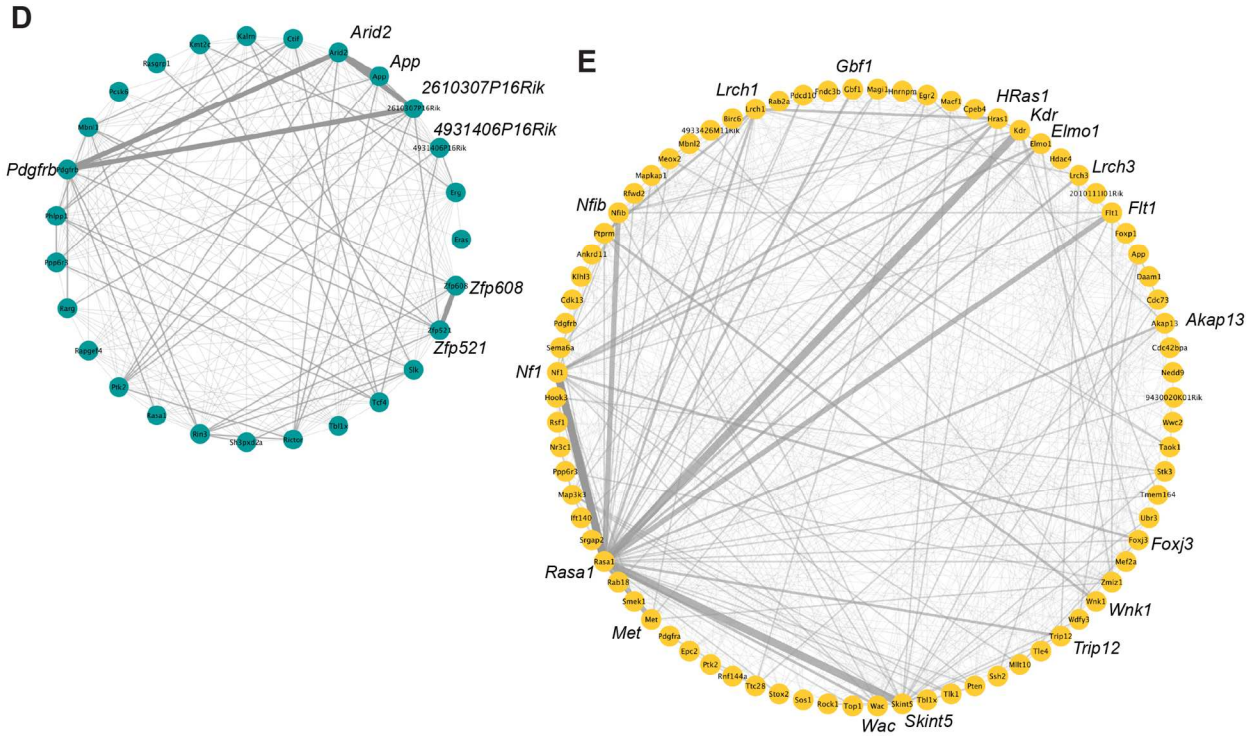

Figure 3.5: gCIS were preferentially segregated based by endothelial bed

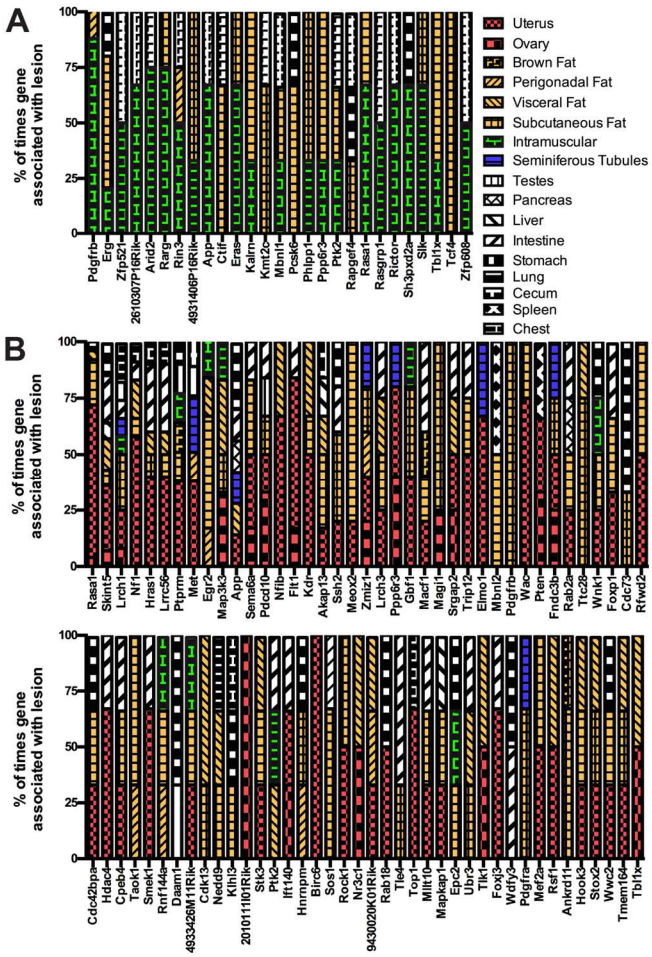

Figure 3.6: Knockdown of novel gene *FNDC3B* and overexpression of *Pdgfrb* affected endothelial cells migration and proliferation

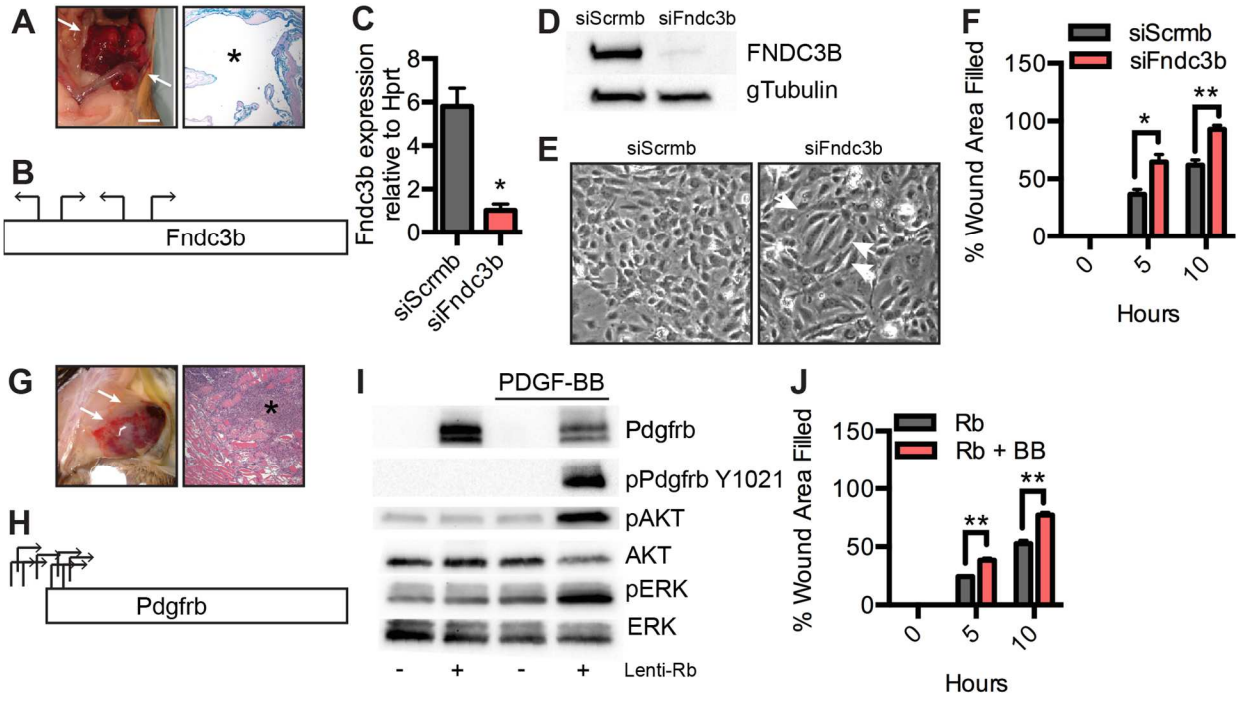

Figure 3.7: Human vascular anomalies contain mutations in genes identified in forward genetic screen

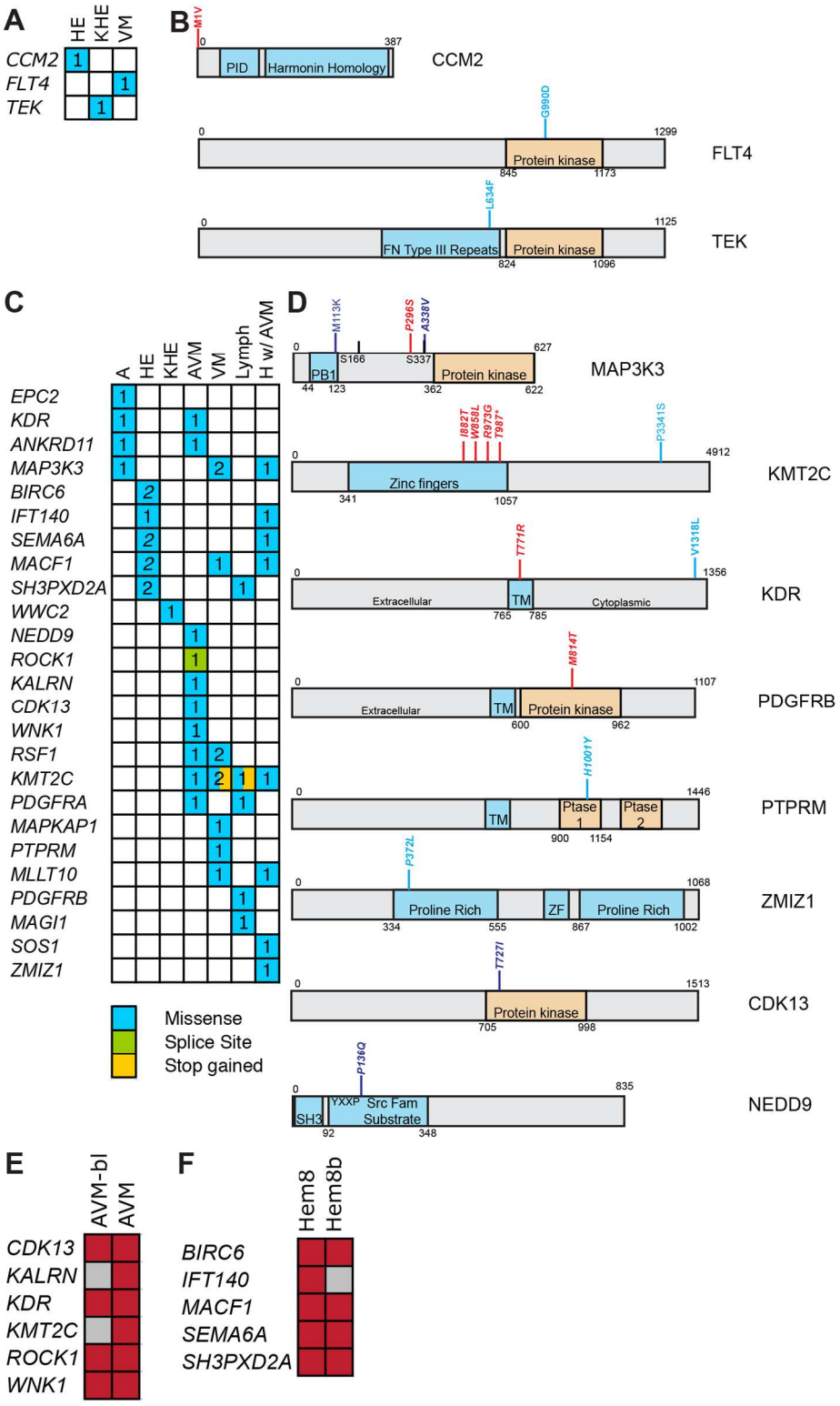

Figure 3.8: Pathways regulating the actin cytoskeleton and hippo pathway converge in endothelial cells

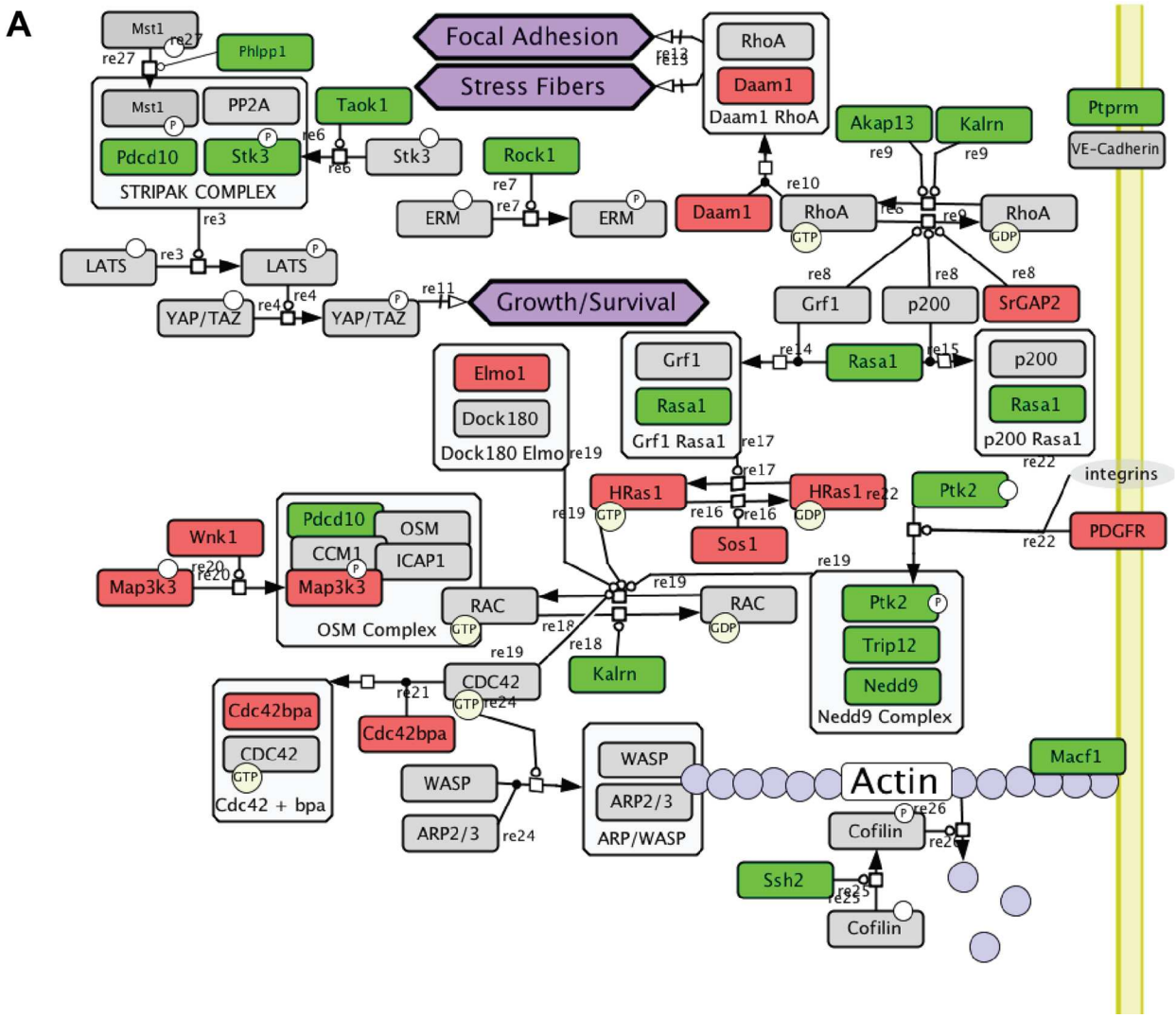

Figure Legends

Figure 3.1: Transposon mutagenesis in endothelial cells yield vascular anomalies

Mice were crossed according to **(A)** and the resulting phenotypes are summarized for the Onc2 **(B, i)** and Onc3 cohort **(B, ii)**. Survival curves for each experimental and control cohort are graphed in **(C)**. The most common tissue bed in which vascular anomalies were found in Onc2 **(D)** and Onc3 **(E)** cohorts are plotted as well as the average number of lesions per animal **(F).** Representative images of VA occurring in uterus, adipose, muscle, lung, and pancreas are in **(G)** (scale= 5mm) and **r**epresentative higher magnification images from uterus, adipose, muscle, pancreas, intestine and testes (scale= 2mm) are in **(H)**.

.

Figure 3.2: Vascular anomalies of endothelial origin were comprised of solid and cavernous lesions

(A) Onc2 and onc3 malformations were stained with X-gal and solid clumps of endothelial tumors and enlarged cavernous lesions, were observed in onc2 and onc3 cohorts, respectively. (top scale= 150μm, bottom scale= 600μm) **(B,C)** CD31 and Ki67 staining reveals onc2 tumors have overall more Ki67 positive endothelial staining than onc3 malformations. **(B)** Onc2 tumors look most like human angiosarcoma, while onc3 malformations look like human vascular malformations. (H&E scale= 150μm, scale IHC 600μm)

Figure 3.3: Endothelial mutagenesis identified known and novel mutations association with vascular anomalies

While there were more insertions per lesion in onc2 compared to onc3 **(A)**, the average number of gCIS were the same for each **(B)**. The gCIS were plotted by frequency and predicted resulting phenotype for onc2 **(C)** and onc3 **(D)** lesion were plotted. Mutagenesis signatures for each lesion is plotted horizontally, where each gene is listed across the top for onc2 **(E)** and onc3 **(F)**. **(G)** Number of times a chromosome contained a transposon was plotted. **(H)** Number of insertions per chromosome per Onc2 sample. **(I)** Number of insertions per chromosome per Onc3 sample. Bold text= predicted GOF

Figure 3.4: Regulation of the actin cytoskeleton is critical to maintain endothelial cell homeostasis

(A) DAVID pathway analysis reveals that Onc2 and Onc3 gCIS highly enrich pathways that regulate the actin cytoskeleton (red). Others include MAPK signaling (purple), various cancer signaling (blue), RTK and cytokine/chemokine signaling (green), and endocytosis pathways (orange). **(B)** Actin cytoskeleton regulatory network visualized as a union of focal adhesion, axon guidance, regulation of actin cytoskeleton, and gap junction pathways. **(C)** Cancer regulatory network visualized as a union of glioma, melanoma, prostate cancer, pathways in cancer, colorectal cancer, endometrial cancer, and renal cell carcinoma pathways. **(D, E)** Gene insertion co-occurrences point towards possible cooperative genes in Onc2 and Onc3 screens, respectively. Lesions often contain mutations that are apart of both cancer and actin cytoskeleton regulatory pathways.

Figure 3.5: gCIS were preferentially segregated based by endothelial bed

(A) Genes were plotted based by the percent of times they occur in different tissues. There was preference for Pdgfrb mutations to occur in muscle, while Tcf4 mutations were only seen in fat. **(B)** Genes were plotted as they are in (A). Here Rasa1 was preferentially mutated in uterine vascular beds, while Cdk13 and Ankrd11 were specific to adipose lesions. Daam1 and Wdfy3 mutations were never found in uterine or adipose lesions.

Figure 3.6: Knockdown of novel gene *Fndc3b* and overexpression of *Pdgfrb* affected endothelial cells migration and proliferation

(A) *Fndc3b* mutations were found in association with aggressive uterine vascular malformation phenotype (enlarged cavernous spaces). **(B)** Transposons were inserted in Fndc3b gene in either orientation and distributed into coding sequence. **(C)** Knockdown efficiency of siFndc3b by RNA expression. **(D)** siFndc3b knockdown at the protein level. **(E)** siFndc3b results in elongated cell morphology. **(F)** siFndc3b HUVEC cells migrate faster than siScrmb treated cells during wound migration assay. **(G)** Pdgfrb insertions were associated with invasive endothelial cell tumor phenotype. **(H)** Transposons were clustered at the beginning of the *Pdgfrb* gene and were all in the same direction of transcription of the gene. **(I)** PDGF-BB causes phosphorylation of Pdgfrb and downstream effectors Akt and Erk. **(J)** Pgfrb was overexpressed in HUVECs and addition of PDGF-BB caused cells to migrate faster.

Figure 3.7: Human vascular anomalies contain mutations in genes identified in forward genetic screen

(A) Whole exome sequencing was performed on 15 vascular anomalies and one corresponding blood sample. Only three rare and potentially damaging mutations were found in known VA

causative genes *Ccm2*, *Flt4*, and *Tek*. **(B)** Amino acid conversions are marked for rare and potentially damaging mutations in *Ccm2*, *Flt4*, and *Tek*. **(C)** 25% of genes identified in forward genetic screen were mutated in human vascular tumor and malformation samples. **(D)** Amino acid conversions are marked for rare and potentially damaging mutations in *Map3k3*, *Kmt2c*, *Kdr*, *Pdgfrb*, *Ptprm*, *Zmiz1*, *Cdk13*, and *Nedd9*. Italicized conversions have CADD C scores above 15 and Polyphen scores close to 1. Dark blue appear <1%, light blue <0.1%, and red 0% in ExAC database. **(E,F)** Acquired mutations identified in tumor when compared to blood (E) or between two tumors from same patient (F). A:angiosarcoma, HE: hemangioendothelioma, KHE: kaposiform hemangioendothelioma, AVM: arterio-venous malformation, VM: venous malformation, Lymph: lymphangioma, H: hemangioma.

Figure 3.8: Pathways regulating the actin cytoskeleton and hippo pathway converge in endothelial cells

(A) Pathways was created by mining the literature for interactions between gCIS found in the screen. Key nodes of regulation surround RhoA and Rac, actin polymerization, the OSM complex, and the STRIPAK complex. Green= predicted LOF mutations. Red= Predicted GOF mutations. Grey= genes in pathways not identified in screen. Purple= phenotypic outcome of signaling

Table 3.1. gCIS and Known Mutations in Vascular Malformations							
SB gCIS	**Linkage Analysis**	**Exome Seq.**	**Whole Genome Seq.**	**Target Gene Seq.**	**Vascular Malformation Associated with Syndrome of Known Etiology**	**Animal Model/ Angiogenesis/ Vasculogenesis**	**Found In Ziyad et al., Human Specimens**
Rasa1	CM [23] CM-AVM [24]	Parkes Weber [60]		Parkes Weber [61-63] Sturge-Weber [64] CM-AVM [62,63,65-67]		[25]	-
Skint5	-	-	-	-	-	-	-
Lrch1	-	-	-	-	-	-	-
Nf1	-	-	-	-	Neurofibromatosis type 1 [38,40-43,68,69]	[25,33,35,36]	
HRas1	-	-	-	[44]	Costello Sydrome [48]	-	-
Lrrc56	-	-	-	-	-	-	-
Met	-	-	-	-	-	-	-
Ptprm						EC permeability [70]	

App	-	-	-	-	-	Beta-amyloid protein in vascular malformations by Congolese stain [71] Zebrafish vascular development [72]	-
Egr2	-	-	-	-	-	-	-
Map3k3						Endothelial Cell Function [73-76]	Angiosarcoma, VM
Akap13	-	-	-	-	-	-	-
Flt1	-	-	-	-	-	****	-
Kdr	-	-	-	-	-	[77,78]	Angiosarcoma AVM
Nfib	-	-	-	-	-	-	-
Pdcd10	[79]			[51,52,80,81]			-
Sema6a						Endothelial repulsion/ angiogenesis [82,83]	HE, H w/ AVM
Gbf1	-	-	-	-	-	-	-

Lrch3	-	-	-	-	-	-	-
Macf1	-	-	-	-	-	-	HE, VM, H w/ AVM
Magi1	-	-	-	-	-	Binds cells adhesion molecules [84,85]	Lymphangioma
Meox2	-	-	-	-	-	[86-91]	-
Ppp6r3	-	-	-	-	-	-	-
Ssh2	-	-	-	-	-	-	-
Zmiz1						Vasculogenesis [92]	H w/ AVM
Elmo1	-	-	-	-	-	[93,94]	-
Fndc3b	-	-	-	-	-	-	-
Foxp1	-	-	-	-	-	[95]	-
Mbnl2	-	-	-	-	-	-	-
Pdgfrb	-	-	-	-	-	[9,96-99]	Lymphangioma

Pten					Proteus-like syndrome, Cowden syndrome, Bannayan-Riley-Ruvalcaba Syndrome (AVM) 45,47,100,101	102	-
Rab2a	-	-	-	-	-	-	-
Srgap2	-	-	-	-	-	-	-
Trip12	-	-	-	-	-	-	-
Ttc28	-	-	-	-	-	-	-
Wac	-	-	-	-	-	-	-
Wnk1	-	-	-	-	-	Angiogenesis/Remodeling 103-105	AVM
2010111I01Rik (mir-23b; mir-27b; mir-24-1)	-	-	-	-	-	EC mechanotranscution 106-110	-
4933426M11Rik	-	-	-	-	-	-	-
9430020K01Rik (Jcad)	-	-	-	-	-	EC Junction Component 111	-

Ankrd11	-	-	-	-	-	-	Angiosarcoma AVM
Birc6	-	-	-	-	-	-	HE
Cdc42bpa	-	-	-	-	-	-	-
Cdc73	-	-	-	-	-	-	-
Cdk13	-	-	-	-	-	-	AVM
Cpeb4	-	-	-	-	-	-	-
Daam1	-	-	-	-	-	EC Proliferation/Migration 112	-
Epc2	-	-	-	-	-	-	Angiosarcoma
Foxj3	-	-	-	-	-	-	-
Hdac4	-	-	-	-	2q37 Deletion Syndrome 113	-	-
Hnrnpm	-	-	-	-	-	-	-
Hook3	-	-	-	-	-	-	-
Ift140	-	-	-	-	-	-	HE, H w/ AVM
Klhl3	-	-	-	-	-	-	-

Mapkap1	-	-	-	-	-	-	VM
Mef2a	-	-	-	-	-	-	-
Mllt10	-	-	-	-	-	-	VM and H w/ AVM
Nedd9	-	-	-	-	-	-	AVM
Nr3c1	-	-	-	-	-	-	-
Pdgfra	-	-	-	-	-	[9,114]	AVM, Lymphangioma
Ptk2	-	-	-	-	-	[115]	-
Rab18	-	-	-	-	-	-	-
Rfwd2	-	-	-	-	-	-	-
Rnf144a	-	-	-	-	-	-	-
Rock1	-	-	-	-	-	[116]	AVM
Rsf1	-	-	-	-	-	-	AVM, VM
Smek1	-	-	-	-	-	-	-
Sos1	-	-	-	-	Noonan syndrome [49,50]	-	H w/ AVM
Stk3	-	-	-	-	-	[117]	-
Stox2	-	-	-	-	-	-	-
Taok1	-	-	-	-	-	-	-
Tbl1x	-	-	-	-	-	-	-

Tle4	-	-	-	-	-	-	-
Tlk1	-	-	-	-	-	-	-
Tmem164	-	-	-	-	-	-	-
Top1	-	-	-	-	-	-	-
Ubr3	-	-	-	-	-	-	-
Wdfy3	-	-	-	-	-	-	-
Wwc2	-	-	-	-	-	-	KHE
Erg	-	-	-	-	-	[118]	-
Zfp521	-	-	-	-	-	-	-
2610307P16Rik	-	-	-	-	-	-	-
Arid2	-	-	-	-	-	[119]	-
Rarg	-	-	-	-	-	-	-
Rin3	-	-	-	-	-	-	-
4931406P16Rik	-	-	-	-	-	-	-
Ctif	-	-	-	-	-	-	-
Eras	-	-	-	-	-	-	-
Kalrn	-	-	-	-	-	-	AVM

Kmt2c	-	-	-	-	-	-	AVM, VM, Lymphangioma, H w/ AVM
Mbnl1	-	-	-	-	-	-	-
Pcsk6	-	-	-	-	-	-	-
Phlpp1	-	-	-	-	-	-	-
Ppp6r3	-	-	-	-	-	-	-
Rapgef4	-	-	-	-	-	-	-
Rasgrp1	-	-	-	-	-	Involved in lymphatic development in zebrafish [120]	-
Rictor	-	-	-	-	-	[121,122]	-
Sh3pxd2a	-	-	-	-	-	-	HE, Lymphangioma
Slk	-	-	-	-	-	-	-
Tcf4	-	-	-	-	-	-	-

Zfp608	-	-	-	-	-	-	-

Table 3.1: gCIS and Known Mutations in Vascular Malformations

References

1. Uebelhoer, M., Boon, L. M. & Vikkula, M. Vascular Anomalies: From Genetics toward Models for Therapeutic Trials. *Cold Spring Harb Perspect Med* **2,** (2012).

2. Zhang, X. *et al.* Up-regulated microRNA-143 transcribed by nuclear factor kappa B enhances hepatocarcinoma metastasis by repressing fibronectin expression. *Hepatology* **50,** 490–499 (2009).

3. Fan, X. *et al.* Up-regulated microRNA-143 in cancer stem cells differentiation promotes prostate cancer cells metastasis by modulating FNDC3B expression. *BMC cancer* **13,** 61 (2013).

4. Katoh, D., Nishizuka, M., Osada, S. & Imagawa, M. Fad104, a Positive Regulator of Adipocyte Differentiation, Suppresses Invasion and Metastasis of Melanoma Cells by Inhibition of STAT3 Activity. *PLoS ONE* **10,** e0117197–18 (2015).

5. Asa, S. A. *et al.* Expression of platelet-derived growth factor and its receptors in spontaneous canine hemangiosarcoma and cutaneous hemangioma. *Histol Histopathol* **27,** 601–607 (2012).

6. Abou Asa, S. *et al.* Analysis of genomic mutation and immunohistochemistry of platelet-derived growth factor receptors in canine vascular tumours. *Vet Comp Oncol* (2013). doi:10.1111/vco.12035

7. Yonemori, K. *et al.* Contrasting prognostic implications of platelet-derived growth factor receptor-β and vascular endothelial growth factor receptor-2 in patients with angiosarcoma. *Annals of Surgical Oncology* **18,** 2841–2850 (2011).

8. Dickerson, E. B., Marley, K., Edris, W. & Tyner, J. W. Imatinib and dasatinib inhibit hemangiosarcoma and implicate PDGFR-β and Src in tumor growth. *Translational …* (2013). doi:10.1593/tlo.12307

9. Yildirim, O. *et al.* Expression of platelet-derived growth factor ligand and receptor in cerebral arteriovenous and cavernous malformations. *J Clin Neurosci* **17,** 1557–1562 (2010).

10. Miyazaki, H. *et al.* Expression of platelet-derived growth factor receptor β is maintained by Prox1 in lymphatic endothelial cells and is required for tumor lymphangiogenesis. *Cancer Sci* **105,** 1116–1123 (2014).

11. Ziyad, S. & Iruela-Arispe, M. L. Molecular Mechanisms of Tumor Angiogenesis. *Genes & Cancer* **2,** 1085–1096 (2011).

12. Eming, S. A., Brachvogel, B., Odorisio, T. & Koch, M. Regulation of angiogenesis: wound healing as a model. *Prog Histochem Cytochem* **42,** 115–170 (2007).

13. Greene, A. K. Current Concepts of Vascular Anomalies. *Journal of Craniofacial Surgery* **23,** 220–224 (2012).

14. Weiss, S. W., Goldblum, J. R. & Folpe, A. L. Enzinger and Weiss's Soft Tissue Tumors.

(2013).

15. Kile, B. T. & Hilton, D. J. The art and design of genetic screens: mouse. *Nat. Rev. Genet.* **6,** 557–567 (2005).

16. Patton, E. E. & Zon, L. I. The art and design of genetic screens: zebrafish. *Nat. Rev. Genet.* **2,** 956–966 (2001).

17. St Johnston, D. The art and design of genetic screens: Drosophila melanogaster. *Nat. Rev. Genet.* **3,** 176–188 (2002).

18. Forsburg, S. L. The art and design of genetic screens: yeast. *Nat. Rev. Genet.* **2,** 659–668 (2001).

19. Keng, V. W. *et al.* A conditional transposon-based insertional mutagenesis screen for genes associated with mouse hepatocellular carcinoma. *Nat Biotechnol* **27,** 264–274 (2009).

20. Moriarity, B. S. *et al.* A Sleeping Beauty forward genetic screen identifies new genes and pathways driving osteosarcoma development and metastasis. *Nat Genet* **47,** 615–624 (2015).

21. Starr, T. K. *et al.* A transposon-based genetic screen in mice identifies genes altered in colorectal cancer. *Science* **323,** 1747–1750 (2009).

22. Bard-Chapeau, E. A. *et al.* Transposon mutagenesis identifies genes driving hepatocellular carcinoma in a chronic hepatitis B mouse model. *Nat Genet* **46,** 24 (2014).

23. Eerola, I. *et al.* Locus for susceptibility for familial capillary malformation ('port-wine stain') maps to 5q. *Eur J Hum Genet* **10,** 375–380 (2002).

24. Eerola, I. *et al.* Capillary malformation-arteriovenous malformation, a new clinical and genetic disorder caused by RASA1 mutations. *Am J Hum Genet* **73,** 1240–1249 (2003).

25. Henkemeyer, M. *et al.* Vascular system defects and neuronal apoptosis in mice lacking Ras GTPase-activating protein. *, Published online: 26 October 1995;* | *doi:10.1038/377695a0* **377,** 695–701 (1995).

26. Lapinski, P. E. *et al.* RASA1 maintains the lymphatic vasculature in a quiescent functional state in mice. *J Clin Invest* **122,** 733–747 (2012).

27. Anand, S. *et al.* MicroRNA-132-mediated loss of p120RasGAP activates the endothelium to facilitate pathological angiogenesis. *Nat Med* **16,** 909–914 (2010).

28. Kulkarni, S. V., Gish, G., van der Geer, P., Henkemeyer, M. & Pawson, T. Role of p120 Ras-GAP in directed cell movement. *J Cell Biol* **149,** 457–470 (2000).

29. Tomar, A., Lim, S.-T., Lim, Y. & Schlaepfer, D. D. A FAK-p120RasGAP-p190RhoGAP complex regulates polarity in migrating cells. *J Cell Sci* **122,** 1852–1862 (2009).

30. Pamonsinlapatham, P. *et al.* p120-Ras GTPase activating protein (RasGAP): a multi-interacting protein in downstream signaling. *Biochimie* **91,** 320–328 (2009).

31. Mai, A. *et al.* Competitive binding of Rab21 and p120RasGAP to integrins regulates receptor traffic and migration. *J Cell Biol* **194,** 291–306 (2011).

32. Pamonsinlapatham, P. *et al.* Capns1, a new binding partner of RasGAP-SH3 domain in K-RasV12 oncogenic cells: Modulation of cell survival and migration. *Cellular Signalling* **20,** 2119–2126 (2008).

33. Gitler, A. D. *et al.* Nf1 has an essential role in endothelial cells. *Nat Genet* **33,** 75–79 (2003).

34. Wu, M., Wallace, M. R. & Muir, D. Nf1 haploinsufficiency augments angiogenesis. *Oncogene* **25,** 2297–2303 (2006).

35. Padmanabhan, A. *et al.* Cardiac and vascular functions of the zebrafish orthologues of the type I neurofibromatosis gene NFI. *Proceedings of the National Academy of Sciences* **106,** 22305–22310 (2009).

36. Bajaj, A., Li, Q.-F., Zheng, Q. & Pumiglia, K. Loss of NF1 expression in human endothelial cells promotes autonomous proliferation and altered vascular morphogenesis. *PLoS ONE* **7,** e49222 (2012).

37. Behjati, S. *et al.* Recurrent PTPRB and PLCG1 mutations in angiosarcoma. *Nat Genet* **46,** 376–379 (2014).

38. Furlanetti, L. L., Santos, M. V., Valera, E. T., Brassesco, M. S. & de Oliveira, R. S. Metachronous occurrence of nonradiation-induced brain cavernous hemangioma and medulloblastoma in a child with neurofibromatosis type I phenotype. *Journal of Pediatric Neurosciences* **7,** 43–46 (2012).

39. Kuorilehto, T. *et al.* Vasculopathy in two cases of NF1-related congenital pseudarthrosis. *Pathol Res Pract* **202,** 687–690 (2006).

40. Rosser, T. L., Vezina, G. & Packer, R. J. Cerebrovascular abnormalities in a population of children with neurofibromatosis type 1. *Neurology* **64,** 553–555 (2005).

41. Ruggieri, M., D'Arrigo, G., Abbate, M., Distefano, A. & Upadhyaya, M. Multiple coronary artery aneurysms in a child with neurofibromatosis type 1. *Eur. J. Pediatr.* **159,** 477–480 (2000).

42. Lin, A. E. *et al.* Cardiovascular malformations and other cardiovascular abnormalities in neurofibromatosis 1. *Am. J. Med. Genet.* **95,** 108–117 (2000).

43. Cairns, A. G. & North, K. N. Cerebrovascular dysplasia in neurofibromatosis type 1. *J. Neurol. Neurosurg. Psychiatr.* **79,** 1165–1170 (2008).

44. Lim, Y. H. *et al.* Somatic Activating RAS Mutations Cause Vascular Tumors Including Pyogenic Granuloma. *J Investig Dermatol* **135,** 1698–1700 (2015).

45. Turnbull, M. M., Humeniuk, V., Stein, B. & Suthers, G. K. Arteriovenous malformations in Cowden syndrome. *Journal of medical genetics* **42,** e50–e50 (2005).

46. Tan, W.-H. *et al.* The spectrum of vascular anomalies in patients with PTEN mutations: implications for diagnosis and management. *Journal of medical genetics* **44,** 594–602 (2007).

47. Zhou, X. P. *et al.* Germline and germline mosaic PTEN mutations associated with a Proteus-like syndrome of hemihypertrophy, lower limb asymmetry, arteriovenous malformations and lipomatosis. *Hum Mol Genet* **9,** 765–768 (2000).

48. Morice Picard, F. *et al.* Cutaneous Manifestations in Costello and Cardiofaciocutaneous Syndrome: Report of 18 Cases and Literature Review. *Pediatr Dermatol* **30,** 665–673 (2013).

49. Semizel, E., Bostan, O. M. & Saglam, H. Bilateral multiple pulmonary arteriovenous fistulas and duplicated renal collecting system in a child with Noonan's syndrome. *CTY* **17,** 229–231 (2007).

50. Joyce, S. *et al.* The lymphatic phenotype in Noonan and Cardiofaciocutaneous syndrome. *Eur J Hum Genet* (2015). doi:10.1038/ejhg.2015.175

51. Bergametti, F. *et al.* Mutations within the programmed cell death 10 gene cause cerebral cavernous malformations. *Am J Hum Genet* **76,** 42–51 (2005).

52. Guclu, B. *et al.* Mutations in apoptosis-related gene, PDCD10, cause cerebral cavernous malformation 3. *Neurosurgery* **57,** 1008–1013 (2005).

53. Fischer, A., Zalvide, J., Faurobert, E., Albiges-Rizo, C. & Tournier-Lasserve, E. Cerebral cavernous malformations: from CCM genes to endothelial cell homeostasis. *Trends Mol Med* **19,** 302–308 (2013).

54. Liquori, C. L. *et al.* Low frequency of PDCD10 mutations in a panel of CCM3 probands: potential for a fourth CCM locus. *Hum Mutat* **27,** 118–118 (2006).

55. Yildirim, O. *et al.* Expression of platelet-derived growth factor ligand and receptor in cerebral arteriovenous and cavernous malformations. *J Clin Neurosci* **17,** 1557–1562 (2010).

56. Nguyen, H.-L., Boon, L. M. & Vikkula, M. Genetics of vascular malformations. *Seminars in Pediatric Surgery* **23,** 221–226 (2014).

57. Brett, B. T. *et al.* Novel Molecular and Computational Methods Improve the Accuracy of Insertion Site Analysis in Sleeping Beauty-Induced Tumors. *PLoS ONE* **6,** 1–11 (2011).

58. Rogers, L. M., Riordan, J. D., Swick, B. L., Meyerholz, D. K. & Dupuy, A. J. Ectopic Expression of Zmiz1 Induces Cutaneous Squamous Cell Malignancies in a Mouse Model of Cancer. *J Investig Dermatol* 1–7 (2013). doi:10.1038/jid.2013.77

59. Ng, S. B. *et al.* Targeted capture and massively parallel sequencing of 12 human exomes. *Nature* **461,** 272–276 (2009).

60. Burrows, P. E. *et al.* Lymphatic abnormalities are associated with RASA1 gene mutations in mouse and man. *Proceedings of the National Academy of Sciences* **110,** 8621–8626 (2013).

61. Revencu, N. *et al.* Parkes Weber syndrome, vein of Galen aneurysmal malformation, and other fast-flow vascular anomalies are caused by RASA1 mutations. *Hum Mutat* **29,** 959–965 (2008).

62. Wooderchak-Donahue, W. *et al.* RASA1 analysis: Clinical and molecular findings in a

series of consecutive cases. *Eur J Med Genet* **55,** 91–95 (2012).

63. Revencu, N. *et al.* RASA1 mutations and associated phenotypes in 68 families with capillary malformation-arteriovenous malformation. *Hum Mutat* **34,** 1632–1641 (2013).

64. Zhou, Q. *et al.* Detection of RASA1 mutations in patients with sporadic Sturge-Weber syndrome. *Childs Nerv Syst* **27,** 603–607 (2011).

65. Thiex, R. *et al.* A novel association between RASA1 mutations and spinal arteriovenous anomalies. *AJNR Am J Neuroradiol* **31,** 775–779 (2010).

66. Boyden, L. M., Orme, C. M., Antaya, R. J. & Choate, K. A. *Capillary malformation–arteriovenous malformation syndrome: Identification of a family with a novel mutation*. (Journal of the American …, 2012).

67. Durrington, H. J. *et al.* A novel RASA1 mutation causing capillary malformation-arteriovenous malformation (CM-AVM) presenting during pregnancy. *Am J Med Genet A* **161A,** 1690–1694 (2013).

68. Kuorilehto, T. *et al.* NF1 gene expression in mouse fracture healing and in experimental rat pseudarthrosis. *J Histochem Cytochem* **54,** 363–370 (2006).

69. Friedman, J. M. *et al.* Cardiovascular disease in neurofibromatosis 1: report of the NF1 Cardiovascular Task Force. *Genet Med* **4,** 105–111 (2002).

70. Sui, X. F. *et al.* Receptor protein tyrosine phosphatase micro regulates the paracellular pathway in human lung microvascular endothelia. *AJPA* **166,** 1247–1258 (2005).

71. Hart, M. N. *et al.* beta-amyloid protein of Alzheimer's disease is found in cerebral and spinal cord vascular malformations. *AJPA* **132,** 167–172 (1988).

72. Luna, S., Cameron, D. J. & Ethell, D. W. Amyloid-β and APP deficiencies cause severe cerebrovascular defects: important work for an old villain. *PLoS ONE* **8,** e75052 (2013).

73. Deng, Y., Yang, J., McCarty, M. & Su, B. MEKK3 is required for endothelium function but is not essential for tumor growth and angiogenesis. *Am J Physiol, Cell Physiol* **293,** C1404–11 (2007).

74. Zhou, Z. *et al.* The Cerebral Cavernous Malformation Pathway Controls Cardiac Development via Regulation of Endocardial MEKK3 Signaling and KLF Expression. *Dev Cell* **32,** 168–180 (2015).

75. Couto, J. A. *et al.* A somatic MAP3K3 mutation is associated with verrucous venous malformation. *Am J Hum Genet* **96,** 480–486 (2015).

76. Fisher, O. S. *et al.* Structure and vascular function of MEKK3-cerebral cavernous malformations 2 complex. *Nat Commun* **6,** 7937 (2015).

77. He, Y. *et al.* Stabilization of VEGFR2 signaling by cerebral cavernous malformation 3 is critical for vascular development. *Science Signaling* **3,** ra26–ra26 (2010).

78. Pavlov, K. A., Gershtein, E. S., Dubova, E. A. & Shchegolev, A. I. Vascular endothelial growth factor and type 2 receptor for this factor in vascular malformations. *Bull. Exp. Biol. Med.* **150,** 481–484 (2011).

79. Craig, H. D. *et al.* Multilocus linkage identifies two new loci for a mendelian form of stroke, cerebral cavernous malformation, at 7p15-13 and 3q25.2-27. *Hum Mol Genet* **7,** 1851–1858 (1998).

80. D'Angelo, R. *et al.* Mutation analysis of CCM1, CCM2 and CCM3 genes in a cohort of Italian patients with cerebral cavernous malformation. *Brain Pathol.* **21,** 215–224 (2011).

81. Stahl, S. *et al.* Novel CCM1, CCM2, and CCM3 mutations in patients with cerebral cavernous malformations: in-frame deletion in CCM2 prevents formation of a CCM1/CCM2/CCM3 protein complex. *Hum Mutat* **29,** 709–717 (2008).

82. Urbich, C. *et al.* MicroRNA-27a/b controls endothelial cell repulsion and angiogenesis by targeting semaphorin 6A. *Blood* **119,** 1607–1616 (2012).

83. Segarra, M. *et al.* Semaphorin 6A regulates angiogenesis by modulating VEGF signaling. *Blood* **120,** 4104–4115 (2012).

84. Wegmann, F., Ebnet, K., Pasquier, Du, L., Vestweber, D. & Butz, S. Endothelial adhesion molecule ESAM binds directly to the multidomain adaptor MAGI-1 and recruits it to cell contacts. *Exp Cell Res* **300,** 121–133 (2004).

85. Sakurai, A. *et al.* MAGI-1 is required for Rap1 activation upon cell-cell contact and for enhancement of vascular endothelial cadherin-mediated cell adhesion. *Molecular Biology of the Cell* **17,** 966–976 (2006).

86. Chen, Y., Leal, A. D., Patel, S. & Gorski, D. H. The Homeobox Gene GAX Activates p21WAF1/CIP1 Expression in Vascular Endothelial Cells through Direct Interaction with Upstream AT-rich Sequences. *J Biol Chem* **282,** 507–517 (2007).

87. Patel, S., Leal, A. D. & Gorski, D. H. The homeobox gene Gax inhibits angiogenesis through inhibition of nuclear factor-kappaB-dependent endothelial cell gene expression. *Cancer Res* **65,** 1414–1424 (2005).

88. Gorski, D. H. & Leal, A. J. Inhibition of endothelial cell activation by the homeobox gene Gax. *J. Surg. Res.* **111,** 91–99 (2003).

89. Chen, Y., Rabson, A. B. & Gorski, D. H. MEOX2 regulates nuclear factor-kappaB activity in vascular endothelial cells through interactions with p65 and IkappaBbeta. *Cardiovasc Res* **87,** 723–731 (2010).

90. Chen, Y. *et al.* Regulation of the expression and activity of the antiangiogenic homeobox gene GAX/MEOX2 by ZEB2 and microRNA-221. *Mol Cell Biol* **30,** 3902–3913 (2010).

91. Douville, J. M., Cheung, D. Y. C., Herbert, K. L., Moffatt, T. & Wigle, J. T. Mechanisms of MEOX1 and MEOX2 regulation of the cyclin dependent kinase inhibitors p21 and p16 in vascular endothelial cells. *PLoS ONE* **6,** e29099 (2011).

92. Beliakoff, J. *et al.* The PIAS-like protein Zimp10 is essential for embryonic viability and proper vascular development. *Mol Cell Biol* **28,** 282–292 (2008).

93. Schäker, K. *et al.* The bipartite rac1 Guanine nucleotide exchange factor engulfment and cell motility 1/dedicator of cytokinesis 180 (elmo1/dock180) protects endothelial

cells from apoptosis in blood vessel development. *J Biol Chem* **290,** 6408–6418 (2015).

94. Epting, D. *et al.* The Rac1 regulator ELMO1 controls vascular morphogenesis in zebrafish. *Circ Res* **107,** 45–55 (2010).

95. Grundmann, S. *et al.* FoxP1 stimulates angiogenesis by repressing the inhibitory guidance protein semaphorin 5B in endothelial cells. *PLoS ONE* **8,** e70873 (2013).

96. Ren, J.-G. *et al.* Downregulation of the transforming growth factor-β/connective tissue growth factor 2 signalling pathway in venous malformations: its target potential for sclerotherapy. *Br J Dermatol* **171,** 242–251 (2014).

97. Marx, M., Perlmutter, R. A. & Madri, J. A. Modulation of platelet-derived growth factor receptor expression in microvascular endothelial cells during in vitro angiogenesis. *J Clin Invest* **93,** 131–139 (1994).

98. Battegay, E. J., Rupp, J., Iruela-Arispe, L., Sage, E. H. & Pech, M. PDGF-BB modulates endothelial proliferation and angiogenesis in vitro via PDGF beta-receptors. *J Cell Biol* **125,** 917–928 (1994).

99. Thommen, R. *et al.* PDGF-BB increases endothelial migration on cord movements during angiogenesis in vitro. *J Cell Biochem* **64,** 403–413 (1997).

100. Srinivasa, R. N. & Burrows, P. E. Dural arteriovenous malformation in a child with Bannayan-Riley-Ruvalcaba Syndrome. *AJNR Am J Neuroradiol* **27,** 1927–1929 (2006).

101. Tan, W.-H. *et al.* The spectrum of vascular anomalies in patients with PTEN mutations: implications for diagnosis and management. *Journal of medical genetics* **44,** 594–602 (2007).

102. Kar, S., Samii, A. & Bertalanffy, H. PTEN/PI3K/Akt/VEGF signaling and the cross talk to KRIT1, CCM2, and PDCD10 proteins in cerebral cavernous malformations. *Neurosurg Rev* 1–9 (2014). doi:10.1007/s10143-014-0597-8

103. Xie, J. *et al.* Endothelial-specific expression of WNK1 kinase is essential for angiogenesis and heart development in mice. *Am J Pathol* **175,** 1315–1327 (2009).

104. Lai, J.-G. *et al.* Zebrafish WNK lysine deficient protein kinase 1 (wnk1) affects angiogenesis associated with VEGF signaling. *PLoS ONE* **9,** e106129 (2014).

105. Dbouk, H. A. *et al.* Actions of the protein kinase WNK1 on endothelial cells are differentially mediated by its substrate kinases OSR1 and SPAK. *Proceedings of the National Academy of Sciences* **111,** 15999–16004 (2014).

106. Wang, K.-C. *et al.* MicroRNA-23b regulates cyclin-dependent kinase-activating kinase complex through cyclin H repression to modulate endothelial transcription and growth under flow. *Arteriosclerosis, Thrombosis, and Vascular Biology* **34,** 1437–1445 (2014).

107. He, J. *et al.* The feedback regulation of PI3K-miR-19a, and MAPK-miR-23b/27b in endothelial cells under shear stress. *Molecules* **18,** 1–13 (2012).

108. Wang, K.-C. *et al.* Role of microRNA-23b in flow-regulation of Rb phosphorylation and endothelial cell growth. *Proceedings of the National Academy of Sciences* **107,** 3234–3239 (2010).

109. Kumar, S., Kim, C. W., Simmons, R. D. & Jo, H. Role of flow-sensitive microRNAs in endothelial dysfunction and atherosclerosis: mechanosensitive athero-miRs. *Arteriosclerosis, Thrombosis, and Vascular Biology* **34,** 2206–2216 (2014).

110. Natarelli, L. & Schober, A. Janus-faced role of Krüppel-like factor 2-dependent regulation of microRNAs in endothelial proliferation. *Arteriosclerosis, Thrombosis, and Vascular Biology* **34,** 1605–1606 (2014).

111. Akashi, M., Higashi, T., Masuda, S., Komori, T. & Furuse, M. A coronary artery disease-associated gene product, JCAD/KIAA1462, is a novel component of endothelial cell-cell junctions. *Biochem Biophys Res Commun* **413,** 224–229 (2011).

112. Ju, R. *et al.* Activation of the planar cell polarity formin DAAM1 leads to inhibition of endothelial cell proliferation, migration, and angiogenesis. *Proc Natl Acad Sci USA* **107,** 6906–6911 (2010).

113. Sakai, Y. *et al.* Testicular sex cord-stromal tumor in a boy with 2q37 deletion syndrome. *BMC Med Genomics* **7,** 19 (2014).

114. Kurth, P., Moenning, A., Jäger, R., Beine, G. & Schorle, H. An activating mutation in the PDGF receptor alpha results in embryonic lethality caused by malformation of the vascular system. *Dev Dyn* **238,** 1064–1072 (2009).

115. Arnold, K. M., Goeckeler, Z. M. & Wysolmerski, R. B. Loss of focal adhesion kinase enhances endothelial barrier function and increases focal adhesions. *Microcirculation* **20,** 637–649 (2013).

116. Kroll, J. *et al.* Inhibition of Rho-dependent kinases ROCK I/II activates VEGF-driven retinal neovascularization and sprouting angiogenesis. *Am J Physiol Heart Circ Physiol* **296,** H893–9 (2009).

117. Oh, S. *et al.* Crucial role for Mst1 and Mst2 kinases in early embryonic development of the mouse. *Mol Cell Biol* **29,** 6309–6320 (2009).

118. Birdsey, G. M. *et al.* Transcription factor Erg regulates angiogenesis and endothelial apoptosis through VE-cadherin. *Blood* **111,** 3498–3506 (2008).

119. He, L. *et al.* BAF200 Is Required for Heart Morphogenesis and Coronary Artery Development. *PLoS ONE* **9,** e109493 (2014).

120. Huang, H. *et al.* The RAS Guanyl Nucleotide-releasing Protein RasGRP1 Is Involved in Lymphatic Development in Zebrafish. *J Biol Chem* **288,** 2355–2364 (2013).

121. ZHENG, N. N., DING, X. D. & ZHANG, H. P. Targeting rictor inhibits mouse vascular tumor cell proliferation and invasion in vitro and tumor growth in vivo. *Neoplasma* **60,** 41–45 (2013).

122. Wang, S. *et al.* Regulation of endothelial cell proliferation and vascular assembly through distinct mTORC2 signaling pathways. *Mol Cell Biol* **35,** 1299–1313 (2015).

Chapter 4:

Mutagenesis Initiated in Murine Hemogenic Endothelium Result in Leukemia

Abstract

Definitive hematopoietic cells arise from hemogenic endothelium during mid-gestation. Because some childhood leukemias can be initiated prenatally, we sought to determine whether mutations at the hemogenic endothelium stage yield hematopoietic malignancies. Here we demonstrate that endothelial-specific transposon mutagenesis in mice promotes the development of hematopoietic cancers that are both myeloid and lymphoid in nature. In addition to highlight genes previously recognized to be associated with leukemias, mutations identified in this screen also uncovered a unique set of cancer-relevant genes in myeloid leukemia (*Pi4ka*) and lymphoid leukemia (*Jdp2, Mbd5, Zb4b42*) not previously linked to blood cancers. Further characterization of *Phosphatidylinositol 4-kinase alpha* (*Pi4ka*), revealed its unsuspected role in hematopoiesis. Targeted inactivation of the Pi4ka catalytic domain or reduction in mRNA expression promoted the expansion of hematopoietic progenitors at the expense of differentiation in several *in vitro* and *in vivo* assays. In summary, these findings establish a link between mutations in hemogenic endothelium and the emergence of leukemia and provide new information that expands our understanding of the critical genes in hematopoiesis.

Introduction

A subset of childhood hematopoietic malignancies such as Down syndrome transient myelodysplastic syndrome (TMS), myeloid leukemia- Down syndrome (ML-DS), and acute lymphocytic leukemia (ALL) are thought to be initiated prenatally [1]. In these conditions, genetic mutations acquired *in utero* first expand a population of progenitors that, upon subsequent secondary hits, progress to leukemia. In the case of Down syndrome-associated hematopoietic malignancies, trisomy is thought to contribute to megakaryocyte-erythroid progenitor expansion at the fetal liver stage by adding an extra dose of Chromosome 21 genes like *Erg* and *Ets2* [2,3]. These amplified loci in turn cooperate with a secondary N-terminal Gata1 truncation, termed Gata1s, to produce TMS [4-6]. Acquisition of further mutations can transform TMS into ML-DS [7]. As in Down syndrome-associated leukemia, parallel evidence from identical twins suggests that chromosomal translocations occurring during prenatal development initiate a subset of ALL, with the acquisition of secondary mutations further promoting malignant progression [8-10]. Given the proposed embryonic origin of initiating mutations in these malignancies, we sought to develop a model system that would allow us to identify genes associated with early developmental progenitors and that eventually result in leukemia.

The development of definitive hematopoietic cells is intertwined with that of endothelial cells lining the vessels through which their progeny flow. In the last decade, a combination of lineage tracing analyses, *in vitro* studies, and live vertebrate embryo imaging evaluations demonstrated that the hematopoietic lineage emerges from a specialized subset of endothelial cells termed hemogenic endothelium (HemEnd) [11-19]. This specialized endothelium exists in a narrow temporal window during development (E10.5-E12.5 in the mouse) [20]. Given this link between hematopoietic stem progenitors and the HemEnd, along with the evidence suggesting fetal origin for some blood cancers, we sought to investigate whether mutagenesis initiated in the HemEnd could drive eventual leukemogenesis.

Here we present the resulting myeloid and lymphoid leukemic phenotypes that resulted from mutagenesis initiated in the HemEnd. We report novel genes associated with leukemia when mutagenesis was initiated at this early embryonic stage. Finally, we highlight the contribution one of the genes identified in this screen, *Pi4ka,* in hematopoiesis. Loss of function of *Pi4ka* impaired normal hematopoietic progression in multiple systems including zebrafish, *in vitro* differentiation of mouse HSC, and in an *in vivo* mouse bone marrow transplantation model.

Results

Targeting mutagenesis to the hemogenic endothelium produces hematopoietic malignancies

To ascertain whether mutations initiated in the hemogenic endothelium (HemEnd) could reveal early causative genes in leukemia, we used a conditional *Sleeping Beauty* (SB) transposon mutagenesis strategy [21] that specifically targeted the endothelium based on its activation by the VE-Cadherin-Cre (VEC-Cre) recombinase (Figure 4.1.1A-B). In this system, VEC-Cre recombinase releases inhibition of the transposase specifically in endothelial cells. The transposase enzyme cuts and pastes the transposable DNA element, randomly into TA dinucleotides distributed throughout the genome [22]. VE-Cadherin-Cre is first expressed in HemEnd by E9.5 in a salt-and-pepper manner with progressive penetration and homogeneous expression by E12.5 [23]. Because the Cre transgene is still expressed in a mosaic pattern in HemEnd (transient phase lasting from E10.5-12.5) by E10.5, some cells were targeted, while others were not, creating a competitive mixture of mutated and non-mutated populations. Initiation of mutagenesis in the hematopoietic compartment was restricted to the HemEnd stage, as VE-Cadherin promoter activity is absent in the hematopoietic lineage [19].

A total of 76 Cre+ animals and 15 Cre- animals were evaluated. 61 Cre+ animals presented with pathology and none of the Cre- animals had abnormalities. From this cohort: 55.3% (n=42) developed hematopoietic abnormalities alone, 9.2% (n=7) developed vascular anomalies, and 13.2% (n=10) developed a combination of both (Figure 4.1.1C, i). Animals with hematopoietic abnormalities were further segregated into those with an enlarged spleen (65.4%, n=34), those with an enlarged thymus (13.5%, n=7), and those with a combination of both (21.2%, n=11) (Figure 4.1.1C, ii). Overall, the affected animals had a mean survival of 179 days (Figure 4.1.1D). Animals with enlarged thymus showed faster disease kinetics when compared

to those with splenomegaly (mean survival of 139 vs 161 days) (Figure 4.11.E). Representative images of pathology are presented in Figure 4.1.1F. Histological analysis revealed expansion of red pulp, often with invasion of hematopoietic cells into the liver (Figure 4.1.2A). The normal cortical and medullary zones of the thymus in affected animals were disrupted and we frequently observed hematopoietic cell infiltration in distal organs like the kidney (Figure 4.1.2B). Affected mice showed an increase in white blood cell counts when compared to Cre negative (Cre-) littermates. This increase was 6.8 fold, 3.7 fold, and 4.5 fold in spleen (S), thymus (T) and S+T mice, respectively (Figure 4.1G). Furthermore, S and S+T mice exhibited an anemic phenotype (reduced red cell (RCB) count and hemoglobin (Hg) concentration) and increased RBC size (MCV) (Figure 4.1H). While animals with compromised spleen and thymus frequently showed abnormal platelet counts compared to Cre- animals, there was no difference in platelets between those affected by large spleen or thymus (Figure 4.1I). Overall, the findings indicate that targeted mutagenesis of HemEnd results in hematopoietic anomalies.

Unbiased transposition pattern in spleen and thymus lesions

The SB mutagenesis system used in this screen enables the precise genomic coordinates of transposon-induced mutations to be determined using linker-mediated PCR and Illumina next-generation sequencing [24]. Subsequent statistical analyses are able to identify recurrently mutated regions in the sample set containing clonally-expanded transposon insertions at a higher rate than would be predicted in the absence of selective pressure. Gene-centric insertion site (gCIS) analysis was used to identify clusters of clonally expanded insertions that were enriched near protein coding regions. Because these analyses assume that transposition occurs randomly throughout the genome, we first confirmed the unbiased distribution of insertions across all chromosomes in our samples (Figure 4.2.2A-C). Indeed, our

data is consistent with the well-established unbiased nature of SB screens in general [21,22,25,26]. Interestingly, the number of gCIS associated with the thymus phenotype was double that of the spleen phenotype, despite the same average number of total insertions per sample (Figure 4.2.2D-E).

Spleen and thymus malignancies show distinct gene insertion signatures

Given the differences in number of gCIS between the S and T phenotypes, we sought to put the gCIS identified in the present screen in context with mutated genes identified in blood cancers created from other murine forward genetic screens. The present screen is the first to exclusively target the hemogenic endothelium, and thus, early definitive HSC. To highlight the similarities and differences, we compared the significant gCIS associated with hematopoietic abnormalities revealed by our screen with mutated genes identified in blood cancers arising from global (non-tissue specific) [27,28] and Vav-Cre (HSC) driven mouse mutagenesis screens [29,30] (Table 4.1 and supplemental Figure 4.2.2F). As anticipated, we observed some degree of overlap, highlighting the ability of our approach to identify genes relevant to hematopoietic malignancy. However, some of the recurrently mutated genes observed were unique to the HemEnd targeting approach, suggesting that their mutation may drive transformation specifically when it occurs in either HemEnd or very early HSC cells, compared to fetal liver HSC. Specifically, we identified three unique genes associated with the thymus-related phenotype when compared to other screens: *Jdp2*, *Mbd5*, and *Zbtb42* (Figure 4.2.1A) and two unique genes associated with the spleen-related phenotype: *Epo* and *Pi4ka* (Figure 4.3.1A). Based on absence of overlap of these genes with those previously identified in screens utilizing unrestricted or Vav-Cre initiated mutagenesis, we hypothesize that our mutations were initiated before E11.5 (Vav-Cre) [29].

The most commonly mutated genes for the enlarged thymus phenotype (Table 4.2) included: *Rasgrp1*, *Akt1*, *Akt2*, *Zbtb42, Notch1*, and *Myc* (Figure 4.2.1B). *Rasgrp1* insertions were associated with about 60% of sequenced lesions (Figure 4.2.1B). Thymus lesions often contained insertions in *Rasgrp1, Akt1* and *Akt2* concurrently (Figure 4.2.1C). The majority of these genes have been previously associated with T-cell malignancy [31-33]. Plotting connections between genes identified within the same lesion highlights a network of genes whose mutation is associated with T-lineage cancer (Figure 4.2.1D). These concurrent hits also revealed key regulatory pathways (Jak-Stat) that are acting early in development to drive lineage specification (Figure 4. 2E).

The most commonly mutated genes detected in enlarged spleens (Table 4.3) were *Eras*, *Erg and Ets1*, which occur in about 40% of samples (Figure 4.3.1A,B). Additional recurrently mutated genes in this population include *Fli1*, *Epo*, and *Runx2* (Figure 4.3.1A). These genes have been previously implicated in myelo-erythropoiesis and hematopoiesis in general providing strong validation to the screen [34-36]. The majority of mutations associated with splenomegaly were also correlated with blast-like cells in the blood and with reduction in polymorphonuclear cells (the predominant cell type of normal bone marrow) in the bone marrow (Figure 4.3.1C and Figure 4.3.2A). In accordance with their frequency of mutation, *Eras* and *Erg* insertions were commonly observed together within the same spleen samples (Figure 4.3.1D). The majority of these affected genes can populate the Jak-Stat pathway (Figure 4.3.1E).

Pi4ka insertion is associated with increased progenitors and abnormal RBC levels

Mutations in *Pi4ka* were also found associated with splenic abnormalities. While scant information is available on *Pi4ka* in hematopoiesis, mutations in this gene have been recently associated with histocytic sarcoma which utilized the myeloid specific Lyz-Cre [37]. As a lipid

kinase that phosphorylates phosphatidyl-inositols at the D4 position, the Pi4ka protein is potentially important in a broad array of signaling events [38]. Two of the three transposon insertions observed in *Pi4ka* were found at the 5' end of the gene, with the third located before the catalytic domain at the 3' end of the gene (Figure 4.4.1A). Each one of these insertions was identified in a lesion from an independent animal, indicating a strong positive selective pressure for mutations of *Pi4ka* in the HemEnd.

Transcriptional analysis indicated that the mutations were associated with decreased *Pi4ka* mRNA supporting that they acted as loss-of-function mutations (Figure 4.4B.1). Histological sectioning of affected spleens revealed expanded red pulp zones compared to Cre- spleens (Figure 4.4.2A). Additional immunohistochemical analyses also indicated a significant decrease of the Pi4ka protein in mutant animals in comparison to Cre- controls (Figure 4.4.1C, top, middle). Cytospin of blood from animals with *Pi4ka* insertions showed a prevalence of blast-like immature cells or myeloid lineage cells (Figure 4.4.1C, bottom). Strikingly, when the *Pi4ka* insertion occurred in absence of additional gCIS mutations (F270), the predominant cell type became a blast-like immature cell, which was also associated with anemia (Figure 4.4.1C, bottom, 4D). On the other hand, when *Pi4ka* occurred in concert in the same lesion as either *Epo* or *Fli1* mutation, lesions appeared myelodysplastic and characterized by more differentiated cells (Figure 4.4.1C, bottom). The increased RBC size (RDW% and MCV) was indicative of a more immature cell type, which is clearly the case in the cytospin images (Figure 4.4.1C, bottom and Figure 4.4.2B).

Loss of pi4kaa function in zebrafish inhibits erythroid differentiation

To evaluate the contribution of pi4kaa (the zebrafish homolog of Pi4ka) in hematopoiesis, we explored loss of function in zebrafish using splice inhibitory morpholinos

targeting the catalytic domain. The morpholino prevented splicing of pi4kaa exons 49 and 50 in a dose dependent manner (Figure 4.5.2A). O-dianisidine staining indicated lower hemoglobin content in the 48hpf morphant embryos compared to controls (Figure 4.5.1A). To quantify the difference in erythroid lineage cells, flow cytometry was performed on control and morpholino treated *gata1*:DsRED (erythroid cells); *fli1*:GFP (endothelial and hematopoieic progenitor cells) or *lcr*:GFP (erythroid cells) embryos at 48hpf in the presence or absence of pi4kaa moprholino. Due to the long half-life of the DsRED protein, measurement of red fluorescence was equivalent to total erythroid lineage cells. *Pi4kaa* inhibition resulted in significantly less erythroid lineage cells in both fish lines (Figure 4.5.1B-C). *fli1*:GFP; *gata1*:DsRED fish were then used to assess the differentiation of erythroid lineage cells in morphants. In control embryos, a prominent *fli1:GFP;gata1:*DsRED double positive population was observed at 24hpf (Figure 4.5.2B). From the DsRED+ population, we determined the median GFP signal (supplemental Figure 4.5.2C). As development proceeds and cells differentiate, this population was decreased. By 48hpf, *gata1*:DsRED cells had lost *fli1*:GFP expression and become *gata1*:DsRED single positive in control embryos. However, the *gata1*:DsRED and *fli1*:GFP double positive population was maintained in pi4ka morphants (about 3.5 times more median *fli1*:GFP expression) (Figure 4.5.1D, Figure 4.5.2F-5G).

To further test whether *fli1*:GFP+; *gata1*:DsRED+ cells were less mature in pi4kaa morphants, we first sorted and compared the morphology of *gata1:*DsRED+,*fli1:*GFP- and *gata1:*DsRED+,*fli1:*GFP+ populations in 48hpf morphants and control embryos (Figure 4.5.1E-F). At 48hpf, pik4aa morphants showed an abundance of immature *gata1:*DsRED+,*fli1:*GFP+ cells, and lacked those normal *gata1:*DsRED+,*fli1:*GFP- mature erythroid cells present in the controls, confirming the abnormal erythropoiesis. The morphant *gata1:*DsRED+,*fli1:*GFP- population also presented an excess of granulocytes, perhaps as a response to the abundance of abnormal erythroid lineage cells. Expression profile analysis for indicators of erythropoiesis

revealed by 24hpf an increase in *gata1* (erythroid progenitor marker), *lmo2* (EMP marker), and *pu.1* (myeloid progenitor marker) mRNA in morphants when compared to controls (Figure 4.5.1G). While *beta-globin* was lower than controls, the mature myeloid markers *mpx* and *l-plastin* were not affected in pi4kaa morphants (Figure 4.5H).

Pi4ka is expressed in mouse HSPC and knockdown impairs progression of mouse hematopoiesis

Given evidence for a role for pi4kaa in zebrafish hematopoiesis, we sought to determine the importance of Pi4ka in mammalian hematopoiesis using mice. First we assessed Pi4ka protein expression in budding hematopoietic stem progenitor clusters (HSPC) clusters from aortic HemEnd. While significant expression was detected in sub-aortic mesenchyme, we were also able to observe clear membrane localization of Pi4ka in budding HSPC (Figure 4.6.1A). We then profiled hematopoietic stem cells for expression of Pi4ka by sorting specific subpopulations of bone marrow cells and evaluating transcript levels (Figure 4.6.1B). We found a significant enrichment of Pi4ka mRNA in HSC (Lineage negative, Sca1 positive, cKit positive) compared to differentiated (Lineage positive) cells, suggesting a role in early hematopoietic stem cells and progenitors. Seeking to understand the role of Pi4ka in HSC, we evaluated the consequence of reducing its expression on differentiation. Sorted adult mouse bone marrow HSC were either treated with lenti-shRNA against *Pi4ka* or scrambled sequence and were subsequently co-cultured on an OP9 stromal layer in the presence of cytokines (Figure 4.6.1C). Flow cytometry after 10 days of culture revealed an increase in immature Mac1+,F4/80+ progenitor cells and decrease in mature Mac1-,F4/80+ myeloid lineage cells (Figure 4.6.1D-E) upon reduction of Pi4ka, when compared to control. We also found a

significant decrease in CD71-, Ter119+ mature erythroid linage cells, when compared to control (Figure 4.6.1F-G).

We next investigated the role of Pi4ka during *in vivo* hematopoietic differentiation. Magnetic column lineage depleted bone marrow, infected with lenti-virus encoding scrambled and *Pi4ka* targeted shRNA, was used to transplant lethally irradiated hosts (Figure 4.7.1A). After 10 weeks mouse recipient bone marrow was assessed for HSC, progenitor (lineage negative) and mature (lineage positive) populations. Results showed that shPi4ka recipient Lin- population was increased 1.3 fold (Figure 4.7.1B and E), LSK population was decreased 0.7 fold (Figure 4.7.1C and F), and Lin+ population was decreased 0.95 fold of shScrmb recipients (Figure 4.7.1D and E).

Discussion

The physiological link between the HemEnd and the HSC has been established by the multiple elegant live imaging and lineage tracing studies in mice and zebrafish [11-19]. This link is likely to also include pathologies, meaning, mutations originated in HemEnd could potentially affect hematopoietic cells. In fact, JAK2V617F mutations (known to cause myeloproliferative neoplasms) were found in endothelial cells of patients with Budd-Chiari syndrome (thrombosis of hepatic vein) or Philadelphia-chromosome negative myeloproliferative neoplasms, but the same mutations were absent from hepatocytes [39,40]. In a second group of studies, BCR-Abl fusion products and protein were also found in endothelial cells of CML patients [41-43]. Nonetheless, the fact that leukemia-causing mutations were present in the endothelium could also be traced to a common and yet, independent progenitor upstream of both lineages.

In the present study, we provide evidence that establishes a link between endothelial and hematopoietic lineages that extends to disease. Mutagenesis initiated specifically in the HemEnd promoted the development of hematopoietic abnormalities. This is consistent with studies of ML-DS [4-6] and childhood acute lymphocytic leukemia [8-10] in which prenatal mutations promote the emergence of post-natal leukemia. In these systems it is believed that initial mutations expand a progenitor population, which is further susceptible to secondary hits. Our screen identified recurrent mutation of ETS family transcription factors *Erg* and *Ets1*, the former known to collaborate with *Gata1s* (inhibitory Gata1 N-terminal truncation mutant) to cause TMS [4-6]. In addition to previously known causative genes in prenatal initiated leukemia, we identified novel candidate genes including *Pi4ka*, *Epo*, *Jdp2*, *Mdb5* and *Zbtb42*.

Furthermore, as validation for our forward genetic screen, we reproduced reduction of *Pi4ka* in independent systems and inquired as to its requirement for normal hematopoiesis. Loss of Pi4ka impaired hematopoiesis progression *in vivo* and *in vitro*. These results are

consistent with literature reporting a requirement for Pi4ka in normal development of other tissues. In zebrafish, pi4kaa was shown to be required for pectoral fin development downstream of FGFR signaling through regulation of the Pi3k-Akt signaling axis [44]. Pi4ka was shown to be essential to Smoothened activation, a pathway critical for several Drosophila developmental processes [45]. Global deletion of Pi4ka in adult mice showed an essential requirement for this gene in gastrointestinal stability [46,47]. Interestingly, both of these studies discussed the possibility that Pi4ka might be needed for intestinal crypt stem cell differentiation and that loss of this protein might contribute to cellular hyperplasia and breakdown of the enterocytes (due to lack of replenishment) observed in the gastrointestinal tracts of Pi4ka knockout animals [46,47]. As in the above-mentioned reports, our findings indicate a critical role of Pi4ka in differentiation in general, but also identified Pi4ka as an important regulator of early hematopoiesis.

We demonstrated that loss of Pi4ka caused a shift in the balance of HSC progenitors and mature populations in the bone marrow of mice transplanted with lineage depleted bone marrow expressing shPi4ka (Figure 4.7.1). Similarly, loss of Pi4ka in HSCs impaired *in vitro* leukocyte differentiation on OP9 stromal cells (Figure 4.6.1). This requirement of Pi4ka is conserved given that loss of pi4kaa in zebrafish caused an accumulation of undifferentiated myelo-erythroid populations at the expense of mature red blood cells (Figure 4.5.1). Taken together these data indicate that early developmental mutations in the HemEnd, and loss of Pi4ka expression in particular, could be the developmental “first hit” that expands a population of hematopoietic progenitor cells, making them susceptible to further mutations that unleash more severe pathologies like dysplasia and/or leukemias (Figure 4.71G).

Methods

Mice

VE-Cadherin-Cre (VEC-Cre); ROSA26-LacZ transgenic mice [23,48] were crossed to conditional ROSA26-LsL-SB transposase T2/Onc2 mice [21] to initiate mutagenesis in hemogenic endothelial cells starting at E9.5. Cre negative and wild-type Bl/6 mice were used as controls. Bl/6 mice were purchased from the UCLA breeding facility or Charles River Laboratories (Wilmington, MA). CD45.1 mice were purchased from Jackson Laboratory (Bar Habor, Maine). CD45.2 mice were lethally irradiated with one dose of 950Gy and were transplanted 24 hours later. Studies were conducted in accordance with UCLA Department of Laboratory Animal Medicine's Animal Research Committee guidelines.

Sequencing of transposon insertion sites and identification of gene-centric common insertion sites (gCISs)

Genomic DNA from tumors was analyzed by ligation-mediated PCR (LM-PCR) to identify transposon integration sites, as previously described [29]. Briefly, genomic DNA was digested with either *Alu*I or *Nla*III restriction enzymes. Double-stranded adapter oligonucleotides were ligated to free DNA ends, followed by two rounds of PCR with nested primers to specifically amplify transposon/genome junctions and add on sequences necessary for sequencing on the Illumina platform. Amplified junctions were purified and sequenced using the Illumina HiSeq machine. Clonal insertion sites were defined as previously described [24]. Gene-centric CIS (gCIS) analyses were used to identify candidate genes implicated in tumorigenesis [24].

Cytoscape Pathways

Cytoscape was used to create pathways visualizations. The Jepetto application was used to find Kegg pathways enriched by gCIS. For spleen pathways, Jak-Stat and Dorsal-Ventral Kegg pathways were merged by union and pruned. For thymus pathways, Jak-Stat and endometrial cancer pathways were merged by union and pruned.

Hematology

Complete Blood Count (CBC) analysis was performed using a Hemavet machine (Drew Scientific, Waterbuy, CT). After red blood cell lysis, leukocytes were spun onto slides using a Shandon Cytospin 4 (ThemoScientific, Waltham, MA). Slides were stained with May-Grunwald and Giemsa stains (Sigma-Aldrich, St. Louis, MO).

Immunohistochemistry/Immunofluorescence

PFA fixed, paraffin embedded tissues were stained with primary antibodies against Pi4ka (4902 Cell Signaling, Danvers, MT) and CD31 (DIA-310 Dianova, Hamburg, Germany). For Pi4ka immunofluorescence, amplification was performed by tyramide- Alexafluor 568 (Life Technologies, Grand Island, NY). Anti-rat Alexafluor 488 (LifeTechnologies) was used to visualized CD31 staining. For IHC, biotinylated secondary antibodies were followed by Avidin-Biotin Complex Elite and DAB Peroxidase kit (Vector Laboratories, Burlingame, CA). Zeiss confocal microscope was used to image fluorescence along with Zen acquisition software (Zeiss, Hamburg, Germany). Olympus DP73 camera and cellSens software was used to image non-fluorescent stains (Olympus, Waltham, MA).

Fish

Zebrafish lines were maintained in accordance with UCLA Department of Laboratory Animal Medicine's Animal Research Committee guidelines. The following lines were used: Tg(gata1:DSRED; fli1:GFP), Tg(lcr:GFP) [49], and wildtype AB fish. lcr:GFP fish were purchased from the UCLA Zebrafish Core Facility. All embryos were treated with 1x PTU (to inhibit pigment formation) at 24hpf. 8pg or 12pg of the splice-inhibitory Pi4ka morpholino 5'-AATGTGTGTAACCTTCTGGAAAGCC-3' [44] was injected with 2pg or 3pg of p53 morpholino, respectively. Splicing efficiency was examined with previously published primers: 5'-GATGGCTCAAAGGGTCTGCTGGCAG-3' and 5'-GTCTCAGTATGGGATTTGGTTCTGG-3'. [44]. O-dianisidine stain was used to stain hemoglobin.

Transcriptional Analysis

RNA was isolated using RNeasy Mini and Micro kits (Qiagen, Valencia, CA). cDNA was made using iScript cDNA sythesis kit (BioRad, Hercules, CA). SYBR Green (BioRad) based qPCR was performed as previously described [50]. Twenty whole zebrafish per treatment were used for RNA isolation. Mouse Pi4ka transcripts were detected using primers targeting the catalytic domain: Forward 5'- TTC ATG GAG ATG TGT GTC CGA GGT-3' Reverse 5'- AGG CCT GTG TCC AAC ATG AGT GTA-3'. Rpl7 Forward: 5'- AAGCGGATTGCCTTGACAGA-3' Reverse: 5'-TTCCTTGAAGCGTTTCCCGA- 3'. Zebrafish primers were described previously [49,51-53].

Cell Culture

OP9 cells (gift from Mikkola lab, UCLA) were cultured in αMEM with 2mM L-glutamine, 1% pen-strep, 20% Hyclone (ThermoScientific) FBS. For OP9/leukocyte co-cultures this media was

supplemented with 5ng/ml TPO, 50ng/ml SCF, 10ng/ml Flt3L, 5ng/ml IL6, and 5ng/ml IL3 (Peprotech, Rocky Hill, NJ).

Flow cytometry and cell sorting

Flow cytometry was performed using BD Fortessa and LSRII machines (BD, Fanklin Lakes, NJ). FACS was performed using BD FACS Aria instruments. For RNA isolation of bone marrow subpopulations, Lin+, HSC (Lin-, cKit+, Sca1+, CD34-), GMP (Lin-, cKit+, Sca1-, CD34-, FcγR+), MEP (Lin-, cKit+, Sca1-, CD34-, FcγR-), and CMP (Lin-, cKit+, Sca1-, CD34+, FcγRlow) cells were sorted from RBC lysed bone marrow. For OP9 cultures, HSC (Lin-, cKit+, Sca1+) cells were sorted after lineage depletion of bone marrow using Miltenyi (Gladbach, Germany) lineage depletion columns. Zebrafish flow cytometry and sorting was based on *fli1*:GFP, *lcr*:GFP, or *gata1*:DsRED fluorescent signal (n=100 per treatment). Dechorionated embryos were digested with 5ug/ml Liberase-TM (Roche, Penzberg, Germany) for 1 hour at 33C as in [54]. Mouse hematopoietic cell differentiation on OP9 cultures was assessed from single cell suspension generated from cultured cells using antibodies against CD45, Mac1(Cd11b), F4/80, Ter119, and CD71. For bone marrow transplantation assays, bone marrow was lineage depleted before treatment with shRNA or control virus.

Lenti shRNA transduction

Lenti-virus targeting Pi4ka was purchased from Origene (TL510615, Rockville, MD). Target or control plasmids along with VSG-G and Δ8.2 packaging plasmids were transfected into 293T cells using Lipofectamine 2000 (LifeTechnologies). Virus was collected and concentrated by centrifugation. For primary HSC or lineage negative cells, high concentration virus was used to

doubly infect cells using Retronectin (Clontech, Mountain View, CA) coated plates (40ug/ml) after an overnight pre-stimulation in serum free StemSPAN (Stemcell Technologies, Vancouver, BC) or StemMACS (Miltenyi) supplemented with 4 times the cytokine concentration used in OP9 co-culture.

Statistical Analysis

Log-rank test was used for survival curve statistics. Paired t-test was used to assess significance between experimental and control conditions for zebrafish and OP9 co-culture experiments. Unpaired t-test was used to assess significant differences between control and treated transplanted mice. Analysis was performed in Prism 6.0 (GraphPad Software). (* $P \leq 0.05$, ** $P \leq 0.01$ ***, $P \leq 0.001$, ****, $P \leq 0.0001$)

Figure 4.1.1: Targeting Mutagenesis to the Hemogenic Endothelium in Mice Produces Hematopoietic Malignancies

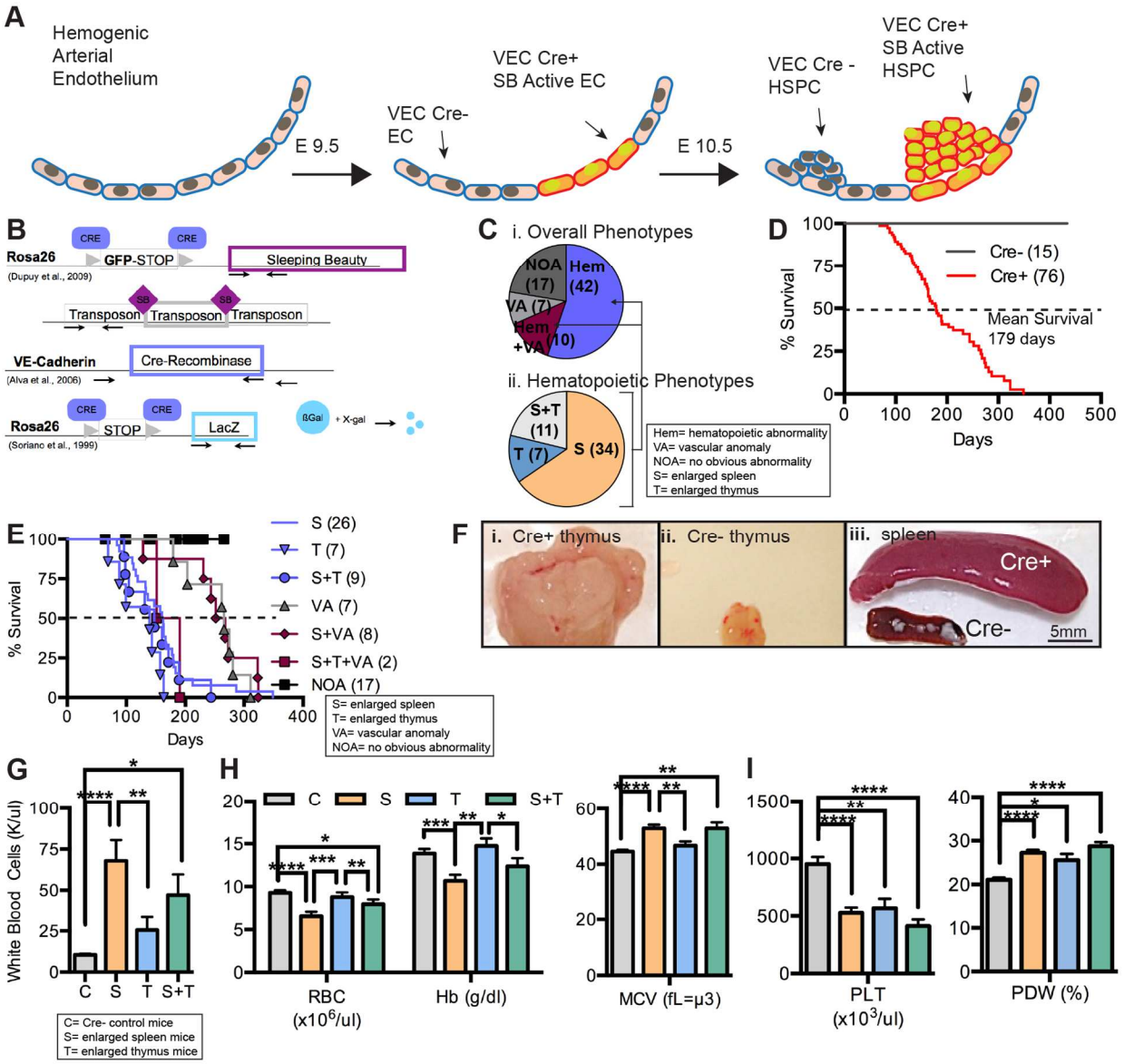

Figure 4.1.2 Histology of Hematopoietic Malignancies

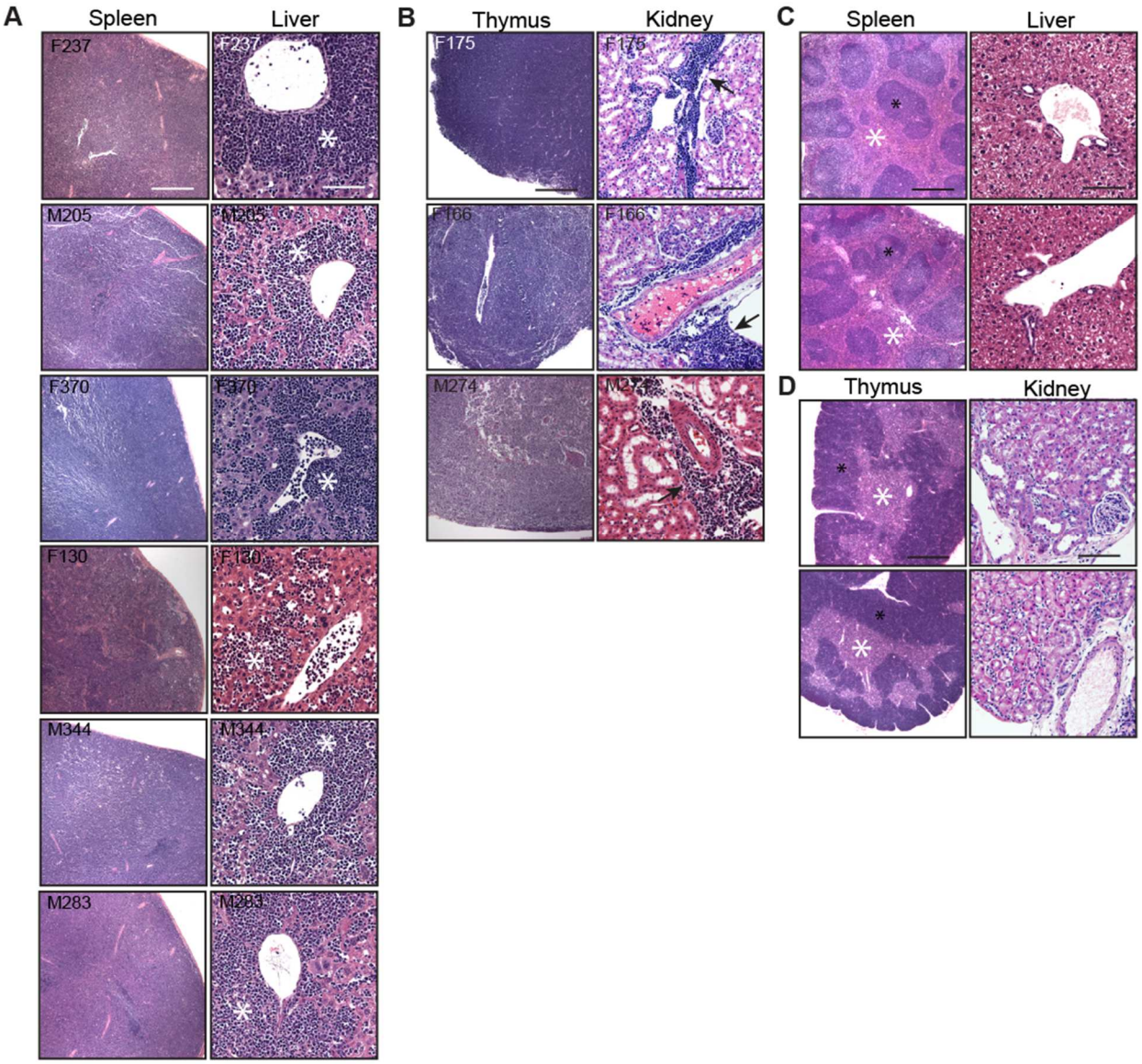

Figure 4.2.1: Thymus Malignancies have Distinct Gene Insertion Signatures

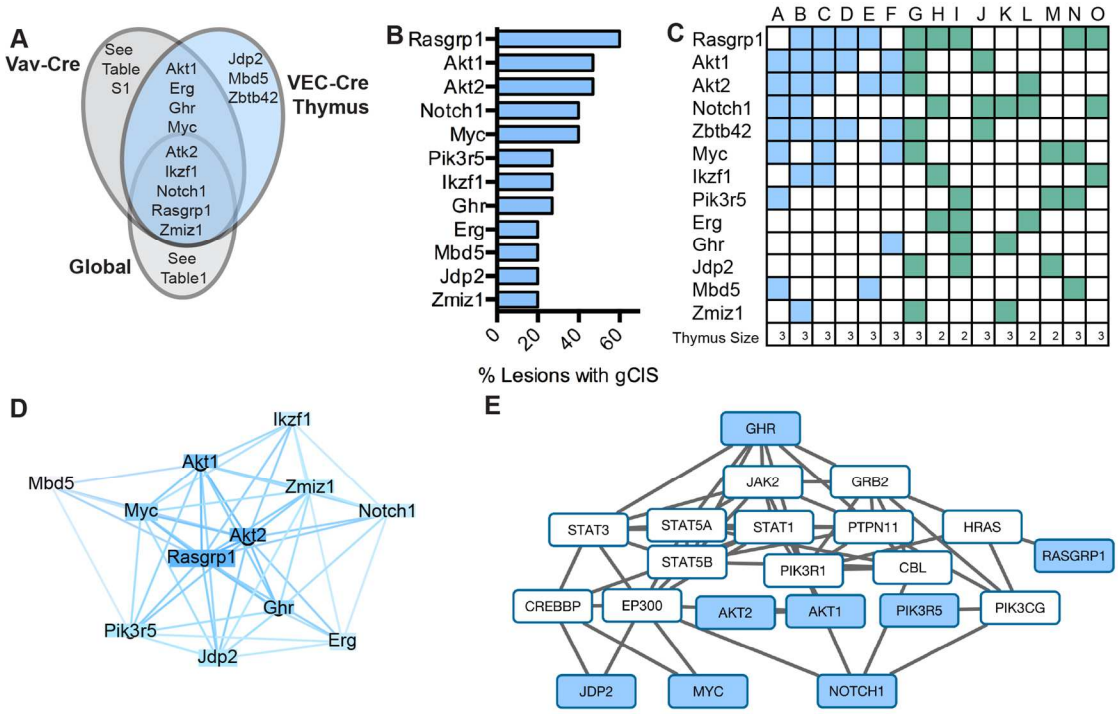

Figure 4.2.2: Transposon insertion characteristics

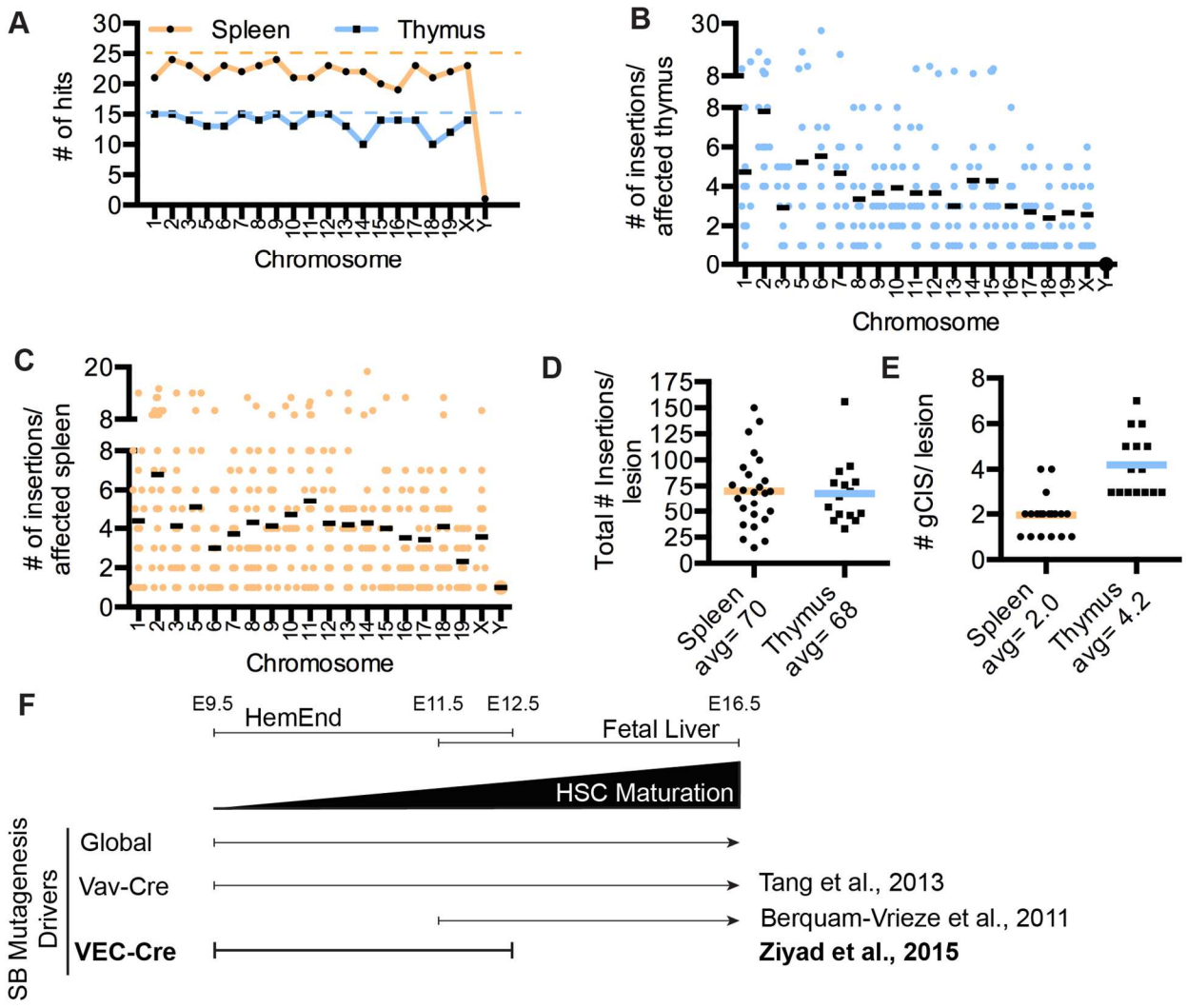

Figure 4.3.1: Spleen Malignancies have Distinct Gene Insertion Signatures

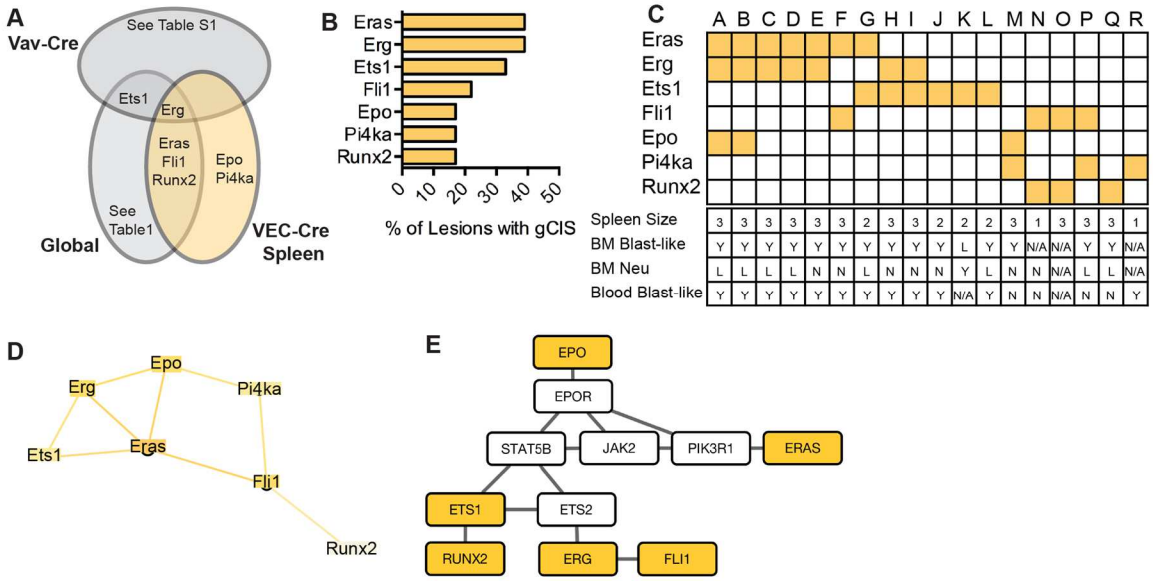

Figure 4.3.2: Cytospin images of blast-like cells

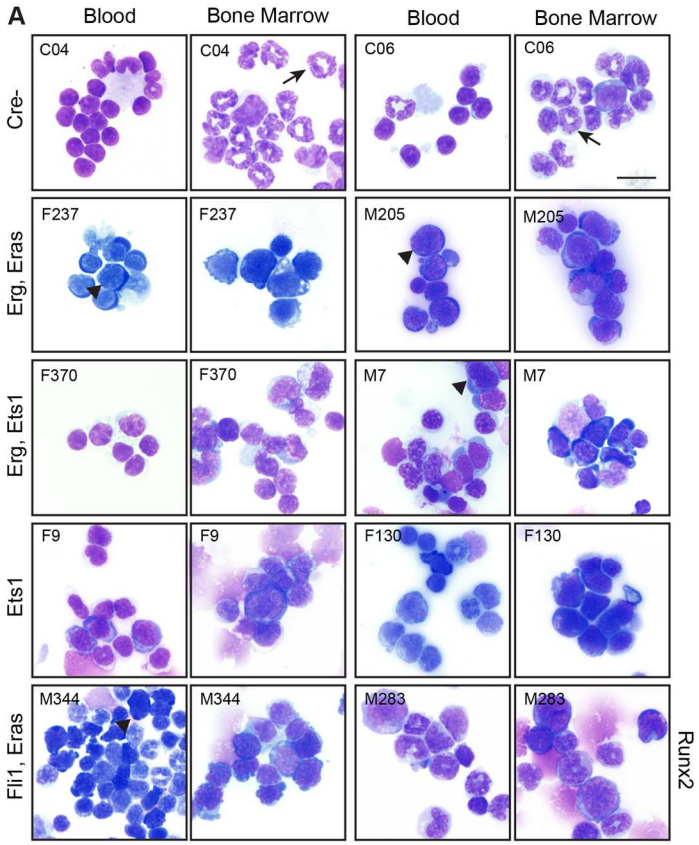

Figure 4.4.1: *Pi4ka* insertion is associated with increased progenitors and decreased RBC and platelets in blood

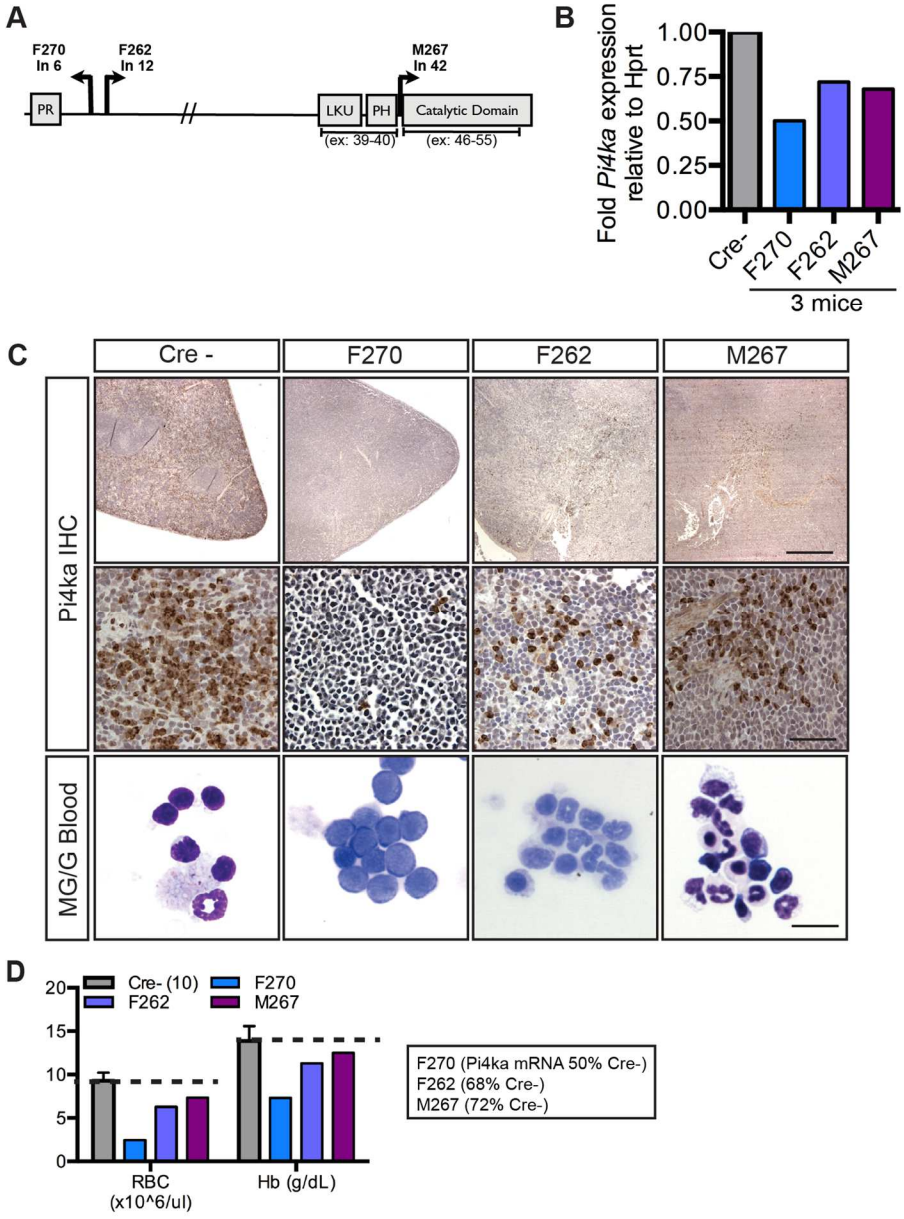

Figure 4.4.2: Histology and CBC counts for *Pi4ka* affected animals

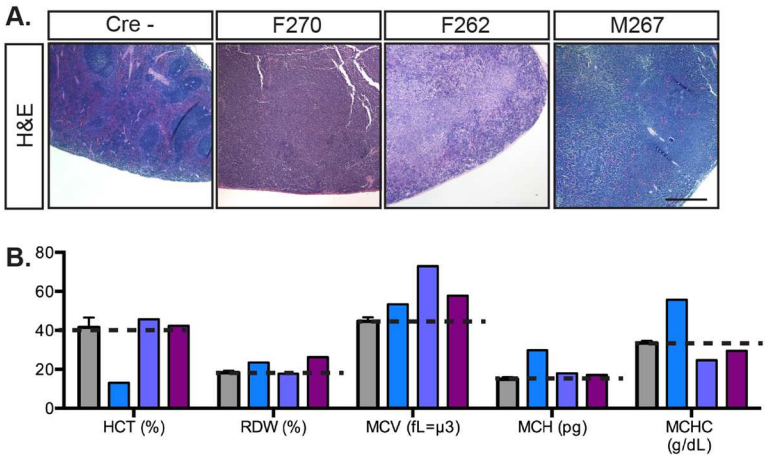

Figure 4.5.1: Loss of pi4kaa function causes reduction in mature RBC in zebrafish

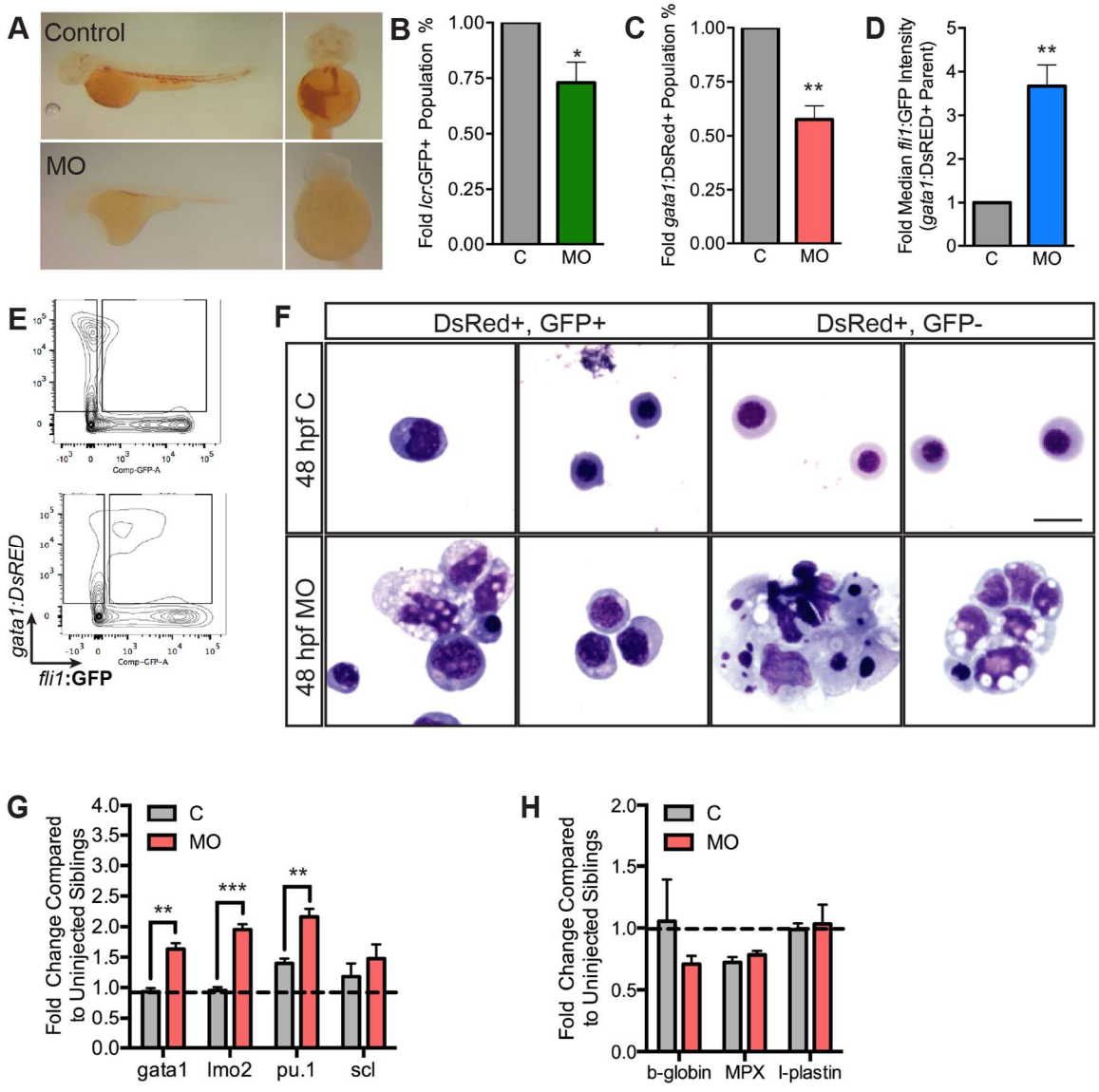

Figure 4.5.2: Morpholino splicing inhibition and gating strategy for zebrafish flow cytometry

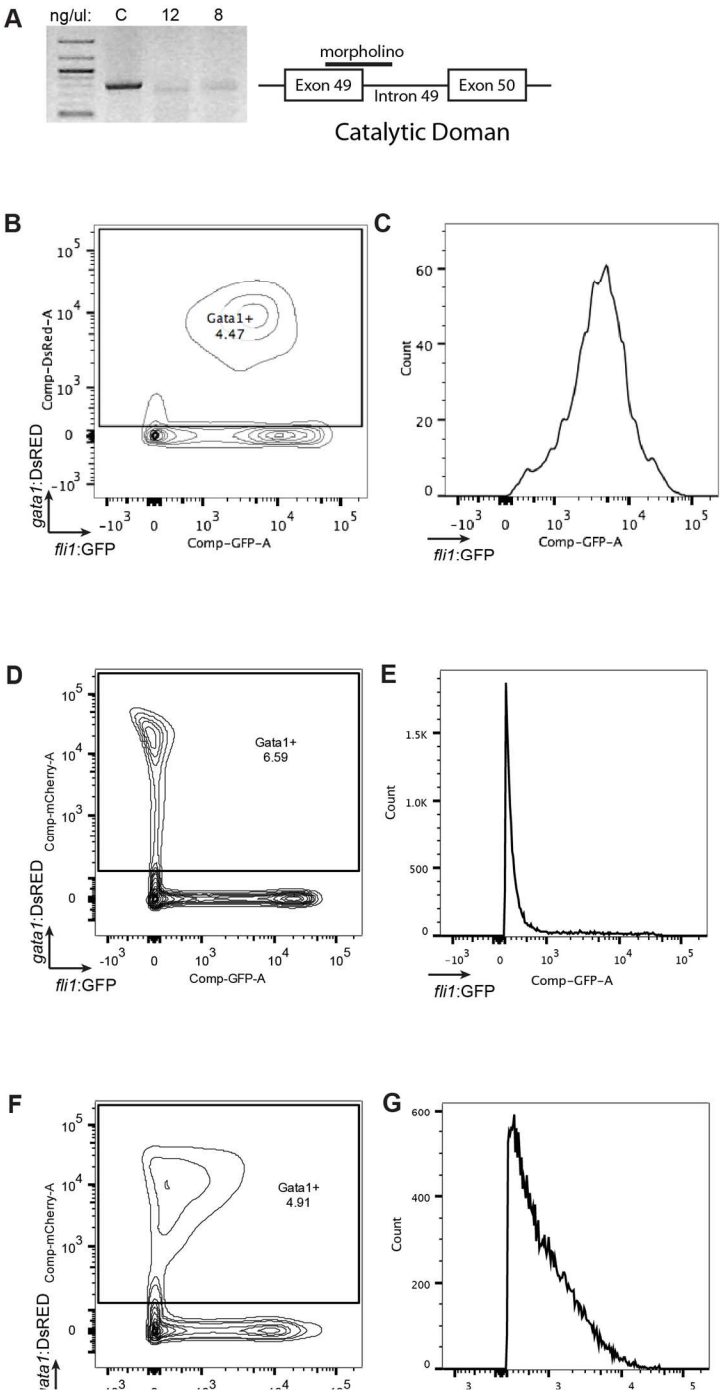

Figure 4.6: Pi4ka is expressed in mouse HSPC and its suppression impairs progression of hematopoiesis *in vitro*

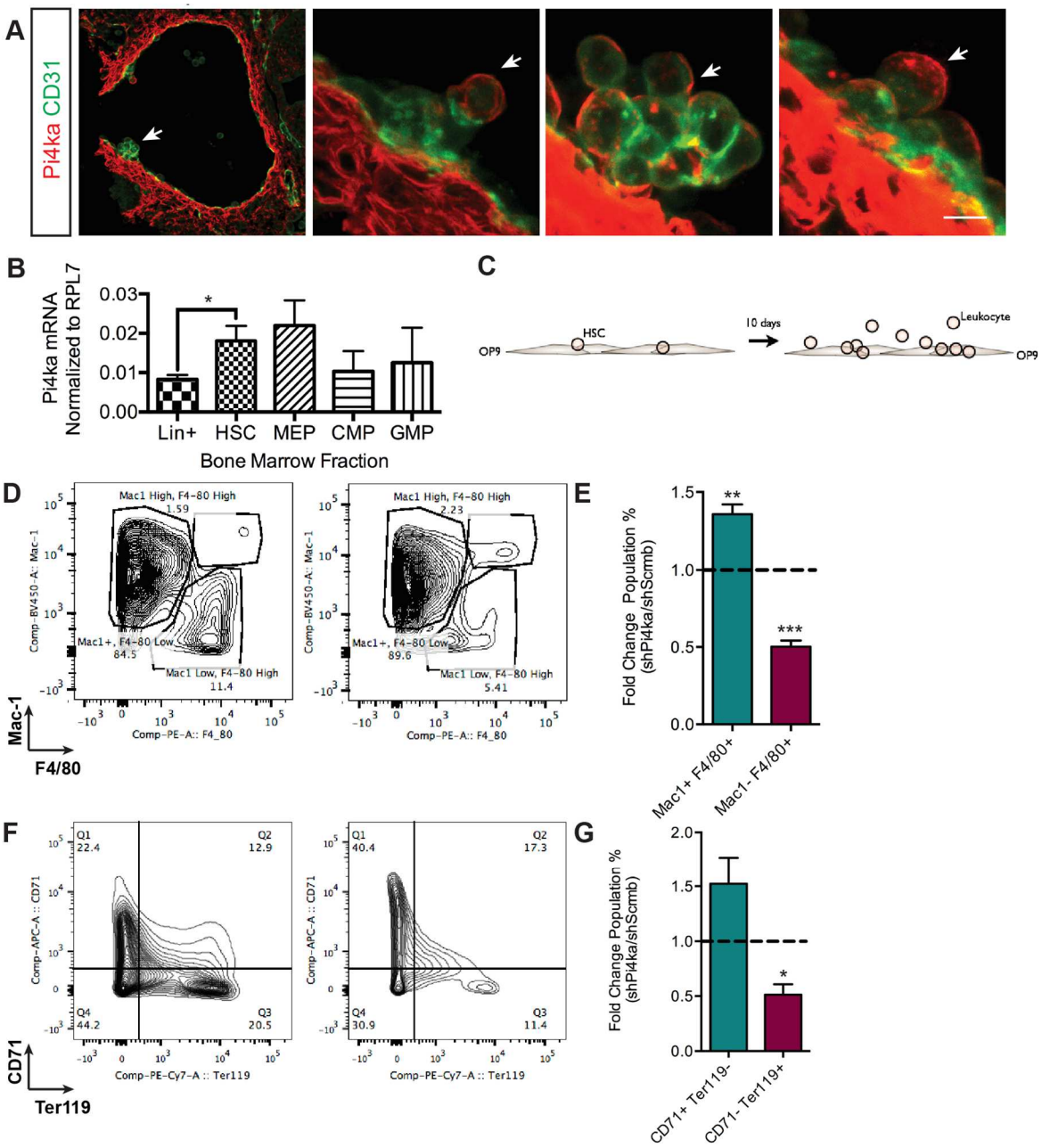

Figure 4.7: *Pi4ka* Knock-down Suppresses Hematopoiesis *in vivo*

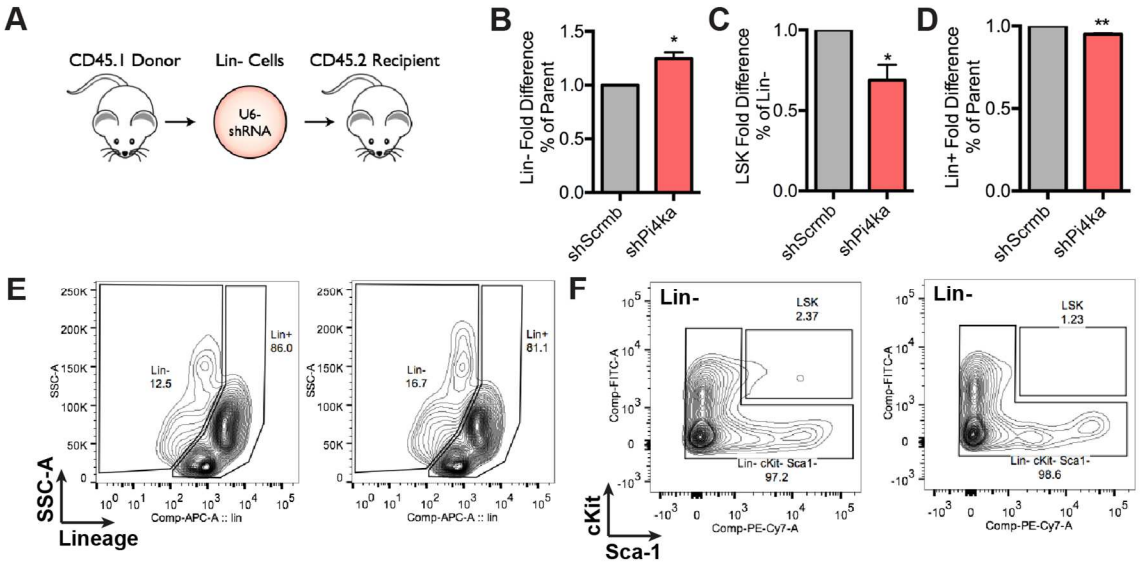

Figure 4.8: Mutations initiated in the hemogenic endothelium result in adult leukemia

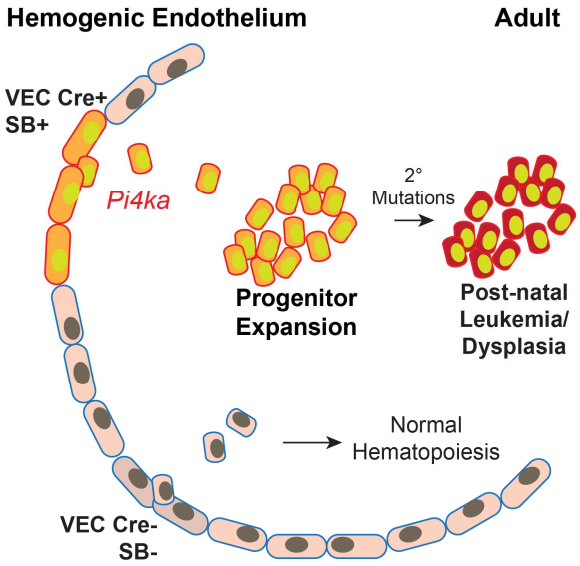

Figure Legends

Figure 4.1.1: Targeting mutagenesis to the hemogenic endothelium in mice produces hematopoietic malignancies

(A) Mutagenesis was initiated in endothelial cells at the onset of VE-Cadherin-Cre (VEC- Cre) expression (at E9.5, including some cells with hemogenic endothelial capacity) mutating emerging definitive HSPC. **(B)** Sleeping Beauty T2/Onc2 mice were crossed with VE-Cad-Cre/ Rosa26-LacZ mice to induce mutagenesis in endothelial cells starting at E9.5. **(C)** (i) Out of a total of 76 Cre+ animals, 42 mice (55.3%) developed hematopoietic abnormalities alone, 7 animals (9.2%) developed vascular tumors and 10 animals (13.2%) developed a combination of both. 17 animals (22.4%) had no obvious abnormalities. (ii) Of the animals with hematopoietic abnormalities 34 (65.4%) developed an enlarged spleen alone, 7 (13.5%) developed an enlarged thymus alone, and 11 (21.2%) developed a combination of both. **(D)** The Cre+ affected animals had an overall median survival of 179 days compared to Cre- animals ($p<0.0001$). **(E)** Survival curve striated by lesion type shows that animals with enlarged thymus had the fastest disease kinetics (blue: T= 139 days, S+T= 147 days), followed by those with enlarged spleen alone (blue: S=161 days), then vascular tumors (maroon: S+T+VT= 170.5 days, S+VT= 260 days, VT=266 days). **(F)** (i) Cre+ enlarged thymus, (ii) Cre- normal thymus, (iii) Cre+ enlarged spleen and Cre- normal spleen (scale 5mm). **(G)** On average, Cre+ animals with enlarged spleens (n=24) had 6.8X excess of WBC, Cre+ enlarged thymus (n=5) animals had 3.7X excess in WBC, and animals with a combination of both (n=10) had 4.5X excess in WBC when compared to Cre- littermates (n=10). **(H)** Cre+ S (n=24) had ~30% less RBC, ~23% less Hb, and ~20% increased MCV. Cre+ S+T mice (n=10) had ~15% less RBC, ~11% less Hb, and ~19% increase in MCV. T mice were not significantly different from Cre- animals using these metrics. **(I)** S, T, and S+T animals all had significantly less platelets and a mean increase in platelet size. (Data are represented as mean ± S.E.M.) Abbreviations: S= enlarged spleen, T=

enlarged thymus, C= Cre- negative, VT= vascular tumors, NOA= no obvious abnormalities, HSPC= hematopoietic stem progenitor cells, Hb= hemoglobin, MCV= mean corpuscular volume PLT= platelet count, PDW%= size distribution of platelets width. See also Figure 4.1.2.

Figure 4.1.2 Histology of hematopoietic malignancies

(A) Animals with enlarged spleens displayed disrupted splenic architecture (expansion of red pulp), often coupled with hematopoietic cell invasion into liver (star indicates invasive hematopoietic cells). **(B)** Enlarged thymus architecture was disrupted and hematopoietic cells often invaded kidney (arrows). **(C)** Normal control spleen is divided into red-pulp (white star) and white pulp (black star) zones. **(D)** Normal control thymus marked by clearly defined cortical (black star) and medullar (white star) zones. (spleen, thymus: scale= 600μm; liver, kidney: scale=100μm)

Figure 4. 2: Thymus malignancies have distinct gene insertion signatures

(A) *Jdp2*, *Mbd5*, and *Zbtb42* mutations were associated with hematopoietic abnormalities that were unique to this screen when compared with HSC targeting screens. **(B)** *Rasgrp1*, *Akt1/2*, *Notch1*, *Zbtb42*, and *Myc* were the most commonly mutated genes in enlarged thymus. **(C)** Enlarged thymus gCIS occurred 3 to 7 times in each lesion (per column), suggesting a requirement for multiple cooperative mutations. T mice (blue) had a different insertion signature compared to S+T mice (green) (3>500mg, 500>2>100mg, 1<100mg). **(D)** Each member of a gene pair directly connected by a line was detected in the same sample, showing *Rasgrp1* insertions are most often present concurrently with mutations in other genes from this group.

(E) gCIS visualized in context of Jak-Stat pathway. T=enlarged thymus, S+T= enlarged spleen and thymus. See also Figure 4.3.2.

Figure 4.2.2: Transposon insertion characteristics

(A) Plotting the number of hits per chromosome shows that every chromosome is hit by the transposon in both enlarged spleen and thymus tissues. Dotted lines indicate the total number of either spleen and thymus and shows that the majority of these lesions have insertions in all of the chromosomes. **(B,C)** The total number of insertions per spleen or thymus per chromosome shows there is little influence of chromosome size on number of insertions. Chromosome 4, the transposon donor chromosome, is removed from analysis due to preponderance of local hopping. **(D)** The average number of insertions per spleen is equal to that of the thymus, yet the average number of gCIS per spleen or thymus is higher in the thymus **(E)**.

Figure 4.3.1: spleen malignancies have distinct gene insertion signatures

(A) *Epo* and *Pi4ka* mutations were unique to this screen. **(B)** *Eras* and *Erg* were the most common gCISs in S mice, being present in about 40% of samples. **(C)** The majority of detected mutation patterns were associated with very large spleens (3> 800mg, 800>2>500mg, 1<500mg), possible blast-like cells in the blood, and reduced polymorpho-nuclear (Neu) cells in the bone marrow of affected animals (each column). **(D)** Network diagram showing spleen intra-lesion connections where each member of a gene pair directly connected by a line was detected in the same sample. **(E)** gCIS in context of Jak-Stat pathway. S= enlarged spleen animals. See also Figure 4.3.2.

Figure 4.3.2: Cytospin images of blast-like cells

(A) Mutations in certain gCIS genes were associated with a prevalence of large blast-like immature cells with high nucleus to cytoplasmic ratio in the blood and bone marrow of affected mice. A dramatic decrease in polymorpho-nuclear cells was observed in the bone marrow of affected animals (scale= 15μm). (arrow= polymorpho-nuclear cell, arrowhead= blast cell)

Figure 4.4.1: *Pi4ka* insertion is associated with increased progenitors and decreased RBC and platelets in blood

(A) Distribution of transposon insertions throughout the *Pi4ka* gene without orientation bias suggests loss of function mutations. **(B)** qPCR of spleens from affected animals showed reduced mRNA expression in spleens with *Pi4ka* insertions compared to Cre- spleens (n=6). **(C)** Immunohistochemistry showed decreased Pi4ka protein in spleens of affected mice (top, scale= 600μm; middle, scale= 60μm). Bottom: Cytospins of RBC lysed blood from affected animals shows increases in blast like cells or myeloid lineage cells from the spleen of affected animals. (scale= 15μm) **(D)** CBC analysis indicated anemia in the animal where *Pi4ka* was the only identified gCIS (F270) and showed the lowest *Pi4ka* mRNA expression. (Data are represented as mean ± S.E.M.) See also Figure 4.4.2.

Figure 4.4.2: Histology and CBC counts for *Pi4ka* affected animals

(A) H&E of Cre- spleens shows normal red and while pulp zone segregation. Spleens with *Pi4ka* insertions have disrupted architecture (scale= 600um). **(B)** The blood from animals with *Pi4ka* insertions had increased blood cell size. (Data are represented as mean ± S.E.M.)

Figure 4.5.1: Loss of pi4kaa function causes reduction in mature RBC in zebrafish

(A) Morphants showed a marked reduction in hemoglobin when compared to controls, as indicated by O-dianiside stain. **(B)** *gata1*:DsRED;*fli1*:GFP (n=4) and **(C)** *lcr*:GFP (n=3) morphant embryos displayed less erythroid lineage cells at 48hpf. **(D)** In 48hpf *gata1:*DsRED;*fli1*:GFP embryos, *fli1*:GFP expression in the *gata1*:DsRED population was 3.5-fold stronger in morphant fish (n=4). **(E)** *gata1*:DsRED+, *fli1:*GFP+ and *gata1*:DsRED+, *fli1:*GFP- populations were sorted. **(F)** Erythroid lineage cell morphology was assessed in sorted cells, revealing loss of mature erythroid cells in morphants (n=2). (scale= 6μm) **(G)** Immature hematopoietic transcription factors *gata-1*, *lmo2*, and *pu.1* were increased in 24hpf morphant embryos compared to controls (n=3-4). **(H)** Mature markers showed no significant differences at this time point, however beta-globin was trending downwards. (Data are represented as mean ± S.E.M.) See also supplemental Figure 4. 5

Figure 4.5.2: Morpholino splicing inhibition and gating strategy for zebrafish flow cytometry

(A) Effects of pi4kaa splice inhibitory morpholino were dose dependent. **(B)** In control embryos, *gata1*:DsRED cells have high *fli1:GFP* expression at 24hpf. **(C)** The median *fli1:*GFP intensity is indicated. **(D)** By 48hpf, *gata1*:DsRED cells lose *fli1:GFP* expression as seen in **(E)**. **(F,G)** In pi4kaa morphant embryos, *gata1*:DsRED cells maintain *fli1*:GFP expression at 48hpf, a phenotype similar to those observed at the 24hpf time point.

Figure 4.6: Pi4ka is expressed in mouse HSPC and its suppression impairs progression of hematopoiesis *in vitro*

(A) Pi4ka (AlexaFluor 568) was observed in the subaortic mesenchyme, but was also found in the membrane of the budding HSPC (CD31 positive, AlexaFluor 488) from hemogenic E9.5 aorta. **(B)** Expression of *Pi4ka* was higher in HSC populations of adult marrow when compared to Lin+ (n=3) **(C)** Co-culture assay (OP9-HSC) for evaluation of HSC differentiation in the presence of cytokines. **(D,E)** HSCs derived from bone marrow were infected with lenti-shRNA targeting *Pi4ka* and evaluated for its ability to differentiate. An increase in the percentage of immature Mac1+, F4/80+ myleloid lineage cells was noted in the *Pi4ka* knock-down conditions after 10 days of co-culture (n=4). **(F,G)** An increase in the percentage of immature CD71+Ter119- cells was also noted in *Pi4ka* knock-down (n=3). (Data are represented as mean ± S.E.M.)

Figure 4.7: *Pi4ka* Knock-down Suppresses Hematopoiesis *in vivo*

(A) Lin depleted CD45.1 bone marrow was infected with shRNA targeting *Pi4ka* or control sequence and used to transplant lethally irradiated CD45.2 hosts. After 10 weeks, bone marrow was harvested. Animals reconstituted with shPi4ka bone marrow (n=3) exhibited increased Lin- **(B)**, decreased LSK **(C)**, and decreased Lin+ **(D)** populations indicating an expansion of the progenitor cells population at the expense of stem and mature populations. **(E,F)** Representative gating strategy for A,B and C. (Data are represented as mean ± S.E.M.)

Figure 4.8: Mutations initiated in the hemogenic endothelium result in adult leukemia

Mutations like Pi4ka are initiated in the hemogenic endothelium or early HSC and cause progenitor cell expansion. Secondary hits then lead to leukemia in the adult.

Table 4.1: Comparison of CIS from HSC targeting SB screens					
Ziyad et al., 2015		Tang et al. 2013	Berquam-Vrieze et al., 2011	Collier et al., 2009	Dupuy et al., 2005
VEC-Cre	VEC-Cre	Vav-Cre/JAK2	Vav-Cre	Global	Global
T2/onc2	T2/onc2	T2/onc	T2/onc2	T2/onc	T2/onc2
Leukemic spleens	Leukemic thymus	Erythroleukemic mice spleens	T-ALL	leukemia/lymphoma (mainly T-cell)	leukemia
Eras	Akt1	**Erg**	**Akt2**	Myb	**Notch1**
Erg	**Akt2**	**Ets1**	Crebbp	Ube2d1	**Rasgrp1**
Ets1	Jdp2	Thsd7a	**Ghr**	Stab2	**Runx2**
Fli1	**Myc**	**Zmiz1**	Foxp1	**Ikzf1**	Sox8
Epo	**Notch1**	Chl1	**Myc**	Csf2	
Pi4ka	Pik3r5	Letm2	Stat5b	Cox10	
Runx2	**Rasgrp1**	Pard3	**Notch1**	Rab5c	
	Zbtb42	Nfyc	**Rasgrp1**	Dusp22	
	Ikzf1	Dock7	**Erg**	Ibrdc2	
	Zmiz1	Scmh1	Runx1	H2afy	
	Erg	Gm5614	**Ets1**	Mef2c	
	Ghr	Shisa9	**Ikzf1**	Cenpk	
	Mbd5	Zfp871	Prlr	Zmiz1	
		Pag1	**Akt1**	Heg1	

		Tcte2	**Zmiz1**	Btla	
		Vav1	Rasgrf1	**Erg**	
		Bcor	Sos1	Heatr5b	
		Enox2		Mbd2	
		Il1rapl1		Pten	
		Chrdl1		**Notch1**	
		Slc9a8		Zbtb34	
		Magea10		**Rasgrp1**	
		Sms		Gm414	
				Ppp3ca	
				Bach2	
				Ptpn12	
				Kit/Kdr	
				AB041803	
				Wnk1	
				Etv6	
				Akt2	
				Klf13	
				Mctp2	
				Eed	
				EG209380	
				Zfp629	
				Dcun1d5	
				Naalad2	
				Fli1	
				BC033915	
				4833427G06Rik	

				Tcf12	
				Eras	
				Tb1x	

Table 4.1: Comparison of CIS from HSC targeting mutagenesis screens

References

1. Marshall, G. M. et al. The prenatal origins of cancer. Nat Rev Cancer 14, 277–289 (2014).

2. Chou, S. T. et al. Trisomy 21-associated defects in human primitive hematopoiesis revealed through induced pluripotent stem cells. Proceedings of the National Academy of Sciences 109, 17573–17578 (2012).

3. Maclean, G. A. et al. Altered hematopoiesis in trisomy 21 as revealed through in vitro differentiation of isogenic human pluripotent cells. Proceedings of the National Academy of Sciences 109, 17567–17572 (2012).

4. Birger, Y. et al. Perturbation of fetal hematopoiesis in a mouse model of Down syndrome's transient myeloproliferative disorder. Blood 122, 988–998 (2013).

5. Stankiewicz, M. ETS2 and ERG promote megakaryopoiesis and synergize with alterations in GATA-1 to immortalize hematopoietic progenitor cells. Blood (2009).

6. Tunstall-Pedoe, O. et al. Abnormalities in the myeloid progenitor compartment in Down syndrome fetal liver precede acquisition of GATA1 mutations. Blood 112, 4507–4511 (2008).

7. Saida, S. et al. Clonal selection in xenografted TAM recapitulates the evolutionary process of myeloid leukemia in Down syndrome. Blood 121, 4377–4387 (2013).

8. Wiemels, J. L. et al. Prenatal origin of acute lymphoblastic leukaemia in children. Lancet 354, 1499–1503 (1999).

9. Ford, A. M. et al. In utero rearrangements in the trithorax-related oncogene in infant leukaemias. Nature 363, 358–360 (1993).

10. Teuffel, O. et al. Prenatal origin of separate evolution of leukemia in identical twins. Leukemia 18, 1624–1629 (2004).

11. Eilken, H. M., Nishikawa, S.-I. & Schroeder, T. Continuous single-cell imaging of blood generation from haemogenic endothelium. Nature 457, 896–900 (2009).

12. Boisset, J.-C. et al. In vivo imaging of haematopoietic cells emerging from the mouse aortic endothelium. Nature 464, 116–120 (2010).

13. Kissa, K. & Herbomel, P. Blood stem cells emerge from aortic endothelium by a novel type of cell transition. Nature 464, 112–115 (2010).

14. Lancrin, C. et al. The haemangioblast generates haematopoietic cells through a haemogenic endothelium stage. Nature 457, 892–895 (2009).

15. Zovein, A. C. et al. Vascular remodeling of the vitelline artery initiates extravascular emergence of hematopoietic clusters. Blood 116, 3435–3444 (2010).

16. Chen, M. J., Yokomizo, T., Zeigler, B. M., Dzierzak, E. & Speck, N. A. Runx1 is required for the endothelial to haematopoietic cell transition but not thereafter. Nature 457, 887–891 (2009).

17. Bertrand, J. Y. et al. Haematopoietic stem cells derive directly from aortic endothelium during development. Nature 464, 108–111 (2010).

18. Rhodes, K. E. et al. The Emergence of Hematopoietic Stem Cells Is Initiated in the Placental Vasculature in the Absence of Circulation. Cell Stem Cell 2, 252–263 (2008).

19. Zovein, A. C. et al. Fate tracing reveals the endothelial origin of hematopoietic stem cells. Cell Stem Cell 3, 625–636 (2008).

20. Zape, J. P. & Zovein, A. C. Hemogenic endothelium: Origins, regulation, and implications for vascular biology. Seminars in Cell and Developmental Biology 1–12 (2011). doi:10.1016/j.semcdb.2011.10.003

21. Dupuy, A. J. et al. A modified sleeping beauty transposon system that can be used to model a wide variety of human cancers in mice. Cancer Res 69, 8150–8156 (2009).

22. Riordan, J. D. et al. Sequencing methods and datasets to improve functional interpretation of sleeping beauty mutagenesis screens. 15, 1–15 (2014).

23. Alva, J. A. et al. VE-Cadherin-Cre-recombinase transgenic mouse: a tool for lineage analysis and gene deletion in endothelial cells. Dev Dyn 235, 759–767 (2006).

24. Brett, B. T. et al. Novel Molecular and Computational Methods Improve the Accuracy of Insertion Site Analysis in Sleeping Beauty-Induced Tumors. PLoS ONE 6, 1–11 (2011).

25. Bard-Chapeau, E. A. et al. Transposon mutagenesis identifies genes driving hepatocellular carcinoma in a chronic hepatitis B mouse model. Nat Genet 46, 24–32 (2014).

26. Keng, V. W. et al. A conditional transposon-based insertional mutagenesis screen for genes associated with mouse hepatocellular carcinoma. Nat Biotechnol 27, 264–274 (2009).

27. Collier, L. S. et al. Whole-body sleeping beauty mutagenesis can cause penetrant leukemia/lymphoma and rare high-grade glioma without associated embryonic lethality. Cancer Res 69, 8429–8437 (2009).

28. Dupuy, A. J., Akagi, K., Largaespada, D. A., Copeland, N. G. & Jenkins, N. A. Mammalian mutagenesis using a highly mobile somatic Sleeping Beauty transposon system. Nature 436, 221–226 (2005).

29. Berquam-Vrieze, K. E. et al. Cell of origin strongly influences genetic selection in a mouse model of T-ALL. Blood 118, 4646–4656 (2011).

30. Tang, J. Z. et al. Transposon mutagenesis reveals cooperation of ETS family transcription factors with signaling pathways in erythro-megakaryocytic leukemia. Proceedings of the National Academy of Sciences 110, 6091–6096 (2013).

31. Oki, T. et al. Aberrant expression of RasGRP1 cooperates with gain-of-function NOTCH1 mutations in T-cell leukemogenesis. Leukemia 26, –1045 (2011).

32. Rasmussen, M. H., Wang, B., Wabl, M., Nielsen, A. L. & Pedersen, F. S. Activation of

alternative Jdp2 promoters and functional protein isoforms in T-cell lymphomas by retroviral insertion mutagenesis. Nucleic Acids Res 37, 4657–4671 (2009).

33. Manabe, N. et al. Src transduces signaling via growth hormone (GH)-activated GH receptor (GHR) tyrosine-phosphorylating GHR and STAT5 in human leukemia cells. Leuk Res 30, 1391–1398 (2006).

34. Zochodne, B. et al. Epo regulates erythroid proliferation and differentiation through distinct signaling pathways: implication for erythropoiesis and Friend virus-induced erythroleukemia. Oncogene 19, 2296–2304 (2000).

35. Huang, H. et al. Differentiation-dependent interactions between RUNX-1 and FLI-1 during megakaryocyte development. Mol Cell Biol 29, 4103–4115 (2009).

36. Athanasiou, M., Mavrothalassitis, G., Sun-Hoffman, L. & Blair, D. G. FLI-1 is a suppressor of erythroid differentiation in human hematopoietic cells. Leukemia 14, 439–445 (2000).

37. Been, R. A. et al. Genetic Signature of Histiocytic Sarcoma Revealed by a Sleeping Beauty Transposon Genetic Screen in Mice. PLoS ONE 9, e97280 (2014).

38. Waugh, M. G. Phosphatidylinositol 4-kinases, phosphatidylinositol 4-phosphate and cancer. Cancer Lett 1–7 (2012). doi:10.1016/j.canlet.2012.06.009

39. Teofili, L. et al. Endothelial progenitor cells are clonal and exhibit the JAK2(V617F) mutation in a subset of thrombotic patients with Ph-negative myeloproliferative neoplasms. Blood 117, 2700–2707 (2011).

40. Sozer, S. et al. The presence of JAK2V617F mutation in the liver endothelial cells of patients with Budd-Chiari syndrome. Blood 113, 5246–5249 (2009).

41. Gunsilius, E. et al. Evidence from a leukaemia model for maintenance of vascular endothelium by bone-marrow-derived endothelial cells. The Lancet 355, 1688–1691 (2000).

42. Prindull, G. Hemangioblasts representing a functional endothelio-hematopoietic entity in ontogeny, postnatal life, and CML neovasculogenesis. Stem Cell Rev 1, 277–284 (2005).

43. Wu, J. et al. Dominant contribution of malignant endothelial cells to endotheliopoiesis in chronic myeloid leukemia. Experimental Hematology 37, 87–91 (2009).

44. Ma, H., Blake, T., Chitnis, A., Liu, P. & Balla, T. Crucial role of phosphatidylinositol 4-kinase III in development of zebrafish pectoral fin is linked to phosphoinositide 3-kinase and FGF signaling. J Cell Sci 122, 4303–4310 (2009).

45. Yavari, A. et al. Role of lipid metabolism in smoothened derepression in hedgehog signaling. Dev Cell 19, 54–65 (2010).

46. Bojjireddy, N. et al. Pharmacological and genetic targeting of pPI4KA reveals its important role in maintaining plasma membrane PtdIns4p and PtdIns(4,5)p2 levels. Journal of Biological Chemistry 1–31 (2014). doi:10.1074/jbc.M113.531426

47. Vaillancourt, F. H. et al. Evaluation of Phosphatidylinositol-4-Kinase III as a Hepatitis C Virus Drug Target. Journal of Virology 86, 11595–11607 (2012).

48. Soriano, P. Generalized lacZ expression with the ROSA26 Cre reporter strain. Nat Genet 21, 70–71 (1999).

49. Ganis, J. J. et al. Zebrafish globin switching occurs in two developmental stages and is controlled by the LCR. Dev Biol 366, 185–194 (2012).

50. Briot, A. et al. Repression of Sox9 by Jag1 is continuously required to suppress the default chondrogenic fate of vascular smooth muscle cells. Dev Cell 31, 707–721 (2014).

51. Oehlers, S. H. et al. The inflammatory bowel disease (IBD) susceptibility genes NOD1 and NOD2 have conserved anti-bacterial roles in zebrafish. Disease Models & Mechanisms 4, 832–841 (2011).

52. Bertrand, J. Y., Kim, A. D., Teng, S. & Traver, D. CD41+ cmyb+ precursors colonize the zebrafish pronephros by a novel migration route to initiate adult hematopoiesis. Development 135, 1853–1862 (2008).

53. Ren, X., Gomez, G. A., Zhang, B. & Lin, S. Scl isoforms act downstream of etsrp to specify angioblasts and definitive hematopoietic stem cells. Blood 115, 5338–5346 (2010).

54. Bertrand, J. Y. et al. Definitive hematopoiesis initiates through a committed erythromyeloid progenitor in the zebrafish embryo. Development 134, 4147–4156 (2007).

Chapter 5:

Conclusions

Summary

In summary, we have demonstrated the role of endothelial cells in three types of pathologies: (1) tumor angiogenesis, (2) vascular anomalies, and (3) leukemia.

(1) First, we described the leaky and non-functional, serpentine morphology of tumor vessels and we discussed the deregulated signaling pathways that govern them. The tumor body was presented as a complex organ made up of cancer cells, immune cells, and stromal cells like fibroblasts and endothelial cells. We highlighted the importance of considering combination therapies that target multiple cells types within the tumor organ for maximal efficacy of treatment.

(2) Next, we presented a mouse model of vascular anomalies that allowed for identification of associated mutations. Novel mutations were identified and validated in vitro. It was found that the majority of the transposon inserted in genes regulating the RhoA and actin cytoskeleton remodeling, cell surface receptor pathways, and Hippo pathways. Mutations in some of the genes identified were found mutated in human vascular anomaly specimens. The findings of this study are very significant to our understanding the governing networks of endothelial cell homeostasis. Clinical scientists now have a new list of genes to focus on in their search for causative genes in human samples. In fact, several of our genes fell in to loci predicted to contain currently unidentified genes causative of Hereditary Hemorrhagic Telangiectasia and Cerebral Cavernous Malformation. Understanding the aberrant signaling pathways that trigger vascular anomalies can also lay the groundwork for targeted therapies.

(3) Finally, we presented data that linked mutations initiated in the hemogenic endothelium (HE) to leukemia in adult animals. Mutagenesis was initiated at embryonic day E9.5, one day before the hemogenic program is turned on at E10.5.

This lead to leukemias that were both myeloid and lymphoid in nature. The network of genes governing the myeloid phenotype involved EpoR signaling through Jak-Stat pathway down to transcription factors Ets1, Runx2, Erg, and Fli1. On the other hand, the lymphoid phenotype was associated with mutations in genes downstream of Ghr, including Akt1/2, Pik3r5, Rasgrp1, Jdp2, Myc and Notch1. Although the link between the hemogenic endothelium and hematopoietic stem cell emergence is well understood, this study established a possible pathological link between the HE and leukemia.

Clinical Implications

Vascular Anomalies

Currently most vascular malformations are routinely trreated with sclerotherapy, embolism, laser treatment or surgery [1,2], while Infantile Hemangioma has shown promising beta-blockers [3]. Knowledge of the pathways has allowed exploration of various treatments in animal models. HHT is driven by the loss of the TGFbeta pathway (*ALK1*, *ENG* and *SMAD4* mutations) so drugs that can increase expression of the remaining receptor/effector have shown clinical promise for patients [4-6] at the cost of side effects. Clinical studies have also shown that the anti-VEGF antibody bevacizumab (Avastin) can greatly improve epistaxis in HHT patients [7]. Most venous malformations are known to be caused by Tie2 activating mutations [8]. A recent study showed that while rapamycin was able to inhibit a mouse model of venous malformation driven by activating Tie mutations, a Tie2 inhibitor (TIE2-TKI) was effective against only some Tie2 mutants [9]. Perhaps the lack of efficacy was due to mutant Tie2 conformational changes that block inhibition of signaling events downstream of WT Tie2 [9]. CCM is known to be characterized by active RhoA signaling and inhibitors of RhoA have been shown to correct the phenotype in mouse models [10,11].

The gCIS from identified in our screen expand the possibilities for targeted therapy. It is well known that CCM is a disease characterized in part by active RhoA signaling. Our screen identified LOF mutations in genes like Akap13 and Kallrn, responsible for helping RhoA catalyze the hydrolysis of GTP. Screening patients for LOF function mutations in those genes could determine whether treatments to increase expression of those genes would dampen the CCM phenotype produced by activated RhoA. Our study suggests that LOF of genes that activate or GOF of genes that inhibit Rac1 (an inhibitor of RhoA) lead to endothelial pathology. In this way therapies that inhibit the function of Wnk1, Cd42bpa, and MEKK3 could help to restore Rac1

inhibition of RhoA. On the other hand drugs that can increase actin depolymerization might be another option since loss of the cofilin activator Ssh2 is associated with endothelial dysfunction. Completely novel modes of endothelial pathogenesis were discovered as well. Kmt2c mutations were very common in the vascular anomalies found in our screen, though it has not yet been reported in endothelial function. Misexpression of Pdgfrb, known well for its role in smooth muscle cells, has also not previously been associated with endothelial pathology, though Imatinib and Dasatinib have been shown to inhibit angiosarcoma growth [12].

Childhood Leukemia

Although no conceivable therapeutic advantage comes with the discovery that mutations initiated in the hemogenic endothelium could carry over into post-natal leukemia, it is still and interesting phenomenon nonetheless. That JAK2, Erg, and BCR-Abl fusion genetic mutations could occur as early as the hemogenic endothelial or even early stem cell stage is a new concept. This is idea is encouraged by the fact that JAK2V617F and BCR-Abl fusion proteins can be detected in endothelial cells from patients affected by myeloproliferative neoplasm and leukemia [13,14].

In conclusion, the data generated from the *in vivo* endothelial specific forward genetic screen bring significant advance to the field of vascular anomalies and is predicted to be used as a major resource for future studies.

References

1. Thiex, R. *et al.* Safety and Clinical Efficacy of Onyx for Embolization of Extracranial Head and Neck Vascular Anomalies. *AJNR Am J Neuroradiol* **32,** 1082–1086 (2011).

2. Uebelhoer, M., Boon, L. M. & Vikkula, M. Vascular Anomalies: From Genetics toward Models for Therapeutic Trials. *Cold Spring Harb Perspect Med* **2,** (2012).

3. Léauté-Labrèze, C. *et al.* Propranolol for severe hemangiomas of infancy. *N Engl J Med* **358,** 2649–2651 (2008).

4. Albiñana, V. & Bernabeu-Herrero, M. E. Estrogen therapy for hereditary haemorrhagic telangiectasia (HHT): Effects of raloxifene, on Endoglin and ALK1 expression in endothelial cells. *Thrombosis & …* (2010).

5. Albiñana, V., Sanz-Rodríguez, F., Recio-Poveda, L., Bernabeu, C. & Botella, L. M. Immunosuppressor FK506 increases endoglin and activin receptor-like kinase 1 expression and modulates transforming growth factor-β1 signaling in endothelial cells. *Mol Pharmacol* **79,** 833–843 (2011).

6. Lebrin, F. *et al.* Thalidomide stimulates vessel maturation and reduces epistaxis in individuals with hereditary hemorrhagic telangiectasia. *Nat Med* **16,** 420–428 (2010).

7. Karnezis, T. T. & Davidson, T. M. Efficacy of intranasal bevacizumab (Avastin) treatment in patients with hereditary hemorrhagic telangiectasia‐associated epistaxis. *Laryngoscope* **121,** 636–638 (2011).

8. Limaye, N. *et al.* Somatic mutations in angiopoietin receptor gene TEK cause solitary and multiple sporadic venous malformations. *Nat Genet* **41,** 118–124 (2009).

9. Boscolo, E. *et al.* Rapamycin improves TIE2-mutated venous malformation in murine model and human subjects. *J Clin Invest* 10.1172/JCI76004–14 (2015). doi:10.1172/JCI76004

10. Stockton, R. A., Shenkar, R., Awad, I. A. & Ginsberg, M. H. Cerebral cavernous malformations proteins inhibit Rho kinase to stabilize vascular integrity. *Journal of Experimental Medicine* **207,** 881–896 (2010).

11. Borikova, A. L. *et al.* Rho kinase inhibition rescues the endothelial cell cerebral cavernous malformation phenotype. *J Biol Chem* **285,** 11760–11764 (2010).

12. Dickerson, E. B. *et al.* Imatinib and Dasatinib Inhibit Hemangiosarcoma and Implicate PDGFR-β and Src in Tumor Growth. *Translational Oncology* **6,** 158–IN7 (2013).

13. Teofili, L. *et al.* Endothelial progenitor cells are clonal and exhibit the JAK2(V617F) mutation in a subset of thrombotic patients with Ph-negative myeloproliferative neoplasms. *Blood* **117,** 2700–2707 (2011).

14. Sozer, S. *et al.* The presence of JAK2V617F mutation in the liver endothelial cells of patients with Budd-Chiari syndrome. *Blood* **113,** 5246–5249 (2009).